Theses, Dissertations and Capstones

2004

HK-2 cells as a human model of glucuronide transport

Eliza E. Robertson

Follow this and additional works at: http://mds.marshall.edu/etd

Part of the Chemicals and Drugs Commons, Nephrology Commons, Pharmacology Commons, Pharmacy and Pharmaceutical Sciences Commons, and the Urogenital System Commons

Recommended Citation

HK-2 CELLS AS A HUMAN MODEL OF GLUCURONIDE TRANSPORT

by

Eliza E. Robertson

Dissertation submitted to
the Graduate College
of
Marshall University
in partial fulfillment of the requirements
for the degree of

Doctor of Philosophy
in
Biomedical Sciences

Approved by

Gary O. Rankin, Ph.D. (Committee Chairperson)
Patrick I. Brown, Ph.D.
Lawrence H. Lash, Ph.D.
Richard M. Niles, Ph.D.
Monica A. Valentovic, Ph.D.

Department of Pharmacology, Marshall University School of Medicine

Fall 2004

ABSTRACT

**HK-2 CELLS AS A HUMAN MODEL OF
GLUCURONIDE TRANSPORT**

by Eliza E. Robertson

Glucuronidation is primarily a pathway of detoxification in most species, but many glucuronide conjugates are associated with toxicity. Numerous drugs are excreted in the urine as glucuronide conjugates. Being organic anions, it is likely that glucuronides are secreted into the urine by organic anion transporters found in renal proximal tubule cells (PTCs). Some drugs that are metabolized by glucuronidation have been shown to cause renal toxicity, yet little is known about the renal handling of glucuronide conjugates. It is hypothesized that glucuronides are transported into renal PTCs by an organic anion transporter (OAT) on the basolateral membrane of the cell. A potential human model for examining renal organic anion transport is the HK-2 cell line, an immortalized adult human male proximal tubule cell line. Little evidence exists that this model is capable of transporting organic anions. Therefore, the purpose of this study was to determine which OATs (1-3) exist in this cell line, if the OATs are functional, and finally, the nature of glucuronide transport. HK-2 cells were grown in keratinocyte serum-free media supplemented with 2% fetal bovine serum. Western blot analysis of membrane fractions of HK-2 cells grown for 5-7 days in T-75 flasks revealed the presence of OAT1 and OAT3, but not OAT2 in the cell membranes. In separate studies, HK-2 cells grown on microporous membranes for 4-9 days transported fluorescein (FL) and p-aminohippurate (PAH), prototypical substrates for OAT1 and OAT3 and estrone sulfate (ES), the prototypical substrate for OAT3. Transport of acetaminophen glucuronide (AG) by HK-2 cells demonstrated time-, temperature- and concentration-dependent uptake suggestive of protein-mediated transport. Transport characteristics of AG in the HK-2 model, such as biphasic concentration-dependent transport and lack of inhibition of transepithelial transport by probenecid are consistent with in vivo transport as found in the literature. These results suggest that HK-2 cells possess functional OATs and demonstrate transport of a model glucuronide compound such that HK-2 cells may be useful as a model to study the renal handling of organic anions, including glucuronide conjugates.

DEDICATION

To my family who has endured the many trials through this long journey, I dedicate this work. You have been my support, my strength and my refuge. To my husband, Dana, thank you for your encouragement and for assuming my role in the family when I could not be there. To my children, Peter and Wesley, thank you for your understanding and your sacrifice when my time was not available for your activities. To my mother, Margie McMorrow, who helped me through the early years with my family, I am ever so grateful. My loving family, I am truly blessed.

ACKNOWLEDGMENTS

TABLE OF CONTENTS

LIST OF FIGURES

LIST OF TABLES

LIST OF SYMBOLS / NOMENCLATURE

A	apical
aa	amino acid(s)
AG	acetaminophen glucuronide
ANOVA	analysis of variance
AP	alkaline phosphatase
APAP	acetaminophen
ATCC	American Tissue Culture Collection
ATP	adenosine-5'-triphosphate
BBM	brush border membrane (apical)
BL	basolateral
BLM	basolateral membrane
BSP	sulfobromophthalein
cAMP	cyclic adenosine monophosphate
cGMP	cyclic guanidine monophosphate
CHO cells	Chinese hamster ovary cells
DDBJ	DNA DataBank of Japan
DHEAS	dehydroepiandrosterone sulfate
DMSO	dimethyl sulfoxide
DPM	disintegrations per minute
$E_217\beta G$	β–Estradiol 17β-D-glucuronide
EcR293	HEK293 cell line expressing ecodysone receptors
EDTA	ethylenediaminetetraacetic acid
EMBL	European Molecular Biology Laboratory
ES	estrone sulfate
F344	Fisher 344 rat
FBS	fetal bovine serum
FL	fluorescein

FLD	fluorescein isothiocyanate dextran
GGT	gamma-glutamyltransferase
HBSS	Hanks' balanced salt solution
HCl	hydrochloric acid
HEK293	human embryonic kidney cell line
HeLa cells	immortal cell line derived from human cervical carcinoma
HEPES	N-[2-hydroxyethyl]piperazine-N-[2-ethanesulfonic acid]
HK	hexokinase
KSFM	Keratinocyte Serum Free Media
LDH	lactate dehydrogenase
LLC-PK1	porcine kidney proximal tubule cell line
LTC_2	leukotriene C2
MDCK	Madin-Darby canine kidney (distal tubule cell line)
MRP	multidrug resistance-associated protein
MW	molecular weight
NAD+	oxidized nicotinamide adenine dinucleotide
NADH	reduced nicotinamide adenine dinucleotide
NaOH	sodium hydroxide
OAT	organic anion transporter
OATP	organic anion transporting polypeptide
OCT	organic cation transporter
PAH	para-aminohippuric acid
PBS	phosphate buffered saline
PCR	polymerase chain reaction
PGE_1	prostaglandin E_1
PGE_2	prostaglandin E_2
$PGF_{2\alpha}$	prostaglandin $F_{2\alpha}$
PSa	permeability-surface area product
PT	proximal tubule
PTC	proximal tubule cell

RT-PCR	reverse transcription polymerase chain reaction
SDS	sodium dodecyl sulfate
SEM	standard error of the mean
Sf9 cells	Spodoptera frugiperda insect cell line
T25	culture flask with a 25 square cm surface area
T75	culture flask with a 75 square cm surface area
TBS	tris-buffered saline
TBST	tris-buffered saline Tween-20
TEMED	tetramethylethylenediamine
TM	transport media (PBS with 5 mM glucose)
UDP	uridine diphosphate
UDPGT	uridine diphospho glucuronysyltransferase
UGA	uridine diphospho glucuronic acid
URAT1	urate transporter
WBTM	Waymouth's buffered transport media
XLO	Xenopus laevis oocyte

CHAPTER I

Introduction

<u>Glucuronides</u>

Glucuronidation is a major route of metabolism of both endogenous and exogenous compounds including many classes of drugs. Primarily, glucuronide conjugates are formed via an enzyme-catalyzed reaction in the liver, creating metabolites that are more water-soluble and more readily excreted in the urine or the feces. Although glucuronidation is considered a detoxification pathway, some glucuronide metabolites have been shown to bind irreversibly to protein and are associated with toxicity. Indeed, many glucuronides have been shown to be associated with nephrotoxicity in humans, yet little is known about how glucuronides accumulate in the human kidney.

<u>Organic Anion Transport</u>

Since glucuronide conjugates are organic anions, it is possible that they are substrates of the renal organic anion transporters. Organic anion transporters are responsible for the uptake of numerous endogenous and xenobiotic organic anions into renal proximal tubule epithelial cells along their basolateral membranes (BLMs). Subsequent secretion of these anions into the glomerular filtrate occurs via carriers in the apical membrane. Hence, transepithelial flux of organic anions is a two-step, protein-mediated process of uptake at the BLM and efflux across the apical, brush-border membrane (BBM). The resultant secretion of these organic anions, including many associated with toxicity, fulfills an important function of the kidney. It is the uptake of these compounds by organic anion transporters that may lead to accumulation and toxic effects in the proximal tubule.

Hypothesis

It is hypothesized that glucuronides are transported into renal proximal tubule cells by an organic anion transporter on the basolateral membrane of the cells.

Model Development

Most studies of renal organic anion transport have been conducted with non-human models. Recent cloning of human organic anion transporters, substrate specificity studies, immunolocalization and gene expression levels have indicated that there are considerable differences in human and animal models which may explain their differing pharmacokinetic profiles for many drugs. Consequently, to study the hypothesis, a human renal model of organic anion transport was chosen. Difficulties in procurement of human tissue often make studies with primary culture or freshly isolated human proximal tubules improbable. A functional human proximal tubule cell line expressing the transporters was a desirable alternative. Dr. Lawrence H. Lash recommended the HK-2 cell line as a likely candidate.

The HK-2 cell line was developed by Dr. Richard Zager, The Fred Hutchinson Cancer Research Center, University of Washington, via transfection of an adult human male proximal tubule cell with the human papilloma virus (HPV 16) E6/E7 genes. Studies indicated that this cell line retains both phenotypical and functional characteristics of a well differentiated proximal tubule cell. Little evidence exists as to the ability of the HK-2 cells to perform active transport of organic anions. A major part of the work described herein is in the development and characterization of the HK-2 cell line relative to organic anion transport.

Studies of the uptake of glucuronide conjugates into HK-2 monolayers proceeded using acetaminophen glucuronide (AG) as the model glucuronide. AG was chosen because evidence in the literature supports renal secretion of AG (Prescott, 1980; Duggin and Mudge, 1975) and because radiolabeled AG was available for purchase. Unlabeled AG as well as other glucuronides were used to study the effect on radiolabeled AG uptake and transepithelial transport.

Throughout this document, BBM and BLM will refer to brush-border and basolateral membranes, respectively, of a renal proximal tubule cell (PTC). The abbreviations BL (basolateral) and A (apical) will refer to the respective membranes of nonproximal tubule cells, such as transfectant models, or to the respective fluid compartments of the porous support membranes upon which the cells are grown.

By convention, the results of transport experiments have been referred to as either *uptake* or *clearance*. However, the term *uptake* describes a single process and is therefore not accurate. Rather, more appropriate terminology is *net intracellular accumulation* implying the amount of substrate remaining in the cells after uptake and efflux have terminated. The terms, *uptake* and *net accumulation*, are used interchangeably in this document.

CHAPTER II

Review of Literature

<u>Glucuronides</u>

<u>Role of Glucuronidation in Metabolism and Disposition</u>

Glucuronidation is a Phase II biotransformation reaction responsible for the elimination of numerous biologically active or potentially toxic substances via conjugation with glucuronic acid. Substrates for this reaction must be lipophilic, and include endogenous compounds, such as steroids, bile acids and hormones, as well as many xenobiotics, including many therapeutic agents and environmental toxicants. Substrates may directly undergo glucuronidation or may first be oxidized in a Phase I reaction, forming an acceptor group for glucuronic acid. Glucuronide formation requires the co-substrate UDP-glucuronic acid (UGA) and is catalyzed by a multi-gene family of enzymes, the UDP-glucuronysyl-transferases (UDPGTs). The reaction takes place in the smooth endoplasmic reticulum and is referred to as a microsomal reaction. Substrates for glucuronidation include compounds with a wide range of acceptor groups, such as alcohols, phenols, carboxylic acids, aliphatic amines and acidic carbon atoms (Miners et al., 1991). Formation of the glucuronide conjugate results in a more hydrophilic compound that typically has the dual effect of inactivating the parent compound and partitioning it to the extracellular compartment, from which it can be more readily excreted in the bile or the urine. Glucuronide formation is depicted in Figure 2.1 (Mulder GJ, 1992; Lohr et al., 1998; Tukey and Strassburg, 2000).
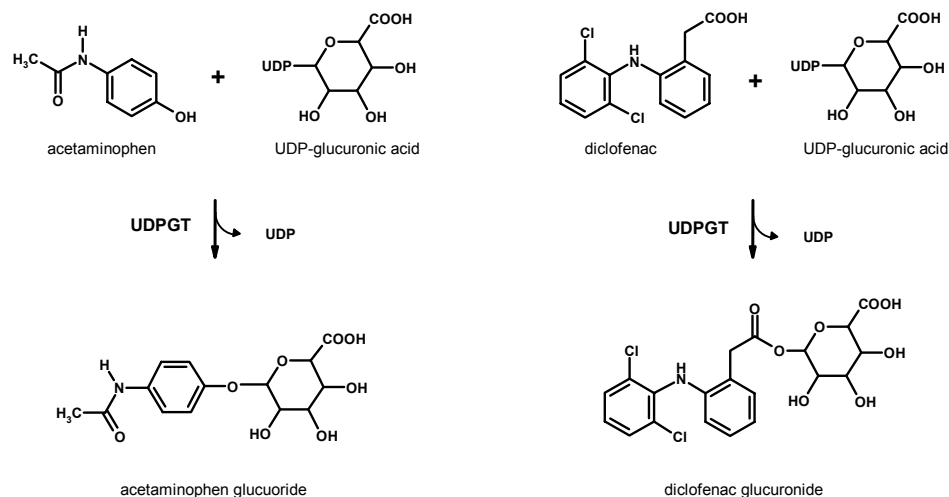
Figure 2.1. **Formation of Acetaminophen Glucuronide and Diclofenac Glucuronide.**

Formation, Hepatic vs. Renal

The largest concentration of the UDPGTs resides in the liver. However, evidence of UDPGT activity in the kidney has been reported (Tukey and Strassburg, 2000). Although the concentration of UGA in human kidney is less than 10% of that of the liver (Cappiello et al., 1991), immunocytochemical studies in rat and human demonstrate the highest concentration of the renal UDPGTs is present in the proximal tubule (Lock and Reed, 1998). Figure 2.2 depicts the biotransformation and secretion of a lipophilic compound in both the liver and the kidney. The contribution of renal vs. hepatic glucuronidation varies for different species and substrates. For example, Morris and Levy (1984) suggested that human renal synthesis of acetaminophen glucuronide (AG) is negligible because elimination of acetaminophen by conjugation is not impaired in anephric patients. In isolated perfused rat kidneys, Newton et al. (1982) found that AG is synthesized from acetaminophen and secreted into the urine at a very low rate. Clearance of indomethacin, however, occurs predominantly by renal glucuronidation in humans (Moolenaar et al., 1992). Evidence also suggests that estradiol is conjugated with glucuronic acid in the kidney forming β−estradiol 17β-D-glucuronide (E$_2$17βG) with subsequent tubular secretion (Kanai et al., 1996).
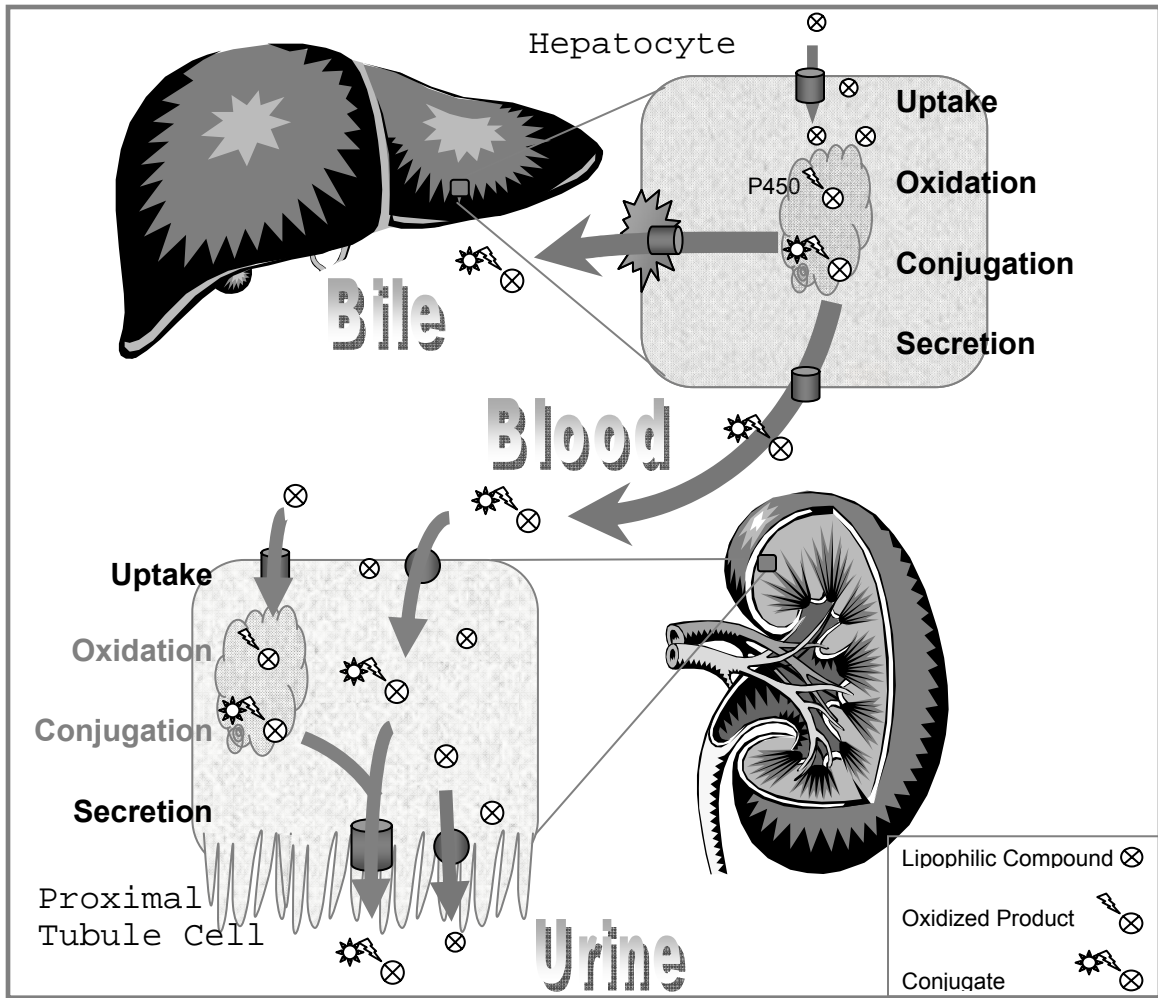
Figure 2.2. General Scheme for Hepatic and Renal Biotransformation and Secretion. Substances may diffuse or be transported into the hepatocyte across the sinusoidal membrane. If they are sufficiently lipophilic, they may enter the smooth endoplasmic reticulum and undergo Phase I and/or Phase II biotransformations such as oxidation by cytochrome P450 enzymes and conjugation with glucuronic acid. Higher molecular weight conjugates (MW > 400) may then be secreted at the canalicular membrane into the bile (represented as a starburst) but may be secreted back into the sinusoid and delivered to the circulation. Lower molecular weight conjugates typically are secreted into the circulation. The conjugate will be more water soluble and may be actively taken up by the renal proximal tubule from the blood delivered to the kidney. Additionally, the parent compound may enter the proximal tubule by diffusion or by carrier-mediated transport and undergo biotransformations in the kidney as in the liver, but to a lesser extent. The conjugates are then secreted into the glomerular filtrate.

Renal Handling of Glucuronide Conjugates

It is well established that glucuronides are efficiently excreted by the kidney (O'Neill et al., 1981; Pantuck et al., 1991; Moolenaar et al., 1992). Numerous drugs are eliminated in the urine as their glucuronide conjugates and have rates of excretion greater than that of creatinine, indicating a secretory process (Prescott et al., 1980, Spahn-Langguth et al., 1996). Most of the information on the renal handling of glucuronides has been attained in the study of the endogenous steroid conjugate, estradiol-17β-glucuronide ($E_2$17βG), which is a high-affinity substrate for basolateral and apical carriers. An extensive review of transport-specific information for glucuronides is covered in the Transport section of this document.

Toxicity Associated with Glucuronides

Several compounds that form glucuronides have been associated with hepatic and renal toxicity (Spahn-Langguth and Benet, 1992; Smith and Liu, 1995; Bailey et al., 2003). Carboxylic acids are the main class of compounds that form labile glucuronides. These conjugates, known as acyl glucuronides, are formed by an ester-linkage of the parent compound with glucuronic acid (see Figure 2.1, diclofenac glucuronide synthesis). Acyl glucuronides, which are stable at low temperature and low pH, are reactive at physiologic temperature and pH (Spahn-Langguth and Benet, 1992). Indeed, acyl glucuronides are known to undergo hydrolysis, intramolecular rearrangement via acyl migration, and formation of protein adducts by intermolecular covalent binding under physiologic conditions. Protein adduct formation is believed to be the mechanism of toxicity (Spahn-Langguth and Benet, 1992). Adverse drug reactions associated with drugs that are metabolized to acyl glucuronides may occur by functional inactivation of target proteins or by hapten formation, resulting in an immune response against the drug-protein adduct (Bailey et al., 2003). Renal proximal tubules are thought to be highly susceptible to the toxic effects of acyl glucuronides due to the ability of the tubules to concentrate the glucuronides (Smith and Liu, 1995).

Renal Excretion of Organic Anions

The Process of Urinary Excretion

More substances are eliminated from the body by renal excretion than by any other route (Klaassen CD, 2001). Renal excretion occurs through three processes: glomerular filtration and tubular excretion by both passive diffusion and active secretion. Glomerular filtration equals about 20% of the renal blood flow. Passive diffusion is thought to be only a minor process in comparison. Protein-bound compounds are typically too large to be filtered and do not diffuse easily, but are readily transferred from plasma proteins at the tubule membrane and secreted by transport-mediated processes in the tubule. Tubular secretion can occur as a facilitated transport mechanism down an electrochemical gradient or as an active process (or dependent upon an active process) requiring energy to move chemicals against an electrochemical gradient. Tubular secretion of organic anions is a very efficient process which occurs in the proximal tubule of the nephron.

Tubular Secretion of Organic Anions

Tubular secretion involves protein-mediated uptake of substrate at the BLM and protein-mediated efflux at the BBM. The transport proteins in the membranes affect the apparent permeability of the membrane to organic anions in a substrate-specific manner. During the secretory process, as studied in perfused tubules (mammalian and non-mammalian), the steady-state concentration of organic anion inside the cells is greater than in the tubule lumen (glomerular filtrate), which is greater than in the peritubular fluid/bathing medium (i.e., $C_i > C_u > C_b$; i = intracellular, u = urinary, b = blood; Figure 2.3; Dantzler, 2002). This process can only occur

Figure 2.3. Concentration Gradient for Fluorescein at Steady-State in the Isolated Perfused Tubule. $C_i > C_u > C_b$

because the BBM is more permeable to the substrate than is the BLM, a condition
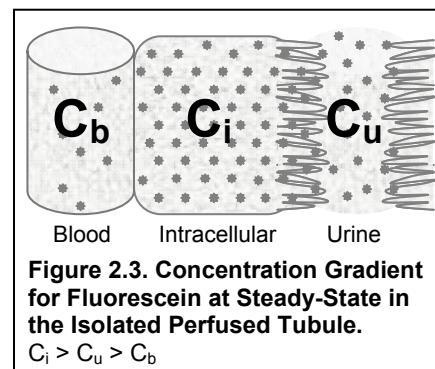
that has been demonstrated in numerous species and is requisite of uptake at the BLM being the rate limiting step in transepithelial transport (Dantzler, 2002). This condition, however, does not hold true for all organic anions. Terlouw et al. (2003) states that in general, the efflux mechanism at the luminal membrane is less efficient than basolateral uptake, resulting in accumulation of organic anions. This condition has been demonstrated for many of the antiviral drugs for which efflux at the BBM is rate limiting, resulting in intracellular accumulation (Russel et al., 2002).

Uptake of substrate at the BLM is often measured as the net accumulation within the cell. Since both cellular energetics (available counter-ions or ATP) and apical efflux will affect net accumulation, uptake is assessed at the initial rate of uptake, during the linear phase for the purpose of kinetic analysis (Sugiyama et al., 2001). Thus, a time course study is conducted to determine the linear phase of uptake.

Transepithelial transport is evaluated by determining the substrate concentrations in both compartments (BL and A) at the end of an incubation period and calculating the substrate clearance. Clearance is the volume of fluid totally cleared of substrate over a period of time (Groves et al., 1999a):

$$Clearance = \frac{[substrate]_A * Volume_A}{[substrate]_{BL} * SA * time} = [\mu l / cm^2 / \min]$$

where A = apical, BL = basolateral and SA = surface area.

Transport Kinetics

The epithelium of the nephron is formed from a single layer of cells known as a monolayer. The kinetics of transport of substrates across a monolayer follows the laws that govern chemical interactions. Kinetic studies are performed during the linear phase of transport (initial velocity) (Sugiyama et al., 2002). By performing a concentration dependent study during the linear phase of transport, the rate of

transport can be evaluated with a rectangular hyperbolic function, namely, the Michaelis-Menten equation:

$$V = \frac{V_{max} * [S]}{K_m + [S]} + d$$

where V = rate of transport, V_{max} = maximum rate of transport, [S] is the substrate concentration, K_m = the substrate concentration which produces 1/2 V_{max}, and d is a nonspecific term to account for nonspecific binding (Groves et al., 1994). A V_{max} is predictive of any interaction that is saturable and correlates with the capacity of the transporter for the substrate, such that a high V_{max} corresponds to a high capacity of transport. The K_m relates to the affinity of the substrate for the transporter, such that the higher the affinity, the lower the K_m.

The Berteloot equation offers an alternative method of analysis for concentration-dependent studies. Data used to analyze transport using this regression is more reflective of the measurements that are made for transport. The data entered for Berteloot regression analysis are the tracer concentration, the concentration of unlabeled substrate and the transport of tracer rather than the total concentration and transport of total substrate as for the Michaelis-Menten analysis. The Berteloot Equation is of the form:

$$V = \frac{V_{max} * [T]}{K_m + [T] + [S]}$$

where V = rate of transport, V_{max} = maximum rate of transport, [T] is the tracer concentration, [S] is the substrate concentration and K_m = the substrate concentration which produces 1/2 V_{max} (Malo and Berteloot, 1991).

Efficiency of transport is defined as the ratio of Vmax to Km (Cihlar and Ho, 2000; Gerk et al., 2002).

$$Efficiency = \frac{V_{max}}{K_m}$$

This is an appropriate tool to evaluate relative efficiencies of BLM vs. BBM transport and relative transport of one substrate vs. another. For example, $E_2 17\beta G$ has a higher affinity (lower K_m) than does taurocholate (TC) for the rOatp2 transporter, but because rOatp2 has a greater capacity (higher V_{max}) for TC, it is much more efficiently transported by rOatp2 than is $E_2 17\beta G$ (Sugiyama et al., 2002).

The permeability of the apical membrane can be evaluated by calculating the permeability-surface area product (PS_a):

$$PS_a = \frac{Apical\ Efflux}{Intracellular\ Accumulation}$$

PS_a is useful in understanding effects at the apical membrane in transepithelial studies using models expressing transporters in BL and A membranes (Sasaki et al., 2002).

Organic Anion Transporters

The OAT Family

The OAT family is a group of transmembrane proteins which function in the transport of organic anions and are associated by a high degree of homology. These transporters belong to the amphiphilic solute transporter family 22a (Slc22a), a subset of the major facilitator superfamily (Sweet et al., 2002). The classical OAT system which was long referred to as the PAH (para-aminohippurate) transporter (Lu et al., 1999) is now known as OAT1 (Sekine et al., 2000; Burckhardt et al.,2000; Sun et al., 2001; Sweet et al., 2001). There are currently 5 known members of the family, named OAT1 to OAT5 (Sun et al., 2001). With advances in technology, the genes encoding transporters OAT1-4 have been characterized, expressed in various cell models and studied to gain a better understanding of their localization and functionality (mechanism, regulation and substrate specificity).

Molecular Studies

Recent molecular cloning of the transporters in several species and immunolocalization studies have dramatically advanced the study of organic anion transport. In 1996, the gene encoding a renal organic anion transporter in mouse, termed NKT (novel kidney transporter), was identified and cloned (Lopez-Nieto et al., 1997). This gene was subsequently identified as the mouse equivalent of OAT1. The following year, two groups of scientists cloned the rat OAT1 (rOAT1) gene (Sekine et al., 1997; Sweet et al., 1997). There have been 4 laboratories that have since reported cloning the human orthologue, hOAT1 (Reid et al., 1998; Hosoyamada et al, 1999; Lu et al., 1999; and Race et al., 1999). Soon after the characterization began of OAT1, followed the discovery of other members of the multispecific organic anion transporters with high homology to OAT1. The cloning of a novel liver transporter (NLT) in rat (Simonson et al., 1994) was later discovered to share a 46% homology to OAT1. NLT was thus termed OAT2 (Sekine et al., 1998). Cloning of yet a third OA transporter from rat, termed OAT3,

was reported in 1999 (Kusuhara et al.) and shares a 49% homology with rOAT1. Human OAT3 (hOAT3) was cloned and reported to share a 51% homology to hOAT1 (Cha et al., 2001). Cloning of human OAT4 by Cha et al. (2000) was soon followed by a report of isolation of a family of OATs, hOAT1 to hOAT5 from the human liver and kidney (Sun et al., 2001). Human OATs, hOAT1-3, are orthologues to rat OATs, rOAT1-3, whereas hOAT4 and hOAT5 had not been identified in species other than human (Sun et al., 2001). The hOAT4 transporter cloned by Sun et al., is not the same transporter as that cloned earlier by Cha and coworkers (2000) and has been identified as structurally nonhomologous to the OAT family. Consequently, hOAT4 refers to the transporter cloned by Cha et al. (2000). Recently rOAT5 which shares only a 55% homology to hOAT5 was isolated from a rat kidney cDNA library and is thought not to represent an orthologue of hOAT5 (Koepsell and Endou, 2003). Thus, there are 3 members of the rat OAT family, and they are orthologous to hOATs 1-3.

A composite of the characteristics reported by the above investigators reveals a family of proteins with a range of 541-568 amino acid residues (aa), 12 putative membrane spanning domains (11 in mouse) and 5 (hOAT1), 4 (hOAT3) and 5 (hOAT4) potential N-glycosylation sites. Isoforms, thought to be splice variants of the individual members, have also been identified. There are 4 isoforms of hOAT1 (563, 550, 506 and 519 aa; Bahn et al., 2000); 2 isoforms of hOAT2 (546 and 538 aa) and 2 of hOAT3 (543 and 568 aa). Although it is unclear as to the purpose of the various isoforms, not all isoforms of a particular transporter have identical substrate specificity and some do not function in transport.

Tables 1-3 are a compilation of the isoforms of hOAT1 and hOAT3 that have been submitted to the sequence databases maintained by the members of the international collaboration of sequence databases: the NIH National Center for Biotechnology Information (NCBI) GenBank, the European Molecular Biology Laboratory (EMBL), and the DNA Database of Japan (DDBJ). The Protein database contains sequence data from the translated coding regions from DNA

sequences in GenBank, EMBL and DDBJ as well as protein sequences submitted to Protein Information Resource (PIR), SWISSPROT, Protein Research Foundation (PRF), and Protein Data Bank (PDB) (sequences from solved structures) (source: National Center for Biotechnology Information, Entrez).

Using the Bioinformatics Harvester, http://harvester.embl.de, a search of the EMBL GenBank DDBJ databases for human organic anion transporters yielded 4 entries for hOAT1 from human kidney and 3 entries for hOAT3. The number of amino acids (aa) recorded for the hOAT1 entries are in agreement with those reported by Bahn et al. (2000) and are those submitted by the individual laboratories and reported in the journal articles (Reid et al., 1998; Hosoyamada et al., 1999; Lu et al., 1999; Race et al., 1999; Cihlar et al., 1999; and Bahn et al., 2000). The EMBL entries for hOAT3 are those submitted by the laboratories and reported by Race et al. (1999), Cha et al. (2000), and one direct submission to the database by Strausberg R in 2002. The GenBank entry for hOAT3 submitted by Cha et al., 2000, lists a 542 aa protein vs. a 543 aa protein as reported by Cha et al. (2000). The third hOAT3 EMBL entry, submitted by Strausberg et al. in 2002 (direct submission, no publication), is a computer derived hypothetical protein and represents a single aa substitution at residue 271 as compared with the 542 aa sequence submitted by Cha et al. (2000) as analyzed by peptide alignment using the Web-based sequence analysis software program Accelrys SeqWeb version 2 .

A fifth isoform of hOAT1 was found through the National Center for Biotechnology Information (NCBI) protein database, http://www.ncbi.nlm.nih.gov/. This 529 aa isoform is listed as isoform e. A complete listing of the proteins and mRNA listed under human OAT1 and/or solute carrier family 22 (organic anion transporter), member 6 (SLC22A6) in the NCBI database is provided in Table 3.

Table 1. hOAT1 Isoforms Listed by the European Molecular Biology Laboratory (EMBL)		
EMBL Accession No.	Amino acid residues	Predicted MW (kD)
O95742	563	61.816
Q8N192	550	60.317
Q9NQC2	506	55.858
Q9NQA6	519	57.357

Table 2. hOAT3 Isoforms Listed by the European Molecular Biology Laboratory (EMBL)		
EMBL Accession No.	Amino acid residues	Predicted MW (kD)
O95820	568	62.070
Q96TC1	542	59.857
*Q8TCC7	542	59.856

* listed as a hypothetical protein

Table 3. National Center for Biotechnology Information (NCBI) GenBank Entries for Human OAT1, SLC22A6						
Nucleotide Accession Number	mRNA bp (variant)	Protein Accession Number	Isoform Name	# Amino acids	Date of Entry	Submitted by
NM_004790	2196 (1)	NP_004781	SLC22A6-a	563	04/2003	Curated by staff
NM_153276	2194 (2)	NP_695008	SLC22A6-b	550	04/2003	Curated by staff
NM_153277	2025 (3)	NP_695009	SLC22A6-c	506	04/2003	Curated by staff
NM_153278	2064 (4)	NP_695010	SLC22A6-d	519	04/2003	Curated by staff
NM_153279	2131 (5)	NP_695011	SLC22A6-e	529	04/2003	Curated by staff
AF057039	2090	AAC70004	hROAT1	550	04/1998	Reid et al.
AF097490	1653	AAD19356	hOAT1	550	10/1999	Race et al.
AF104038	2088	AAD10052	hPAHT	550	10/1998	Lu et al.
AF124373	2118	AAD55356	OAT1	550	09/1999	Cihlar et al.
AB009697	2151	BAA75072	hOAT1-1	563	12/1997	Hosoyamada et al.
AB009698	2113	BAA75073	hOAT1-2	550	12/1997	Hosoyamada et al.
AJ249369 exons1-10	8635 (DNA)	CAB77184	OAT of OAT1 gene	563	09/1999	Bahn et al.
AJ251529	1521	CAB94830	OAT1-3	506	12/1999	Bahn et al.
AJ271205	1560	CAB94830	OAT1-4	519	01/2000	Bahn et al.
BC033682	2180	AAH33682	SLC22A6	550	07/2002	Strausberg R
AK055764	2180	--	--	--	10/2001	Isogai T et al

<u>Western Analysis</u>

Currently, the only known commercial supplier of antibodies for the OATs is Alpha Diagnostics International. However, several investigators have raised antibodies and conducted immunohistochemical and/or Western analysis. All antibodies were raised against synthetic peptides of sequences at or near the carboxy terminus. Table 4 summarizes their findings for OAT1 and OAT3 by Western analysis. The table also includes the predicted molecular weight of the OAT clones. These predicted values are indicated by an asterisk.

Due to the vast differences in molecular weight for the OATs reported, the study of Bergwerk et al (1996) is worthy of mention. In this study, Bergwerk and colleagues performed a Western analysis of a cloned organic anion transport protein from rat. The transporter had not been identified, but it was reported to function in a sodium-independent manner and Northern analysis had identified RNA in liver and kidney only. Protein for the liver revealed an 80 kD protein that migrated to 65 kD after deglycosylation. In the kidney, under non-reducing conditions, the protein migrated to 83 kD but on reduction, it resolved into peptides of 33 and 37 kD. Molecular weights marked with a double asterisk in Table 4 indicate deglycosylated protein. Additionally, a column is included in the table to indicate if the preparation included a reducing agent.

**Table 4. Molecular Weight of OAT1 and OAT3 Proteins
Based on Western Analysis or Predicted Gene Products**

* indicates predicted MW
** indicates the bands recognized after deglycosylation

Investigator	Species/Organ/Model	Reduced	OAT1 (kD)	OAT3 (kD)
Cihlar et al., 1999	Human kidney cortex	no	80-90; 60**	--
Hosoyamada et al., 1999	Human renal clone	--	61.8*	--
Race et al., 1999	Human renal clone	--	60.3*	62.1*
Reid, 1999	Human renal clone	--	60*	--
Motohashi et al., 2002	Human kidney tissue	no	84	80
Hasegawa et al., 2002	Rat kidney tissue	yes	--	65
Hasegawa et al., 2002	rOAT3 expressing LLC-PK1 cells	yes	--	54
Ji et al., 2002	Rat kidney	yes	77	72
Kojima et al., 2002	Rat kidney	no	--	130
Kikuchi et al., 2003	Rat kidney	?	--	65; ~40**
Kikuchi et al., 2003	Rat brain capillaries	?	--	75; ~40**
Nagata et al., 2002	Rat kidney	yes	69	Slightly > 63
Nagata et al., 2002	rOAT1 and rOAT3 expressing LLC-PK1	yes	69	50, 63
Nagata et al., 2002	Rat kidney / brain	yes	69	50, 63 / 63
Tojo et al., 1999	Rat renal cortex	yes	57	--

Models for Transport Studies

Traditional models for organic anion transport include renal slices, freshly isolated cells or tubules (Visarius et al., 1996; Groves et al., 1998; Lash, 1998), isolated perfused tubules (Newton et al., 1982), membrane vesicles (Pritchard, 1995; Sweet et al., 1997; Van Aubel et al., 2000; Burckhardt et al., 2001) and primary culture (Groves et al, 1999a; Lash, 1998). With the recent cloning of many of the transporters, the most common models utilized in organic anion transport studies currently are cell lines or oocytes expressing one or multiple transporters. These expression systems are commonly referred to as transfectants (Sugiyama et al., 2001). Human organic anion transporter transfectants include HeLa cells (Lu et al., 1999), Xenopus laevis oocytes (referred to hereafter as oocytes) (Cha et al., 2001), transformed mouse S2 PT cells (Takeda et al, 2000) and Chinese hamster ovary (CHO) cells (Cihlar and Ho, 2002). A list of the human OAT transfectants referenced in this document is provided in Table 5. Transfectants of some of the apical transporters and rOATs include LLC-PK1 cells (Sugiyama et al., 2001; Nagata et al., 2002), MDCK cells (Ilias et al., 2002, Sasaki et al., 2002) and HEK293 cells (Uchino et al., 2000). Inside-out membrane vesicles of Sf9 insect cell transfectants are utilized for the study of the multidrug resistance associated protein (MRP) efflux transporters (Van Aubel et al., 2002; Reid et al., 2003; Bodo et al., 2003; Zelcer et al., 2003).

Table 5. Human Organic Anion Transporter Expression Systems

Transporter	Expression System	Reference
hOAT1	Oocytes	Cihlar et al., 1999 Hosoyamada et al., 1999 Race et al., 1999
	CHO cells	Cihlar and Ho, 2000
	Mouse S2 PTCs	Babu et al., 2002 Jung et al., 2001 Takeda et al., 2000, 2001
	HeLa cells	Lu et al., 1999
hOAT2	Mouse S2 PTCs	Babu et al., 2002 Enomoto et al., 2002 Takeda et al., 2000, 2001
	EcR293 cells	Sun et al., 2001
hOAT3	Oocytes	Cha et al., 2001
	Mouse S2 PTCs	Babu et al., 2002 Jung et al., 2001 Takeda et al., 2000, 2001, 2002
hOAT4	Oocytes	Cha et al., 2000
	Mouse S2 PTCs	Enomoto et al., 2002

Immunohistochemical staining performed by Motohashi et al. (2002) demonstrated a wide distribution of hOAT1 in the proximal tubule. In contrast, no staining of the S1 or S3 segment was seen in rat, suggesting rOAT1 confinement to the S2 portion (Tojo et al., 1999). By confocal microscopy, however, Kojima et al., (2002) found rOAT1 in S2>>S1, S3; rOAT3 in S1, S2, S3 >> other sites along the nephron; and rOAT2 in apical membrane of the thick ascending loop (TAL) and the collecting duct (CD), but not in the proximal tubule (PT). For structure of the nephron, refer to Figure 2.4. Motohashi et al. (2002) also found the highest mRNA expression levels among the transporters (hOAT1, hOAT2, hOAT3, hOAT4 and five organic cation transporters) to be that of hOAT3 at approximately 3 x hOAT1 levels with hOAT1 levels the second highest and hOAT2 levels very low (nearly 1/20 x hOAT3). Staining for hOAT3 in renal slices was concentrated in the cortical proximal tubules with some cortical proximal tubules negative for hOAT3. No staining was seen in the proximal tubules of the medullary rays.
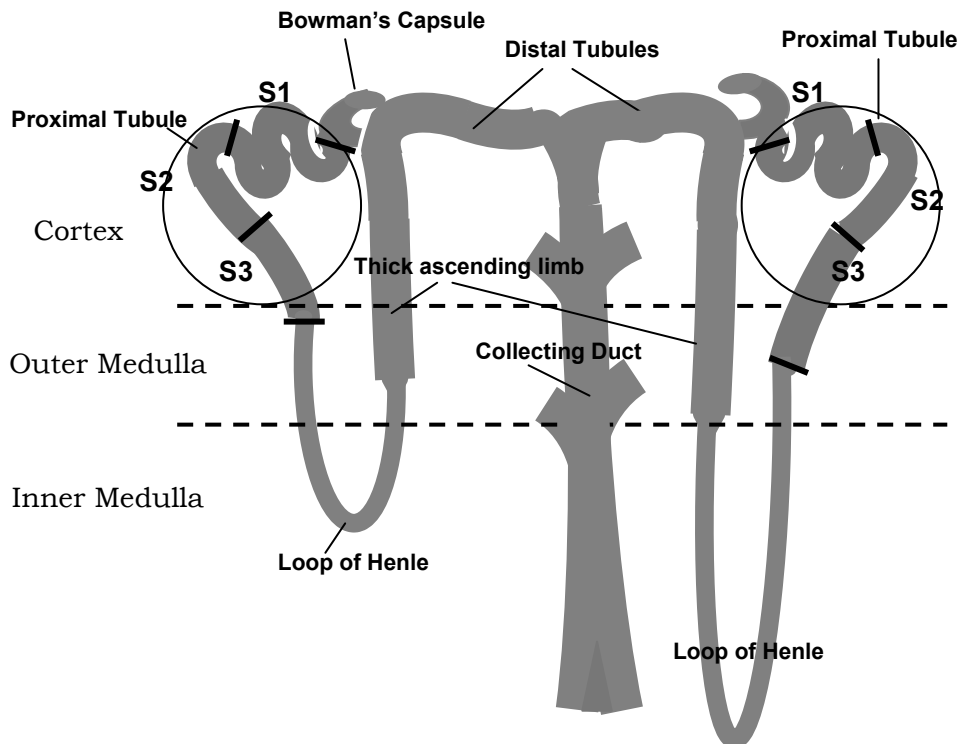
Figure 2.4. Structure of the Nephron.

Several immunohistochemical studies have demonstrated that hOAT1, rOAT1, hOAT3 and rOAT3 are localized to the BLM of the proximal tubule (Hosoyamada et al., 1999; Motohashi et al., 2002; Tojo et al.,1999; Cha et al., 2001; Hasegawa et al., 2002; Kojima et al., 2002). (Although traditionally, discussions on the OATs of the BLM have been restricted to OAT1 and OAT3 (Hosoyamada et al, 1999; Cha et al., 2001), it has recently been reported that OAT2 is also localized to the BLM of the human proximal tubule (Enomoto et al., 2002)). hOAT2 mRNA levels in the human kidney cortex are about 1/20 the levels of hOAT3 (Motohashi et al., 2002). In rat, rOAT2 has been localized to the luminal membrane of other sections of the nephron (Kojima et al., 2002) and was found by Northern blot analysis to be expressed only weakly in kidney and at much higher concentrations in the liver (Sekine et al., 1998). hOAT4 has been localized to the apical membrane (Babu et al., 2002). Therefore, discussions of the BL transporters will focus predominately on OAT1 and OAT3, but will include information on OAT2 and to a lesser extent on OAT4 where pertinent.

Two additional BL transporters of the human proximal tubule are the sulfate exchanger, SAT1, which has been shown to mediate uptake of organic anions (Burckhardt and Burckhardt, 2003) and the multidrug resistance associated protein MPR6 (Russel et al., 2002). Other possibilities include other members of the MRP family and the OATP family of transporters. MRP5, OATPA, OATPB, OATPD and OATPE are expressed in the human kidney, but distribution along the nephron has not been determined (Russel et al., 2002; Tamai et al., 2001).

OAT1 vs. OAT3

OAT1 is thought to be the classic sodium-dependent organic anion transporter also known as the PAH transporter (Van Aubel et al., 2000). It is a multispecific transporter mediating uptake of substrates against an electrochemical gradient in exchange for a dicarboxylate, such as α–ketoglutarate (αKG) (Pritchard and Miller, 1996). Organic anion

22

exchange for dicarboxylate (most commonly αKG or glutarate) has been demonstrated in several OAT1 clone expression models (Appiwattanakul et al., 1999; Lu et al., 1999; Cihlar and Ho, 2000). The mechanism of exchange is explained in the next section. Typical substrates of OAT1 are amphiphilic exhibiting a negative or partial negative charge and a domain of hydrophobicity, although some neutral hydrophobic substrates such as steroid hormones and aniline derivative analgesics are also transported by OAT1. Interaction with the transporter increases with the strength of the ionic charge and the number of hydrogen bond acceptors. Thus, in general, amphiphilic compounds with a low pK_a tend to display a high-affinity for OAT1 (Ullrich et al., 1997; Burckhardt et al., 2001).

Studying the effects of biotransformation, Ullrich and coworkers (1990) found that glucuronidation reduces or abolishes the interaction with the PAH transporter. They suggested that this might be due to the reduced hydrophobicity of the conjugates.

The prototypical substrates for OAT1 are PAH and fluorescein (FL) (Miller and Pritchard, 1997; Dantzler, 2002), with a mean K_m of 11.9 µM for PAH (Burckhardt et al., 2003b). No K_m has been reported for FL. Substrates transported by OAT1 include cAMP, cGMP, folate, indoxyl sulfate, PGE_2, many antiviral agents (acyclovir, cidofovir, zidovudine), many antibiotics (benzylpenicillin, cephaloridine, tetracycline), methotrexate, many diuretics (acetazolamide, bumetanide, ethacrynic acid, furosemide), heavy metal chelators (DMPS), nonsteroidal anti-inflammatory drugs (NSAIDs: acetylsalicylate, indomethacin, salicylate) and ochratoxin A (Burckhardt et al., 2003b).

Unlike OAT1, OAT3 demonstrates the ability to transport sulfate and glucuronide steroid conjugates. Estrone sulfate (ES) is the prototypical substrate for OAT3 with a K_m of 3.1 µM (Cha et al., 2001). OAT3 (human

and rat) also transports estradiol glucuronide (E$_2$17βG) with a K$_m$ of 8.3 μM in rat (Sugiyama et al., 2001) and dehydroepiandrosterone sulfate (DHEAS) with high-affinity. Overlap of substrate specificity between OAT1 and OAT3 is, however, common.   PAH, the prototypical substrate for OAT1, is transported by OAT3 with a K$_m$ of 87 μM (Cha et al., 2001).   The characterization of OAT3 has not been as extensive as that of OAT1. However, transport of cAMP, glutarate, methotrexate, PGE$_2$, PGF$_{2α}$, salicylate, taurocholate, urate, zidovudine, valacyclovir has been demonstrated for OAT3 (Burckhardt et al., 2003b). In contrast to OAT1, which can be trans-stimulated by preloading with PAH, OAT3 (rat and human) could not be trans-stimulated with preloaded ES (or PAH in rat) (human - Cha et al., 2001; rat - Kusuhara et al., 1999). Sweet et al. (2003), however, have demonstrated rOAT3-mediated trans-stimulated uptake of ES and PAH by glutarate in rOAT3 expressing oocytes. Finally, OAT3 is thought to mediate the BL step of the reabsorption of urate in humans (Koepsell and Endou, 2003).

Probenecid is the prototypical inhibitor of both OAT3 and OAT1 with slightly lower inhibition constant for OAT3-mediated ES transport than OAT1-mediated PAH transport (K$_i$ = 9 μM and 12 μM, respectively) (Takeda et al., 2001). Sensitivity to the inhibitory effects of probenecid, however, may be determined equally by the substrate. Takeda and colleagues (2002) found that hOAT1-mediated transport of acyclovir (ACV) was only weakly inhibited by probenecid (~20% inhibition) vs. strong inhibition (~80-90%) of hOAT1-mediated PAH transport by probenecid reported in earlier studies (Takeda et al., 2001). They speculate that this difference may be attributed to the difference in substrate affinity. In the 2001 study, Takeda et al. determined the K$_m$ for PAH vs. ACV to be 20.1 and 342.3 μM, respectively. Other inhibitors include substrates for both OAT1 as well as OAT3, thereby making it difficult to distinguish OAT1 vs. OAT3 transport solely based on inhibition studies. The literature reports for inhibitors are often conflicting.

For example, cimetidine has been considered a substrate and specific inhibitor of OAT3 (Cha et al., 2001; Nagata et al., 2002). However, cimetidine inhibited hOAT1-mediated uptake in a mouse PTC transfectant model (Jung et al., 2001) and was found to be transported with low-affinity by hOAT1 and flounder fOAT1 (Burckhardt et al, 2003a). In contrast, cimetidine was found to have no effect on PAH transport by rOAT1 in LLC-PK1 cells (Nagata et al, 2002). Likewise, reports of the effects of indomethacin as a specific inhibitor of OAT1 are at odds. In contrast to the studies by Kusuhara et al. (1999) and Deguchi et al. (2002), who found indomethacin had no effect on uptake of ES or indoxyl sulfate by OAT3, Feng et al. (2001) reported indomethacin caused inhibition of OAT3-mediated cimetidine uptake. Thus, inhibition of substrate transport is determined by both the inhibitor and the substrate for each transporter.

OAT2

PAH and αKG transport by hOAT2 has been reported by Sun et al. (2001). In this study, however, they were unable to demonstrate inhibition of hOAT2-mediated uptake of PAH by αKG. They found no hOAT2-mediated transport of DHEAS or salicylate. Interestingly, in studies of rOAT2 expressing oocytes, salicylate has been used as the model substrate (Sekine et al., 1998). A lower affinity of probenecid for hOAT2 vs. hOAT1 or hOAT3 has been demonstrated (K_i = 766 μM) (Enomoto et al., 2002).

SAT1

The sulfate-anion antiporter 1 (SAT1) is responsible for the sodium-dependent uptake of sulfate from the BLM into the PTC. Substrates include sulfated steroid hormones and some bile acids (Ullrich et al., 1990). Probenecid, several antibiotics, diuretics and NSAIDs were inhibitory. PAH did not inhibit SAT1-mediated sulfate uptake (Ullrich et al., 1990).

Little is known regarding substrates for MRP6. Initial studies demonstrated a lack of transport of the typical substrates of the MRP family, such as $E_2 17\beta G$ and LTC_4 (Russel et al., 2002). Subsequent studies, however, showed transport of LTC_4, the glutathione conjugate of N-ethylmaleimide and at a very low rate, $E_2 17\beta G$ (Ilias et al., 2002). Mutation of MRP6 has been associated with pseudoxanthoma elasticum, a connective tissue disorder (Ilias et al., 2002). MRP6 is a primary active transporter in that it is ATP-dependent (Ilias et al., 2002).

Transport Mechanisms at the Basolateral Membrane

Uptake of organic anions across the BLM is an uphill process, requiring the translocation of a negatively charged molecule into a negatively charged environment with the ability to create an intracellular > extracellular concentration gradient. Therefore, the process cannot involve a simple facilitator mechanism without some component of energy input, thereby being dependent upon an active process or an exchange with a solute moving down its electrochemical gradient. It has been demonstrated that OAT1 is an organic anion/dicarboxylate exchanger and is indirectly coupled to the basolaterally-distributed Na^+/K^+ ATP-ase (Shimada et al., 1987; Pritchard, 1988). Uptake by OAT1 is thus a tertiary active process, dependent on a dicarboxylate-gradient established by co-transport of Na^+ and dicarboxylate, a secondary active process, which is in-turn, dependent upon the Na^+-gradient established by the primary active Na^+/K^+ ATP-ase (see Figure 2.5, page 33.)

Recently, OAT3 has also been shown to function in like manner to OAT1 in oocytes coexpressed with rOAT3 and the Na^+-dicarboxylate co-transporter, rb-NaDC-1 (Sweet et al., 2003). Past studies however, have indicated that OAT3 function is independent of the Na^+ gradient, and the authors (Sweet

et al., 2003) have stressed the importance of a reevaluation of the respective roles of OAT1 vs. OAT3. The authors additionally speculate that since OAT2 is known to transport dicarboxylates, it too may utilize the same mechanism, thereby rendering the BLM OATs indistinguishable based solely on energetics.

SAT1 functions as an antiporter and is sodium-dependent (Russel et al., 2002). MRP6 is likely a primary active transporter utilizing the energy of ATP hydrolysis (Ilias et al., 2002).

The Apical Transporters

Because transepithelial transport and net intracellular accumulation are dependent upon both BL uptake and A efflux, the apical transporters will be included in this discussion where appropriate.

The only member of the OAT family to be localized to the apical/brush border membrane (BBM) in human is OAT4 (Babu et al., 2002). However, there are other important organic anion transporters not belonging to the OAT family that are resident in the BBM. Apical transporters known to mediate transport of organic anions in the human PTC include MRP2, MRP4, NPT1 and URAT1. It is also possible that a member of the OATP family is located in the BBM.

OAT4

When expressed in Xenopus laevis oocytes, hOAT4-mediated high-affinity transport of ES (K_m = 1.01 µM) and DHEAS (K_m = 0.63 µM) and prostaglandins PGE_2 and $PGF_{2\alpha}$ in a sodium independent manner (Cha et al., 2000). In the study, no inhibitory effects on hOAT4-mediated transport of ES were seen with glucuronide conjugates, including both AG and $E_2 17\beta G$. As a class, glucuronide conjugates showed little or no inhibitory effect on hOAT4 (Cha et al., 2000). OAT4 transport is bidirectional and is thought to physiologically function in the reabsorption of prostaglandins and

organic anions and in the secretion of organic anions (Koepsell et al., 2003). Probenecid was demonstrated to strongly inhibit hOAT4-mediated translocation of ochratoxin A with a K_i of 44.4 μM (Babu et al., 2002). PAH and glutarate showed no inhibitory effect on hOAT4-mediated transport (Cha et al., 2000).

MRP2

Multidrug resistance associated protein 2 (MRP2) has been termed the apical conjugate export pump (Keppler et al., 2000). MRP2 is a primary active pump utilizing the energy derived from the hydrolysis of ATP to mediate efflux of substrates into the glomerular filtrate. It is localized to the BBM in PTCs and to the canalicular membrane of hepatocytes. Substrates of MRP2 include conjugated and unconjugated organic anions such as glutathione conjugates, glucuronide conjugates, leukotrienes, methotrexate, ochratoxin A and PAH (Konig et al., 1999). The K_m for $E_2 17\beta G$ is 7.2 μM (Konig et al., 1999) vs. 880 μM for PAH (Leier et al., 2000). Van Aubel and colleagues reported a Km of 1.9 mM and a Vmax of 187 pmol·mg^{-1}·min^{-1} for rabbit MRP2 PAH transport and a stimulatory rather than inhibitory effect of α-naphthyl-β-D-glucuronide on PAH transport. DHEAS and ES were determined *not* to be substrates for MRP2 (Sasaki et al., 2002). Rather, Sasaki and coworkers found that ES stimulated MRP2-mediated transport.

The hepatobiliary disposition of AG and acetaminophen sulfate (AS) were studied in isolated perfused livers of MRP2-deficient rats (Xiong et al., 2000). Xiong and colleagues found that AG and AS biliary excretion was decreased to 0.3% and 20% of control, respectively, with overall bile flow decreased to 25% of control, in MRP2-deficient rats. They also found a 7-fold increase in the BL efflux of AG, consistent with an upregulation in BL transporters to compensate for the deficiency of MRP2. Probenecid, furosemide, indomethacin, and several conjugated bile acids stimulated

MRP2-mediated transport of $E_2$17βG in inside-out membrane vesicles expressing human MRP2 (Bodo et al., 2003b). Bodo et al. determined that there is an allosteric stimulation by bile acids of MRP2 co-transport of bile acids and glucuronide conjugates. In contrast, Ilias et al. (2002) demonstrated 78% inhibition of MRP2-mediated transport of the glutathione conjugate of N-ethylmaleimide by probenecid in the insect membrane-vesicle transfectant model.

MRP4

MRP4 is a novel multidrug resistant protein reported by Van Aubel and colleagues (2002) to be localized to the BBM of human PTCs. This probenecid sensitive, ATP-dependent efflux pump has been shown to transport cAMP, cGMP, antiviral nucleoside analogues (Van Aubel et al., 2002), PGE_1 and PGE_2 with high-affinity (Reid et al., 2003). Furthermore, Thromboxane B2, several other prostaglandins and several NSAIDs were potent inhibitors (and possibly substrates) of MRP4-mediated transport (Reid et al., 2003). Van Aubel and coworkers (2002) found that $E_2$17βG is a low-affinity substrate for MRP4 and based on inhibition studies, propose that the other glucuronides tested (α-naphthyl-β-D-glucuronide and p-nitro-phenyl-β-D-glucuronide) are also substrates. The MRP4 transporter has since been identified in several other tissues including liver where it is localized to the sinusoidal membrane (BL) and has been shown to mediate high-affinity transport of DHEAS (Zelcer et al., 2003).

NPT1

The human type I sodium-dependent inorganic phosphate transporter, NPT1, originally thought to function primarily in the reabsorption of phosphate from the glomerular filtrate, has since been determined to transport organic anions. Uchino et al. (2000) have determined that NPT1 transports organic anions such as PAH and $E_2$17βG in a Cl⁻-sensitive

manner, demonstrating decreased uptake (influx) of PAH with increasing extracellular Cl$^-$ levels. In the same study, increasing concentrations of extracellular Cl$^-$ had no effect on efflux of preloaded PAH via NPT1. NPT1 is thought, therefore, to function in the efflux of organic anions into the glomerular filtrate (Uchino et al., 2000). The NPT1 K_m for PAH is 2.66 mM and NPT1-mediated transport is strongly inhibited by probenecid (Uchino et al., 2000). It is thought that NPT1 may represent the voltage-dependent PAH transporter or anion exchange mechanism for PAH at the apical membrane (Russel et al., 2002).

URAT1

URAT1 is the apical transporter responsible for the reabsorption of urate in the human kidney. It functions as a sodium-independent exchanger with Cl$^-$ or with organic anions (Koepsell and Endou, 2003). Urate uptake by URAT1 (K_m = 371 µM) is trans-stimulated to a higher degree by organic anions than by Cl$^-$ and was determined not to be driven by membrane potential (Enomoto et al., 2002b). PAH, however, showed no cis-inhibitory or trans-stimulatory effect on urate uptake. ES caused a cis-stimulatory effect on 1-hour urate uptake, but no data were given for the trans effect of ES on URAT1-mediated uptake. No trans-stimulation was demonstrated by αKG. Agents known to cause in vivo uricosuric effects, i.e., reduce hyperuricemia, such as probenecid, NSAIDs (salicylate and indomethacin) and diuretic drugs, showed cis-inhibition but no trans-stimulation of urate uptake. Agents known to cause hyperuricemia, such as the anti-tuberculosis agent, pyrazinamide and to a greater extent, its aromatic monocarboxylate metabolite pyrazinecarboxylic acid (PZA), both cis-inhibited and trans-stimulated uptake of urate by URAT1. Aliphatic monocarboxylates, such as lactate, also cis-inhibited/trans-stimulated urate uptake, but to a lesser extent (Enomoto et al., 2002b).

OATP

Unlike the OATs, there appears to be no one-to-one orthology of the OATPs between rodents and human. In rat, Oatp1 is resident in the BBM of the pars recta (Bergwerk et al., 1996) and Oatp2, an isoform of human OATPA, is localized to the BLM (Gao et al., 2000) and to the apical membrane (Sugiyama et al., 2002) of brain capillary endothelial cells. The OATPs in the human liver are localized to the BLM. In the human kidney, mRNA for OATPA, OATPB, OATPD and OATPE has been detected (Hagenbuch and Meier, 2003). OATPD and OATPE both contain a carboxy-terminus consensus sequence that is typically associated with localization to the apical membrane (Russel et al., 2002). Thus, the possibility of OATP(s) present in human PTCs exists and localization could be apical, BL or both. In rat, Oatp2 is thought to be responsible for the efflux transport of glucuronides across the blood-brain barrier (BBB) (Sugiyama et al., 2001). Sugiyama and coworkers (2001) found Oatp2 to be responsible for 40% of the efflux of $E_2 17\beta G$ across the BBB. In a later study, it was determined that Oatp2 has at least two substrate recognition sites and that $E_2 17\beta G$ stimulated the Oatp2-mediated transport of taurocholate but inhibited transport of digoxin (Sugiyama et al., 2002). OATP substrates are mainly high molecular weight amphipathic molecules that are normally bound to protein (albumin) and the transporters are thought to be organic anion exchangers (Hagenbuch and Meier, 2003). Of the 7 human OATP transporters listed in a substrate specificity table by Van Montfoort et al. (2003), 4 of 5 tested transported DHEAS, 5 of 7 transported $E_2 17\beta G$ and all 7 transported ES. The affinities for these substrates were very high. PAH was only tested for one transporter (OATPA) and was found not to be a substrate.

Mechanisms of the Apical Transporters

 Mechanisms of the apical transporters are discussed above, beginning on page 27, under the sections for each transporter. Briefly, the mechanism of OAT4-mediated efflux is unknown; MRP2 and MRP4 function as primary active transporters, utilizing the energy of ATP; the mechanism for NPT1 function is uncertain, but is thought to function in the secretion of organic anion (OA^-) in a Cl^--sensitive manner; and URAT1 functions as an OA^- (urate and others) exchanger with Cl^- or organic anions (Figure 2.5).

Basolateral
Peritubular Fluid

Luminal
Glomerular Filtrate

0mV   -5mV

-60mV

K$^+$ ATPase

Na$^+$ Na$^+$

α-KG   α-KG

OAT1/OAT3   OA$^-$

OA$^-$?   OA$^-$

SO$_4^-$ SAT1

A$^-$/OA$^-$

urate   URAT1
OA$^-$/Cl$^-$

OA$^-$ ATP   MRP2/MRP4
ADP

OA$^-$ OATP ?

OA$^-$ OAT4

Cl$^-$ Cl$^-$ NPT1

OA$^-$
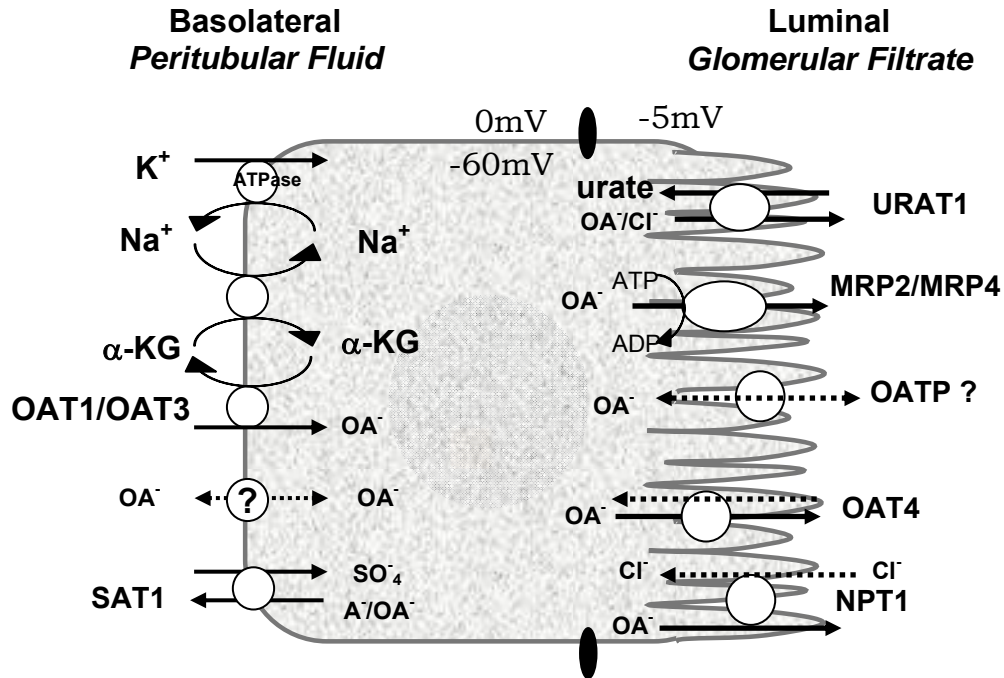
Figure 2.5. Basolateral and Apical Organic Anion Transporters of the Human Proximal Tubule. The BL organic anion transporters known to be present in the human PTC are OAT1, OAT3 and SAT1. OAT1, and possibly OAT3, functions as a tertiary active protein, mediating exchange of dicarboxylate for OA$^-$ in a Na$^+$-dependent manner. SAT1 is a SO$_4^-$ exchanger, responsible for efflux of OA$^-$ and uptake of SO$_4^-$ and several SO$_4^-$ conjugates. The apical transporters, responsible for efflux or organic anions, include OAT4, URAT1, MRP2, MRP4 and NPT1. URAT1 functions as an exchanger, mediating reabsorption of uric acid (or OA$^-$) with efflux of OA$^-$. MRP2 and MRP4 are primary active proteins utilizing the energy of ATP for efflux of OA$^-$. The mechanism of NPT1 is uncertain, however, it is known to mediate efflux or OA$^-$ in a Cl$^-$-sensitive manner. The mechanism of OAT4 is unknown. Other possible transporters resident in both the BBM and BLM include both OATP and MRP proteins.

<u>Organic Anion Transporter Substrates and Regulation</u>

According to Dantzler (2002), during the secretory process as studied in perfused tubules (both mammalian and non-mammalian), the steady-state concentration of organic anion inside the cells is greater than that in the tubule lumen, which is greater than that in the peritubular fluid (bathing medium). This is consistent with the observation that the BBM (luminal) has a higher apparent permeability to PAH than does the BLM and that transport into the cell across the BLM is the rate limiting step (Dantzler, 2002). This is, however, not always the case. According to Terlouw et al. (2003), efflux of anions at the BBM, in general, is less efficient than BL uptake, resulting in intracellular accumulation. This has been demonstrated for many of the antiviral drugs for which efflux at the BBM is rate limiting resulting in intracellular accumulation (Russel et al., 2002). Thus, relative membrane contributions to the rate of secretion vary depending on the substrate.

Very little is known about the renal transport of glucuronides. Efficient tubular secretion of glucuronides is well established. Apical transporters that have been identified as transporters of glucuronides include MRP2, MRP4 and NPT1. OAT4 does not transport glucuronides and no data exist regarding URAT1 affinity for glucuronides. In hepatocytes, Sallustio et al. (2000) report that concentration gradients of 1:50:5,000 in the circulation, hepatocytes and bile, respectively are found for acyl-glucuronides. MRP2 is considered to be the major conjugate efflux pump in the liver responsible for excretion of glucuronides into the bile. Transport of $E_2 17\beta G$ in oocytes expressing human renal OAT3 (Cha et al., 2001) is the only report of glucuronide uptake by a BLM transporter. As a class, glucuronides have not been investigated in carrier specific uptake at the BLM.

A list of the BL and A transporters in the kidney and their substrate specificity are given in Table 6. The properties and substrate specificities listed are not intended to be all inclusive, but to cover the basic characteristics and prototypical substrates for the transporters and/or those substrates utilized for this project.

Table 6. Substrates and Inhibitors of Renal Organic Anion Transporters				
Transporter	**Species**	**Substrate (K_m)**	**Inhibitors (K_i)**	**Reference**
OAT1 (BL)	Human	PAH (11.9µM), FL αKG, Glutarate	Probenecid (12µM)	Burckhardt et al., 2003b
Oat1 (BL)	Rat	PAH (14µM, 70 µM)	Probenecid	Russel, 2002
Oat1 (BL)	Mouse	PAH, ~~ES~~ ~~Taurocholate~~	Probenecid	Sweet et al., 2002
OAT2 (BL)	Human	PAH, αKG ~~DHEAS~~	Probenecid[2] (766µM)	Sun et al., 2000 Enomoto[2] et al, 2002
OAT3 (BL)	Human	PAH (87µM), FL ES (3µM), $E_2$17βG DHEAS	Probenecid (9µM) ~~Ouabain[4]~~	Cha et al.[1], 2001
OAT3 (BL)	Rat	PAH, ES $E_2$17βG (8.43µM)	Probenecid	Sugiyama et al, 2001
Oat3 (BL)	Mouse	PAH, ES Taurocholate	Probenecid	Sweet et al., 2002
OAT4 (A)	Human	DHEAS (0.63µM) ES (1.3 µM)	BSP, Probenecid ~~Glucuronide Conj~~ ~~$E_2$17βG~~, ~~AG~~, ~~PAH~~	Cha et al., 2000
NPT1 (A)	Human	PAH (2.66 mM) $E_2$17βG urate	Probenecid	Uchino et al., 2000
MRP2 (A)	Human	$E_2$17βG[2] (7 µM) PAH[3] (880 µM) ~~ES[4]~~ ~~DHEAS[4]~~	(Probenecid[1], and ES[4] **stimulate** transport)	Bodo et al.[1], 2003b Konig et al.[2], 1999 Leier et al.[3], 2000 Sasaki et al.[4], 2002
MRP2 (A)	Rat (hepatic)	AG[1]		Xiong et al.[1]., 2000
MRP4 (A in PTC, BL in hepatocytes)	Human	DHEAS[3] (2µM) $E_2$17βG[2,3]	Probenecid[1] Glucuronides[2] NSAIDs[2]	Reid et al.[1], 2003 Van Aubel[2] et al., 2002 Zelcer[3] et al., 2003
Oatp1	Rat	$E_2$17βG (2.58 µM)	Probenecid ~~PAH~~	Sugiyama et al., 2001
Oatp2	Rat	$E_2$17βG (17 µM)	Probenecid ~~PAH~~	Sugiyama et al., 2001
OATP-A (BL in brain)	mRNA in human kidney	$E_2$17βG, ~~PAH~~ ES (59 µM) DHEAS (7 µM)		Hagenbuch et al., 2003 Tirona et al., 2002 V Montfoort et al, 2003
OATP-B (BL in liver)	"	ES (6 µM) DHEAS ~~Glucuronides~~		Tamai et al.[2], 2001 Tirona et al., 2002
OATP-D	"	ES		Hagenbuch et al, 2003
OATP-E	"	ES $E_2$17βG		Hagenbuch et al., 2003 Tirona et al., 2002
SAT1(BL)	human	sulfates	Probenecid	Burckhardt and Burckhardt (2003)

This table is not designed to be all-inclusive, but to list those substances utilized in transport studies for this project. Strikethrough (e.g. ~~PAH~~) indicates the agent was *not* transported by or did *not* inhibit the transporter.

AG Transport

Acetaminophen glucuronide
MW = 349.3
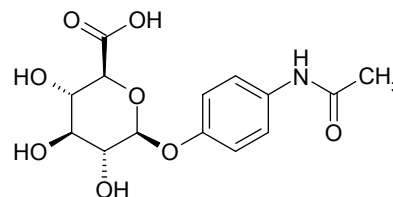
Acetaminophen glucuronide (AG) binding to plasma proteins in human is low (<10%) such that AG is freely filtered at the glomerulus (Morris and Levy, 1984). In early studies of acetaminophen (APAP) metabolism in humans, Prescott (1980) demonstrated that at therapeutic doses of APAP, renal clearances of AG and acetaminophen sulfate (AS) often exceeded the rate of glomerular filtration and that the respective percentage of APAP metabolite excretion in the urine was 55 and 40%. In contrast, the renal clearance of AG on average was found not to exceed that of creatinine 1-3 hours after an oral dose of APAP in human as determined by Morris and Levy (1984). In a study of renal tubular transport of APAP and its conjugates in the dog, Duggin and Mudge (1975) found that at low plasma concentrations, AG is secreted by an active transport process, whereas at high concentrations, it is reabsorbed. They also found that net renal tubular secretion of AS but *not* AG was inhibited by probenecid. The hepatobiliary disposition of AG and AS was studied in isolated perfused livers of MRP2-deficient rats (Xiong et al., 2000). In the MRP2-deficient rats, Xiong and colleagues found that biliary excretion of AG and AS was decreased to 0.3% and 20% of control, respectively, with an overall decrease in bile flow by 25% of control. They also found a 7-fold increase in the BL efflux of AG which they hypothesized may be attributed to upregulation of MRP3 as demonstrated in multiple studies of MRP2-deficient models as well as the work of Hirohashi et al. (1999) that demonstrated transport of multiple glucuronide conjugates by MRP3.

DHEAS Transport

Dehydroepiandrosterone sulfate
MW = 390.5
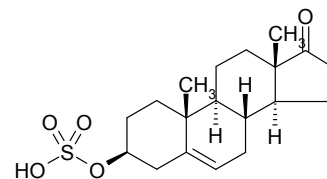
Dehydroepiandrosterone sulfate (DHEAS) is the most abundant steroid hormone in the human circulation. It is synthesized by the adrenal gland. DHEAS is a high-affinity substrate for hOAT4 (K_m = 0.63 µM, Cha et al., 2000). Transport by hOAT3 was also demonstrated. Although the K_m was not reported for hOAT3, high uptake by hOAT3-expressing oocytes was indicated (Cha et al., 2001). No data were given as to the affinity of DHEAS for OAT1. DHEAS is not a substrate for MRP2 (Sasaki et al., 2002) but is a high-affinity substrate for MRP4 (K_m = 2 µM, Zelcer et al., 2003). Four of 5 human OATPs tested transported DHEAS (Van Montfoort et al., 2003).

E$_2$17βG Transport

Estradiol 17β-glucuronide
MW = 470.5
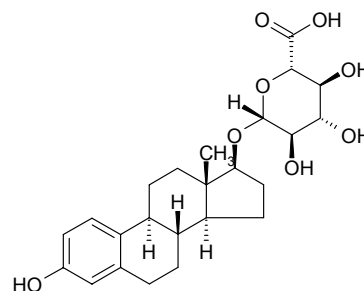
Estradiol glucuronide (E$_2$17βG) hOAT3-mediated transport in oocytes was reported by Cha et al. (2001). In earlier studies, (2000), Cha and coworkers found no inhibitory effects on hOAT4-mediated transport by E$_2$17βG. Sugiyama et al. (2001) found that E$_2$17βG efflux from the brain was mediated by Oatp2 (40%) and by OAT3 (20%). MPR2 (K_m = 7 µM; Konig et al., 1999) , MPR3 (Bodo et al., 2003b) and MRP4 (low-affinity; Van Aubel et al., 2002) all transport E$_2$17βG. Transport of E$_2$17βG by MRP3 in LLC-PK1 cells was inhibited by methylumbelliferone glucuronide but stimulated by methyl-umbelliferone sulfate (Hirohashi et al., 1999).   Stimulation rather than inhibition of transport of E$_2$17βG also resulted from coincubation with probenecid, indomethacin, furosemide and several conjugated bile acids mediated by human MRP2 expressed in insect cell line inside-out

membrane vesicles (Bodo et al., 2003b). In contrast, Bodo and colleagues found inhibition of MRP3-mediated transport by these same substances. In hepatocytes, $E_2$17βG causes a rapid inhibition of bile flow (85% inhibition within 10 min) coinciding with retrieval of MRP2 into intracellular sites (Mottino et al., 2002, 2003). $E_2$17βG is also a substrate for NPT1 (Uchino et al., 2000). Five of 7 human OATPs tested transported $E_2$17βG (Van Montfoort et al., 2003).   Thus, $E_2$17βG is a substrate for multiple transporters including OAT3 (BL) and MRP2, MRP4 and NPT1 (A) present in human renal PTCs and has been shown to affect regulation of MRP2.

ES Transport

Estrone-3-sulfate
MW = 372.4
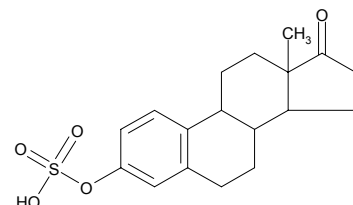
Estrone sulfate (ES) is the prototypical substrate for OAT3 and OAT4 (Cha et al., 2001, 2000). Cha and colleagues demonstrated a K_m of 3.1 µM and 1.01 µM for ES transport mediated by hOAT3 and hOAT4, respectively. Unlike the ability of PAH to trans-stimulate transport of PAH by hOAT1 (Sweet and Pritchard, 1997), neither hOAT3 nor hOAT4 transport of ES was trans-stimulated by ES (Cha et al., 2000, 2001).   Experiments in mouse renal cortical slices indicate that OAT3 is not the only BL transporter responsible for ES uptake (Sweet et al., 2002).   In URAT1-expressing oocytes, ES cis-stimulated uptake of urate in exchange for Cl^- by URAT1 (Enomoto et al., 2002b).   ES and DHEAS were determined *not* to be substrates for MRP2 (Sasaki et al., 2002). Rather, Sasaki and coworkers found that ES stimulated transport of substrate mediated by MRP2. ES was found to have no inhibitory effect on rOAT1-mediated transport of PAH (Sweet et al, 2002.) Finally, all 7 of the human OATPs tested transported ES (Van Montfoort et al., 2003).   Thus, ES is transported into the cell by multiple transporters at the BLM, is effluxed at the BBM by OAT4 and stimulates efflux at the BBM mediated by URAT1 and MRP2.

MUG

Methylumbelliferyl glucuronide
MW = 352.3
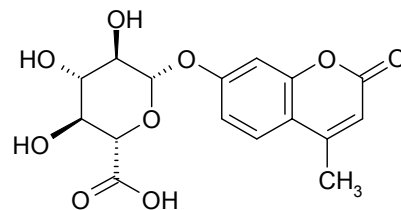
Methylumbelliferyl glucuronide (MUG) is a
low molecular weight glucuronide. Little is found in the literature as to its
transport properties, however, it has been used to investigate the inhibitory
properties of glucuronide transport. Transport of $E_2 17\beta G$ by MRP3 in LLC-
PK1 cells was inhibited by methylumbelliferone[f] glucuronide but stimulated
by methyumbelliferone sulfate (Hirohashi et al., 1999). MUG showed no
inhibitory effect on hOAT4-mediated transport (Cha et al., 2000).

PAH Transport

p-aminohippurate
MW = 194.2
pK_a = 3.2
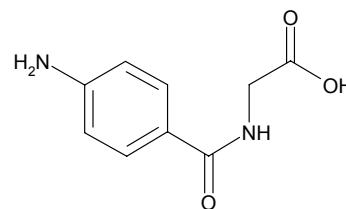
PAH is the prototypical substrate for OAT1 (K_m = 11.9 μM; Burckhardt et al.,
2003b). It is also transported on the BLM of the PTC by OAT3 (K_m =
87 μM; Cha et al., 2001). The apparent permeabilities of the BLM and the
BBM to PAH have been measured in several species with the BBM (apical)
permeability always greater than the BLM (Dantzler, 2002). Pritchard
(1988) determined that PAH uptake is coupled to dicarboxylate (αKG)
efflux, and later studies demonstrated trans-stimulation can also be
achieved with PAH itself. Trans-stimulation of PAH with αKG results from
an increase in the Vmax with little change in the Km (Dantzler, 2002). In
human BBM vesicles, voltage-driven PAH transport and αKG/PAH
exchange were demonstrated (Burckhardt et al., 2001). PAH had no cis-
inhibitory or trans-stimulatory effect on the uptake of urate by URAT1-

[f] Methylumbelliferone glucuronide could not be found in any chemical databanks as is thus thought to be methylumbelliferyl
glucuronide (MUG). MUG is the conjugate of 4-methylumbelliferone and glucuronic acid.

expressing oocytes (Enomoto et al., 2002b) and was found to have no effect on hOAT4-mediated transport (Cha et al., 2000). PAH is a low-affinity substrate for both MRP2 (K_m = 880 µM, Leier et al., 2000) and NPT1 (K_m = 2.66 mM, Uchino et al., 2000). PAH affinity for the OATPs has only been reported for one human OATP transporter: PAH was found not to be a substrate for OATPA (Van Montfoort et al., 2003). PAH is not transported by rOATP1 nor rOATP2 (Sugiyama et al., 2001).

Probenecid, the Transport Inhibitor

Probenecid
MW = 285.4
pKa 3.4
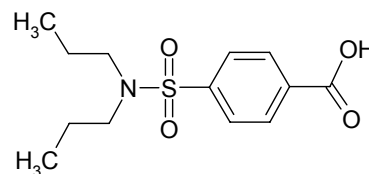
Probenecid is a highly lipid-soluble derivative of benzoic acid. It was originally discovered during the search for a drug to depress the renal excretion of penicillin (Goodman and Gillman, 1990). Probenecid is secreted by the proximal tubule but is almost completely reabsorbed by back diffusion along the nephron unless the urine is alkaline (Goodman and Gillman, 1990). Probenecid inhibits, but is not a substrate for OAT1. It is also an inhibitor of OAT3, URAT1, NPT1, MRP4 and the OATP transporters. Refer to Table 6 for K_i values for the specific inhibitors. Probenecid acts as a uricosuric agent by inhibiting the reabsorption of urate by URAT1 (Enomoto et al., 2000b). In stop-flow studies of isolated canine proximal tubules, probenecid had no effect on AG net tubular secretion (Duggin and Mudge,1975). In the liver, probenecid and ouabain stimulate bile flow (Dickinson et al., 1979). Consistent with this finding, Bodo et al. (2003b) demonstrated that, in transport of $E_2$17βG, probenecid inhibits MRP3, the BL export transporter in hepatocytes, whereas probenecid stimulates MRP2, the canalicular (apical) export transporter in hepatocytes. Finally, probenecid also inhibits the formation of glucuronide conjugates (Savina et al., 1992).

<u>Regulation</u>

Both OAT1 and OAT3-mediated uptake are inversely proportional to protein kinase C (PKC) activity (Terlouw et al., 2003; Lu et al, 1999) and directly proportional to cAMP signaling. Transporter activity has also been shown to be acutely stimulated by epidermal growth factor (EGF) and the mitogen activated protein kinase (MEK/ERK) pathway (Sauvant et al., 2001). EGF can acutely upregulate OAT3 activity via the extracellular MEK signaling pathway. Induction of transporter expression (OAT1) can be affected by a 24 hour pretreatment with 5 mM sodium butyrate (Nagata et al., 2002; Sugiyama et al., 2001).

Regulation for MRP2 is more thoroughly characterized than are the OATs. MRP2 activity and expression are regulated at three levels: 1. endocytic retrieval/exocytic insertion (occurs within min); 2. translational regulation (within several hours); 3. transcriptional regulation (within days) (Gerk and Vore, 2002). Rapid retrieval and retargeting of MRP2 to the BLM in hepatocytes in response to activation by PKC was reported to occur within 30 min as detected by immunoreactive MRP2 (Kubitz et al., 2001). Insertion of MRP2 into the canalicular membrane of rat hepatocytes has been demonstrated by stimulation with cAMP, resulting in a 3-fold increase in MRP2 within min (Kipp et al., 2001). Insertion and retrieval of MRP2 also occurs in response to hypo- and hyperosmolarity, respectively (Kubitz et al., 1997; Schmitt et al., 2001). Also in hepatocytes, $E_2 17\beta G$ causes a rapid inhibition of bile flow (85% inhibition within 10 min) coinciding with retrieval of MRP2 into intracellular sites (Mottino et al., 2002, 2003).

HK-2 Cell Model

HK-2 Cells

The HK-2 cells used for this project were purchased from American Type Culture Collection (ATCC). The literature provided with the cells recommended culturing the cells in Keratinocyte Serum Free Media (KSFM) supplemented with 5 ng/ml epidermal growth factor (EGF) and 40 µg/ml bovine pituitary extract. Normal adult male proximal tubule cells were immortalized by transfection with human papilloma virus 16 (HPV-16) E6/E7 proteins and were reported to retain phenotypic and functional characteristics of well differentiated proximal tubule cells (Ryan et al., 1994). Cells retain Na^+-dependent glucose transport and parathyroid responsive, antidiuretic hormone unresponsive hormone sensitivies. Several investigators report successful use of different types of media used for the culture of HK-2 cells, including Dulbecco's Modified Eagle Medium (DMEM)/Ham's F12 with supplements, and Roswell Park Memorial Institute (RPMI) Defined Media. Additionally, many investigators supplement culture media with 2 to 10% fetal bovine serum (FBS).

HK-2 Cells and Transport

HK-2 cells have been used in transport studies of riboflavin (Kumar et al., 1998) and to study the function of the P-glycoprotein pump, MDR1, which is expressed in the BBM of HK-2 cells (Romiti et al., 2002). Studies of extracellular glutathione peroxidase have demonstrated polarization of HK-2 cells on permeable membranes (Whitin et al., 2002). In this study, the membrane resistance was measured and determined to be 100 Ohms. Whitin and colleagues plated Transwell membranes coated with human placental collagen Type IV at a seeding density of 3.0×10^5 cells/cm^2 and used fluorescein-labeled dextran to determine paracelluar diffusion.

CHAPTER III

Methods

<u>Cell Culture</u>

<u>Materials</u>

HK-2 human kidney, proximal tubule cells, transformed (ATCC, CRL-2190)

Keratinocyte Serum Free Media (KSFM, Invitrogen Lifetechnologies, 17005-042)

Fetal Bovine Serum, 100 ml, heat inactivated (Invitrogen Lifetechnologies, 10082139)

Trypsin-EDTA (0.25% Trypsin, 1mM EDTA.4Na) (Invitrogen Lifetechnologies, 25200)

Collagen Type IV from human placenta (Sigma, C-5533)

Collagen Type I from rat tail (Sigma, C-7661)

Costar Brand Transwell-Clear Inserts, No. 3450 (Fisher Scientific,07-200-170)

Millipore Millicell Culture plate inserts (Fisher Scientific, PIHP 030-50)

Corning Brand Culture Flasks, T25 (Fisher Scientific, 10-126-28)

Corning Brand Culture Flasks, T75 (Fisher Scientific, 10-126-37)

Falcon polystyrene 35 mm dishes (Fisher Scientific, 08-722A)

Wheaton Cryule Vial (Cryovials) (Fisher Scientific, 03-341-18N)

Nalgene Cryogenic Controlled-Rate Freezing Container (Fisher Scientific, 15-350-50)

<u>Equipment</u>

IEC PR-7000M centrifuge, rotor 966, International Equipment Company

Steril®GARD II Class II Type A/B3 Biosafety Cabinet, The Baker Company

Nuaire US Autoflow CO_2 water-jacketed incubator

Zeiss Axiovert25 phase contrast microscope

Cultureware and Media

HK-2 cells purchased from American Type Culture Collection (ATCC, Manassas, VA), were cultured in T25 and T75 tissue culture flasks or on 35 mm culture plates. Cells used for transport studies were grown on 30 mm Millicell-PCF Millipore Millicell© Culture Plate Inserts (early studies) or 24 mm Costar® Transwell-Clear polyester tissue culture-treated, microporous membranes. Culture media consisted of keratinocyte serum-free media (GIBCO/Invitrogen) containing 5 ng/ml human epidermal growth factor and 40 µg/ml bovine pituitary extract as recommended by ATCC and supplemented with 2% fetal bovine serum. Antibiotics (50 µg/ml streptomycin and 48 U penicillin) were added to the culture media during subculturing only. For transport studies and when indicated, inserts were treated with 0.025 mg/insert Type IV human placental collagen (Sigma C-5533) prepared in 0.5 M glacial acetic acid.

Subculture and Feeding

All conditions were under Biosafety Level 2 containment, performed in a Class II Biosafety Hood using sterile pipets and plastic/glassware, wearing a laboratory coat and double-gloved. Subculture was performed weekly or when the monolayers reached 80% confluence as assessed by phase-contrast microscopy. Media from flask-grown cells were poured into a waste flask. The monolayers were rinsed with 1.5 ml/T25, 3 ml/T75 HEPES Buffered Saline Solution (HBSS) then trypsinized for 10 min to lift cells from flasks. Trypsinization was performed by adding 1.5 ml/T25 or 3 ml/T75 0.25% trypsin, 0.05% EDTA (Invitrogen), decanting after 30 seconds and incubating the monolayer in the residual trypsin solution. When cells were released from the flasks (10 min), culture medium was added to each flask (5 ml/T25, 8 ml/T75) and swirled over the cells. The cell suspension was transferred to a 15 ml or 50 ml centrifuge tube and centrifuged at 270 x g for 5 min at $4^{\circ}C$ (IEC PR-7000M centrifuge, rotor 966). The supernatant

was discarded and the pellet resuspended in culture medium. Using a hemacytometer, the cell suspension was enumerated and the cells seeded into new flasks, plates or inserts. Cells grown in T75 flasks were seeded at a density of 4.0×10^6 cells in 25 ml or split at a one to four ratio and fed twice weekly. Cells grown in T25 flasks were seeded at a density of 1 to 1.5×10^6 cells in 12 ml or at a one to four ratio and were fed every other day. Millicell inserts were seeded at 4.0×10^5 cells in 2.0 ml culture medium in the basolateral compartment with 1.5 ml culture medium added to the apical compartment. Cells were fed every other day. Transwells were seeded at 4.0×10^5 cells or superseeded at 1.41×10^6 cells in 2.6 ml culture medium in the basolateral compartment with 1.5 ml culture medium added to the apical compartment. Cells were fed every other day or daily. Cells were maintained in an incubator at $37^{o}C$ and 5% CO_2.

Cryopreservation of Cell Line

Cells from intermittent passages were cryopreserved in a solution of 85% culture medium prepared without fetal bovine serum (FBS), 10% FBS and 5% dimethyl sulfoxide (DMSO) at a cell suspension of $1-1.5 \times 10^6$ cells/ml. The cryosuspension was prepared as a double-strength cryomedium (0.35 ml culture medium, 0.10 ml FBS, 0.05 ml DMSO per vial) to which a cell suspension (0.5 ml x 2.0 to 3.0×10^5 cells/ml culture medium) was added dropwise to the cryovial for a final volume of 1 ml cryosuspension. The cryovials were placed in a Nalgene cryofreezer temperature control unit and placed in a $-20^{o}C$ freezer overnight, transferred to a $-80^{o}C$ freezer for 4 hours then placed in liquid nitrogen or in a $-135^{o}C$ freezer for long-term storage.

Cell Pellets for Assays or Western Blot Analysis

Cells grown in 35 mm plates, T25 or T75 flasks were rinsed X 2 with 1-3 ml HBSS, then scraped with a Teflon scraper, transfered into 15 ml or 50 ml centrifuge tubes and centrifuged at 270 x g for 5 min at $4^{o}C$ (IEC PR-7000M centrifuge, rotor 966). Supernantant was discarded. Cells were stored at $-80^{o}C$ if not used immediately.

Cell Line Characterization

Materials

Adenosine 5'-triphosphate (Sigma, A-2383)

Alkaline phosphatase staining kit (Sigma, 85L-3R)

Phosphatase substrate (Sigma, 104)

Glucose-6-phosphate deydrogenase Type VII (Sigma, G-7877)

γ-Glutamyltransferase Kit (Sigma, 545-A)

Protein assay kit, dye reagent (Bio-Rad Laboratories, 500-0006)

Bovine Serum Albumin, (Sigma, A-6003)

Equipment

Perkin-Elmer HTS 7000 bioassay reader

Gillford III spectrophotometer

Beckman UV/Vis spectrophotometer

Growth

Ideal growing conditions were determined by comparing growth of cells with variations in culture medium, culture plate type or plate preparation. These growth comparisons were performed on a minimum of n=4 per culture plate and were evaluated based on cell count and/or protein content per flask/plate. Cell count was performed using a hemacytometer and was expressed as number of cells per plate or flask type.

Protein Determination

Protein determination by the method of Bradford (1976) was measured spectrophotometrically at 595 nm using bovine serum albumin as standard and Biorad® protein assay dye reagent. Utilizing 5 μl aliquots of cell lysate, measurements were performed in duplicate for each flask, plate or membrane. Protein content was expressed as mg protein per plate or flask type or as a measurement of the amount of cellular protein (mg) used in a specific assay.

Proximal Tubule Cell Markers

Characterization of HK-2 cells by known proximal tubule cell markers was performed using cells from subculture cell suspensions and from cells scraped with a Teflon cell lifter from 35 mm plates, T25 and T75 flasks. Alkaline phosphatase (AP) levels were measured using Diagnostic Kit 104 purchased from Sigma Chemical Company measured as nmol p-nitrophenol liberated/min/mg protein by spectrophotometric absorbance at 410 nm or by a staining procedure using Sigma Diagnostics Alkaline Phosphatase kit, procedure number 85, as a semi-quantitative demonstration of AP activity using α-naphthyl phosphate as a substrate and fast blue RR as the diazonium salt to stain cells expressing AP. The stained monolayers were evaluated as positive or negative for AP based on visibility of stain on cell membranes under light microscopy. Hexokinase (HK) levels were determined by the method of Joshi and Jagannathan (1966) as a measure of nmol $NADP^+$ reduced/min/mg protein spectrophotometrically at 340 nm. Gamma-glutamyltransferase (GGT) levels were determined by colorimetric absorbance at 540 nm with the use of Sigma kit 545, based on the formation of a colored product in a secondary reaction after a GGT catalyzed reaction liberating p-nitroaniline. GGT levels were expressed as GGT units/mg protein.

<u>Toxicity Studies</u>

<u>Materials</u>

Acetaminophen (APAP) (Aldrich, A730-2)

Acetaminophen glucuronide (AG) (Sigma, A-4438)

Diclofenac sodium (Sigma, D-6899)

Lactate dehydrogenase kit (Sigma, 228)

Gilford Stasar III spectrophotometer (Fisher Scientific)

<u>Lactate Dehydrogenase Release</u>

Five to seven day old monolayers of HK-2 cells grown on 35 mm plates were incubated in 0, 200 μM or 500 μM acetaminophen or acetaminophen glucuronide (AG) for 30, 60 and 120 min in incubation medium (phosphate buffered saline solution (PBS) with 5 mM glucose) on an orbital shaker at 60 cycles per min in an environment of 95% air/5% CO_2 at 37°C. Incubation medium was removed from the culture well and cells were scraped from the plate and solubilized in 1 ml PBS/0.1% Triton-X100. Cell suspensions were transferred to microcentrifuge tubes, vortexed for 1 min, then centrifuged at 7200 x g for 3 min. Using Diagnostic Kit LDL-20 from Sigma Chemical Company, LDH activity was calculated as the change in spectrophotometric absorbance at 340 nm over time corresponding to LDH-catalyzed reduction of $NADP^+$ to NADPH. Cell viability was determined by measuring release of lactate dehydrogenase (LDH) into the incubation media as compared with the total LDH and expressed as % LDH release according to the following equation.

$$\% \; LDH \; release = \frac{LDH \; released \; in \; the \; medium \; x \; 100\%}{LDH \; retained \; in \; cells + LDH \; released \; in \; the \; medium}$$

LDH release in control vs. treated data per each incubation period was statistically analyzed by One-Way ANOVA at 95% probability with a statistically significant increase in LDH release indicative of toxicity.

Transport Characterization and Experimentation

Materials

4-Acetamidophenyl-ring-UL-^{14}C glucuronide sodium ([^{14}C]AG) (Sigma, A-1329)

Dehydroepiandrosterone sulfate sodium salt, [1,2,6,7-^{3}H(N)] ([^{3}H]DHEAS) (PerkinElmer LS, NET-860)

p-[Glycyl-1-^{14}C]-Aminohippuric Acid ([^{14}C]PAH) (PerkinElmer LS, NEC-563)

Estrone sulfate, ammonium salt, [6,7-^{3}H(N)] ([^{3}H]ES) (PerkinElmer LS, NET-203)

Acetaminophen (APAP) (Aldrich, A730-2)

Acetaminophen glucuronide (AG) (Sigma, A-4438)

Dehydroepiandrosterone sulfate sodium salt (Sigma, D-5297)

β–Estradiol 17β-D-glucuronide (Sigma, E-1127)

Estrone sulfate sodium salt (ES) (Sigma, E-0251)

Fluorescein isothiocyanate dextran (FLD) (Sigma, FD-4)

Fluorescein sodium salt (FL) (Sigma, F-6377)

p-Aminohippuric acid (PAH) (Sigma, A-1422)

Probenecid (Sigma, P-8761)

Ouabain (Sigma, O-3125)

ScintiVerse II, universal liquid scintillation cocktail (Fisher Scientific, SX12-4)

Equipment

Wallac 1409 liquid scintillation counter
Perkin-Elmer HTS 7000 bioassay reader
Dubnoff Incu-Shaker Model 3575
Innova 2000 Platform Shaker

Semipermeable membranes used for transport studies were purchased from Fisher Scientific: 30 mm Millicell-PCF Millipore Millicell© Culture Plate Inserts (early studies) or 24 mm Costar® Transwell-Clear polyester tissue culture treated

microporous membranes. Transport media (TM) consisted of PBS with 5 mM glucose or Waymouth's Buffered Transport Media (WBTM). Ingredients are listed in the appendix. All reagents were purchased from Sigma Chemical Company unless otherwise stated. When indicated, inserts were treated with 25 µg/insert Type IV human placental collagen (Sigma, C-5533) prepared in 0.5 M glacial acetic acid.

Transepithelial Transport

Four to nine day old monolayers of HK-2 cells grown on membranes were rinsed with a transport media of phosphate buffered saline solution containing 5 mM glucose (TM), pH 7.4. TM was added to both compartments of the insert: 1.5 ml apical (A) and 2.6 ml basolateral (BL) (Figure 3.1). Monolayers were incubated for 10 min in TM to equilibrate. At time 0, substrate was added to the BL or the A compartment ($\leq$ 1% compartment volume) with gentle swirling to ensure even concentration throughout media. In experiments studying both uptake and clearance, incubation medium was prepared as a batch rather than per insert and medium was aspirated from the outside of the plate before placing the insert into the TM containing the substrate. Plates were incubated at 37°C, 5% CO_2, 95% air on an orbital shaker at 60 cycles per min. Upon expiration of the incubation period, 1.0 ml aliquots were removed from each compartment and transferred to microcentrifuge tubes.   Aliquots (100 µl) were then assayed in triplicate for fluorescence with a Perkin-Elmer HTS 7000 bioassay reader (485/535 nm excitation/emission). For radiolabeled substrates, 120 µl aliquots were removed from each compartment and transferred to microcentrifuge tubes. Aliquots (30 - 50 µl) were transferred to scintillation vials to which 5 ml RIA-Solve II or Scintiverse II Cocktail scintillant was added.   Samples were vortexed then assayed for radioactivity using a Wallac 1409 liquid scintillation counter. For each experiment, parallel plates were incubated with 100 µM FLD to determine paracellular diffusion and/or non-specific uptake and efflux across the monolayer. To quantify transport,

clearance of substrate was calculated as the volume of treated media totally cleared of substrate and received into the trans compartment, normalized to the surface area (SA) of the membrane. For BL to A transport,

$$Clearance = \frac{[substrate]_A * Volume_A}{[substrate]_{BL} * SA * time} = [\mu l / cm^2 / min]$$

Clearance was corrected for diffusion by subtracting the clearance of FLD.

Diffusion Studies

Diffusion studies were conducted as transport studies (above) using fluorescein isothiocyanate dextran (FLD) as the diffusing agent and expressed as $\mu l/cm^2$ or $\mu l/cm^2/min$. To determine relative confluence of monolayers, diffusion rates of 3-7 day old monolayers were compared to diffusion rates of blank plates (no cells) at time 5, 15, 30 and 60 min.

Figure 3.1. Microporous Membrane
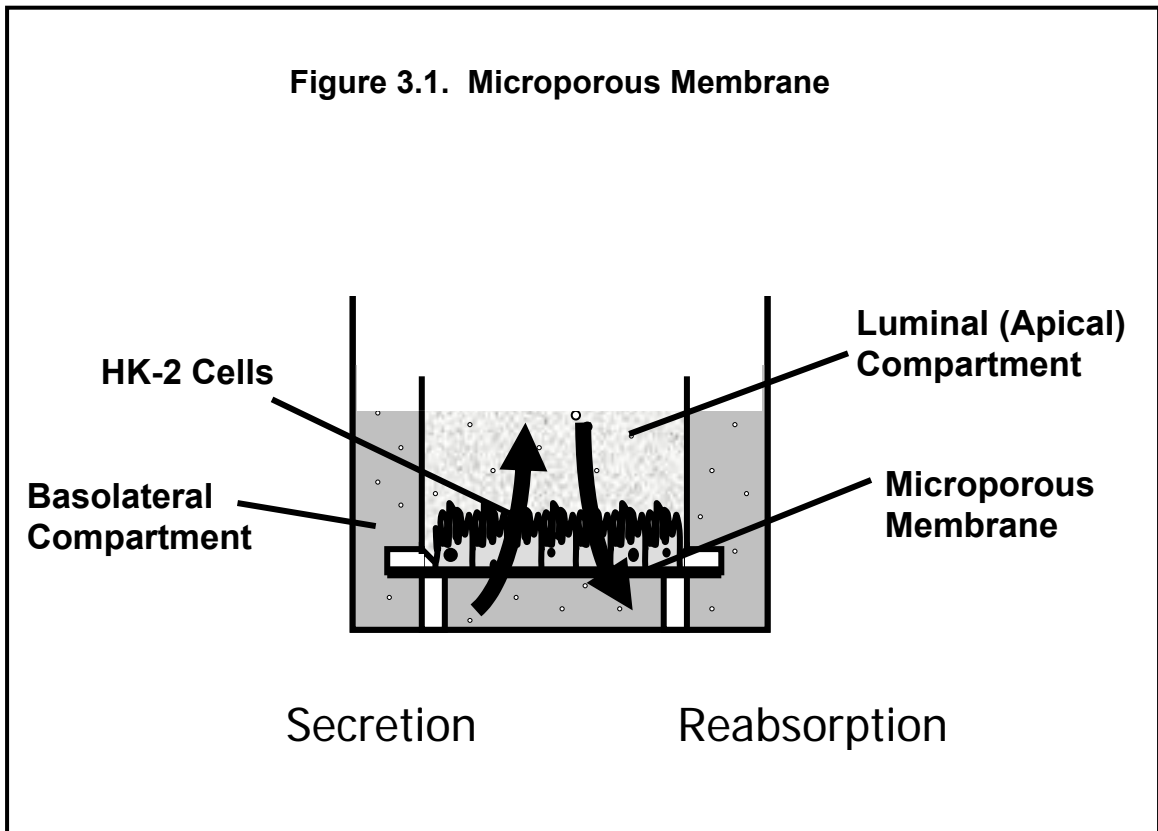
<u>Uptake Studies</u>

Four to eleven day old monolayers seeded on Transwell membranes were used for uptake studies. Culture media from HK-2 monolayers was aspirated and monolayers were then rinsed with transport media (TM or WBTM) warmed in a $37^{\circ}C$ water bath. After thorough aspiration, 1.5 ml transport media was added to the A compartment and at time 0, the insert was placed in the BL compartment (one well of a 6-well plate) containing 2.6 ml transport media containing substrate with or without inhibitors. For apical uptake studies, the insert was placed into the BL compartment and transport media containing substrate was placed in the A compartment at time 0. The monolayers were placed in an incubator at $37^{\circ}C$, 5% CO_2, 95% air or were placed in a $37^{\circ}C$ water bath for the shorter incubation periods (5 min or less). Upon expiration of the incubation period, the insert was transferred to a well containing 2.6 ml ice-cold transport media and rinsed x 2 in a total volume of 5 ml ice-cold transport media. The inserts were aspirated and the bottom of each insert was blotted with a Kim® wipe unless otherwise indicated. Various methods were used to collect and lyse the cells. Cells were either A) solubilized overnight in 1 ml 0.1 N NaOH after removal of the membrane from the insert housing; B) solubilized by the addition of 400 μl 1% SDS/0.1 N NaOH directly to the intact membrane, placed on an orbital shaker at 120 cycles/min for 30 min, then neutralized with 200 μl 0.2 N HCl; or C) cells were scraped from the membranes with a Teflon cell lifter and solubilized in 500 μl 1 N NaOH overnight, neutralized by adding 250 μl 2 N HCl. Aliquots or entire lysates were assayed for radioactivity using a Wallac 1409 liquid scintillation counter. Uptake was expressed as fmol/cm^2/min or pmol/mg protein/min and was calculated by one of the two the formulas:

$$Uptake\ (fmol/\text{cm}^2) = DPM * \frac{1 uCi}{2.22 x 10^{\wedge}6 DPM} * \frac{1}{Activity} \frac{umol}{uCi} * \frac{10^{\wedge}9\ fmol}{umol} * \frac{1}{SA}$$

$$Uptake\ (pmol/mg) = DPM * \frac{1 uCi}{2.22 x 10^{\wedge}6 DPM} * \frac{1}{Activity} \frac{umol}{uCi} * \frac{10^{\wedge}6\ pmol}{umol} * \frac{1}{mg\ protein}$$

in which *DPM* is the disintegrations per min as measured by the scintillation counter, *Activity* is that indicated per isotope from the manufacturer and *SA* is the surface area of the membrane. For those data expressed per mg protein, parallel plates were used to determine protein by removing membranes from the housing and lysing the cells in 1 ml 0.1 N NaOH overnight. Aliquots (5 µl) were used for protein determination using a Biorad protein assay kit as described above on page 47.

Dynamic Model Uptake Studies

For the dynamic model, the uptake experiments were conducted as described above but with the medium in the apical compartment replaced with fresh WBTM by continuous simultaneous removal and replacement of medium over the incubation period utilizing two disposable 1 ml pipettes. Medium was slowly added with one pipette while removed at the same rate with the other pipette for a total volume exchange of 9 ml.

Statistics

Each Millicell insert or Transwell membrane represents an N of 1. The data are represented as means ± standard error of the mean (SEM) of N = 2 to 7 experiments. Statistical analysis between two groups was performed using the Student's t-Test assuming equal variances or for multiple groups using One Way ANOVA or Repeated Measures One Way ANOVA followed by a Dunnett's post test for comparison back to control or by Tukey's method for multiple comparisons. Significance was reported at $p < 0.05$.

Western Blot Analysis

Materials

HK-2 human kidney, PTCs, transformed (ATCC, CRL-2190)

Fisher 344 rat PTCs (kindly provided by Sarah Miles, graduate student)

Human (56 year old Caucasian female) PTCs (kindly provided by Dr. LH Lash, Wayne State USOM)

OAT1 antibodies, affinity pure (Alpha Diagnostic International, OAT11-A)

OAT2 antibodies, affinity pure (Alpha Diagnostic International, OAT21-A)

OAT3 antibodies, affinity pure (Alpha Diagnostic International, OAT31-A)

Endo H (endoglycosidase H) (New England Biolabs, P0702S)

Benchmark™ Pre-Stained Protein Ladder (Invitrogen, 10748-010) [†]

ECL™ Western Blotting Detection Reagents (Amersham Biosciences, RPN2106)[†]

Hyperfilm™ ECL high performance chemiluminescence film (Amersham Biosciences, RPN2114K) [†]

Goat anti-rabbit IgG-HRP (Santa Cruz Biotechnology, SC-2004) [†]

Equipment

Trans-Blot Electrophoretic Transfer Cell (BioRad)[†]

Beckman Optimal XL-100K Ultracentrifuge, Rotor SW 60 Ti

Beckman J6 MI centrifuge, rotor 4.2

Beckman Avanti centrifuge, rotor J14

Micromax RF Centrifuge, International Equipment Company[†]

[†] All reagents and equipment for Western blot analysis were kindly provided by Dr. Kelley Kiningham.

Cell Procurement

HK-2 cells were grown as described above on page 44. Human renal PTCs were kindly provided by Dr. Lawrence Lash. F344 PTCs were isolated by Sarah Miles according to the following procedure.

F344 PT isolation

Male Fischer 344 rats were anestisized (pentobarbital sodium, 50mg/kg, i.p.) and renal proximal tubule (PT) fragments were isolated following the procedure described by Gesek et al. (1987) and modified by Aleo et al. (1991). Additional modifications were made, initiating renal retrograde perfusion by the procedure of Jones et al. (1979). Following perfusion, kidneys were decapsulated, and cortical tissue dissected away from the medulla, minced, and placed in a 50 ml plastic beaker with 25 ml of oxygenated collagenase containing Incubation buffer (see appendix for composition). Digestion of cortical tissue was initiated at 37ºC in a shaking waterbath (60 rpm) with continuous oxygenation. After 15 min, solid kidney tissue was allowed to settle in the beaker and freed PTs remaining in suspension in the incubation buffer were removed by transfer pipette and placed in a 50 ml centrifuge tube. The suspension was centrifuged at 50 x g for 2 min at 4º C in a Beckman J6MI centrifuge (JS 4.2 rotor). The supernatant was removed and reserved for further cortical tissue digestion and the pellet was resuspended in oxygenated ice cold 1x Krebs-Henseleit (KH) buffer (see appendix for composition) and kept on ice. The remaining tissue was digested with an additional 25 ml of Incubation buffer for additional 5 min intervals until cortical tissue was completely digested. Total incubation time was typically 25 min. PTs were removed at the end of each 5 min interval, centrifuged as described and combined. The total pellet was then rinsed three times by resuspension in 25 ml ice cold 1x KH buffer and centrifugation at 50 x g for 2 min. The final PT pellet was then resuspended in 10 ml 1x KH buffer. This suspension of PT tubules was then divided in half and each 5 ml resuspended in polycarbonate round bottom centrifuge tubes each containing 30 ml oxygenated

45% Percoll solution (see appendix for compositon). A 5 ml 100% Percoll cushion was then injected into the bottom of each tube using a transfer pipette (Fig. 3.1A). PTs were then centrifuged at 17,000 x g for 10 min at 4º C in a Beckman Avanti™ Ultracentrifuge (JA 14 rotor) stopping without brake. Following centrifugation PTs formed a uniform layer above the cushion layer (Fig. 3.1B). This layer was removed using a transfer pipette, and rinsed three times in 1x KH buffer at 500 x g for 5 min at 4º C in a Beckman J6MI centrifuge (JS 4.2 rotor). PT pellets were stored at -80^oC.

Cell Fractionation

Plasma membrane fractions and whole cell lysates of HK-2 cells were prepared from 7 day old monolayers scraped from T75 flasks or from Transwell membranes, pelleted at 270 x g and frozen. Cell pellets (HK-2, human PTC and F344 rat PTC) were resuspended in 1 ml homogenization buffer (HB, appendix), homogenized (15 slow strokes) and centrifuged (100 x g, 2 min) to remove intact cells. To separate membrane from cytosolic fractions, 3 different methods were used. The supernatants (whole cell lystes) were centrifuged at 100,000 x g for 1 hour at 4^oC (procedure provided by Dr. Mary Vore) to isolate crude membrane fractions or at 15,000 x g for 30 min at 4^oC (Kikuchi et al., 2003) to isolate plasma membrane fractions. Proteins from the membrane pellets were extracted in 100 - 200 µl HB containing 1% Triton-X100 by frequent vortexing for 1 hour followed by overnight tumbling at 4^oC. The extracts were centrifuged for 30 min at 14,000 x g, 4^oC and the supernatants (membrane proteins) were assayed for protein content.

Deglycosylation

Selected samples were incubated for 2 hours at 37^oC in a buffer containing 2500 units Endo H, a deglycosylating enzyme (Kit P0702S, New England BioLabs, buffers supplied with the kit). As a control, an equal volume of water was added to the incubating buffer instead of enzyme.

SDS-PAGE and Western Blot Procedure

Each sample was solubilized in loading buffer (4% sodium dodecyl sulfate, 62.6 mM Tris, 10% glycerol) with or without 5% 2-mercaptoethanol, loaded at 200-250 µg HK-2 protein/lane and 100 µg F344 rat or human kidney PTC protein/lane and separated by polyacrylamide gel electrophoresis on a 12.5% or 8% gel overnight at 4^oC (12.5% gel for 15 hours at 70 V; 8% gel for 15 hours at 74V). Proteins were transferred onto a nitrocellulose membrane, blocked with 5% nonfat dry milk in Tris-buffered saline containing 0.3% Tween 20 for 1 hour at 25^oC and incubated overnight at 4^oC with anti-ratOAT1, OAT2 or OAT3 antibodies reported by the manufacturer to be specific for respective OATs and cross-reactive with the respective human orthologues (1:333, Alpha Diagnostics International). The bound antibody was detected on x-ray film by enhanced chemiluminescence with horseradish peroxidase-conjugated anti-rabbit IgG antibody. Buffer and gel formulations are recorded in the appendix.

CHAPTER IV

Results

HK-2 Growth and Characterization

Growth of HK-2 cells was measured for cells grown in Keratinocyte Serum Free Media (KSFM) for 4 days in the absence or presence of 2% or 5% FBS. No significant effect was observed on proliferation in the presence of FBS (Table 7). Protein content was numerically greater in the presence of FBS (Table 8), yet was statistically insignificant. Data for both studies were analyzed by One Way ANOVA. Although no difference was demonstrated in the effect of FBS on growth, the 2% FBS supplementation was favored and was adopted as standard procedure for subculture and feeding. In HK-2 cells, with supplementation of 2% FBS, the protein content per 10^6 cells was only half that of freshly isolated F344 rat PTCs (550 µg protein/10^6 cells; Lash and Tokarz, 1989).

Table 7. Effect of FBS on Cell Proliferation		
Medium	Harvest Density / Seeding Density	No. of monolayers
KSFM	4.48 ± 0.41	3
+ 2% FBS	4.20 ± 0.35	4
+ 5% FBS	4.28 ± 0.29	11

Table 8. Effect of FBS on Protein Level		
Medium	µg protein/10^6 cells	No. of monolayers
KSFM	172 ± 54.2	4
+ 2% FBS	270 ± 25.2	6
+ 5% FBS	221 ± 18.0	6

The growth rate of cells grown in T75 culture flasks in KSFM supplemented with 2% FBS was monitored over time, from passages 29 to 40. Cells were plated at a density of 4.0 x 10^6 cells/T75 flask. After 7 days, cells were harvested. Table 9 summarizes the findings for harvest cell count and the harvest to seeding ratio.

Table 9. Growth Rate of HK-2 Cells Grown in T75 Culture Flasks			
	Mean	SEM	Sample Size
7 Day <u>Harvest Density</u> Seeding Density	3.70	.067	10
7 Day Harvest*	1.35×10^7 cells	3.5×10^5	4

* Seeded at 4.0 x 10^6 cells/T75

Characteristic renal tubule cell enzymes were measured for HK-2 cells grown in 35 mm culture dishes. Gamma-glutamyltransferase (GGT) and Alkaline Phosphatase (AP) are brush-border enzymes known to be expressed in the proximal tubule (Lash and Tokarz, 1989). Thus, high concentrations for both enzymes were expected. Hexokinase (HK) is an enzyme involved in glycolytic metabolism and is expressed at higher concentrations in the distal tubule than in the proximal tubule (Lash and Tokarz, 1989). The results of the enzyme assays are presented in Table 10. Typically, these enzymes are measured for freshly isolated PTCs for comparison with the enzyme levels of freshly isolated distal tubule cells (DTCs) to verify purity of the isolate or for comparison for levels for primary culture PTC vs. DTC. Enzyme measurements in the case of a cell line are more for the purpose of demonstrating presence of the enzyme in character with the cell type. GGT levels for HK-2 cells were comparable to those found for primary culture of F344 rat PTC (32.2 U/10^6 cells; Lash et al., 1995). HK-2 HK levels were less than those of freshly isolated F344 rat PTC (111 U/10^6 cells; Lash and Tokarz, 1989). AP could not be detected by a spectrophotometric assay, however, the enzyme was positively detected with the use of a staining procedure. This detection method is frequently employed for cell lines and has been used to detect AP in HK-2 cells by other investigators as well (Raucusen, 1997).

Table 10. HK-2 Cellular Enzyme Levels	
Enzyme	Level of Activity in HK-2 cells
GGT	32.93 ± 2.83 U/10^6 cells 126.67 ± 10.89 U/mg protein
HK	57.06 ± 7.36 U/10^6 cells 219.46 ± 30.12 U/mg protein
AP	Stain +

GGT gamma-glutamyltransferase, HK hexokinase, AP alkaline phosphatase

Figure 4.1.1 is a photo of HK-2 cells grown in a T-75 culture flask. Morphological characteristics of the cell line include stellate cytoplasmic processes extending from the cell bodies. These processes are thought to be responsible for cell migration. When cells are plated on hydrophilic porous membranes of Millicell-CM inserts, fewer of these processes are present (Figure 4.1.2). For reasons discussed in the Transport section below, these inserts were not used for transport studies. HK-2 cells grown on Transwell-Clear inserts display shorter processes (Figure 4.1.3), but when superseeded (1.41×10^6 cells/insert) onto the Transwell-Clear inserts, no migration is necessary, and very few processes are present (Figure 4.1.4). Superseeding on Transwell-Clear inserts was selected for transport studies and is discussed in more detail in the Transport section.

Figure 4.1.1. HK-2 Cells plated on a T75 Culture Flask. Five day old HK-2 cells, passage 30, were seeded on a T75 culture flask at 4.0 x 10^6 cells. 100X Magnification on Zeiss Axiovert Phase Contrast Microscope.

Figure 4.1.2. HK-2 Cells seeded on a Millicell-CM Microporous Membrane. Five day old HK-2 cells, passage 29, were seeded on a Millicell-CM insert at 4.0 x 10^6 cells. 100X magnification on Zeiss Axiovert Phase Contrast Microscope.
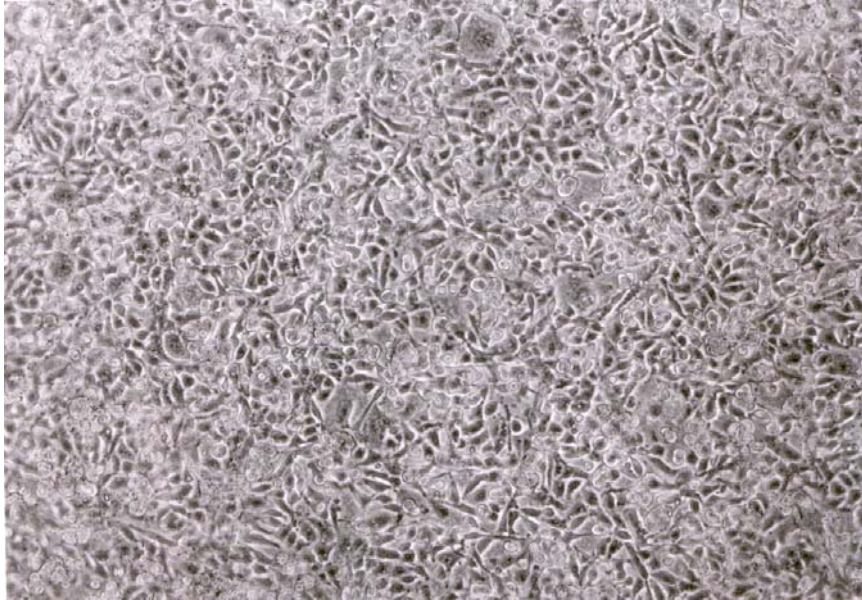
Figure 4.1.3. HK-2 Cells seeded on a Transwell Microporous Membrane.
Four day old HK-2 cells, passage 31, were seeded on a Transwell-Clear membrane at 4.0 x 10^5 cells. 100X , Zeiss Axiovert Phase Contrast Microscope.
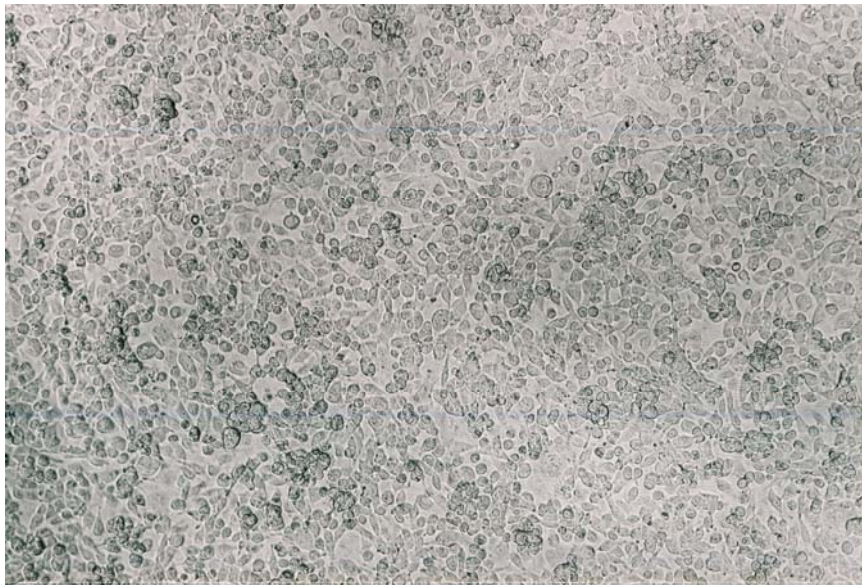
Figure 4.1.4. HK-2 Cells superseeded on a Transwell-Clear Microporous Membrane.   Three day old HK-2 cells were seeded on a Transwell-Clear microporous membrane at 1.41 x 10^6 cells. 100X, Zeiss Axiovert Phase Contrast Microscope.

<u>Molecular Analysis of Organic Anion Transporters</u>

Western blot analysis of the organic anion transporters, OAT1 and OAT3, was performed using crude membrane fractions isolated from Fisher 344 rat (F344) PTCs and HK-2 cells (Figures 4.2.1 and 4.2.2). Figure 4.2.3 also contains a blot for OAT2 demonstrating lack of detection of the protein in HK-2 cells. Lack of OAT2 in HK-2 cells is not surprising since OAT2 is expressed at high levels in the liver, but at low levels in the kidney. F344 rat PTCs were isolated in our lab by Sarah Miles.

The blot shown in Figure 4.2.3 consists of plasma membrane fractions from freshly isolated human PTCs isolated from renal cortical tissue of a 56 year old caucasian female, kindly provided by Dr. Lawrence Lash, and from HK-2 cells. Proteins were subjected to nonreducing vs. reducing homogenization buffer and loading buffer and/or the deglycosylating enzyme EndoH as indicated in the caption below the figure. No effects were apparent for membrane proteins treated with reducing vs. nonreducing conditions or for those proteins incubated with deglycosylating enzyme vs. control. Because no positive control was used for the deglycosylating enzyme, it is possible that the enzyme was inactive.

For all blots, molecular weight is given for protein bands only above 50 kD because the lower molecular weight proteins are thought to be due to incompletely synthesized proteins. Antibodies for OAT1 and OAT3, purchased from Alpha Diagnostics International (ADI), were synthesized against peptides homologous to the amino-terminus and would therefore bind whole and partial proteins. The antibodies against OAT2, also from ADI, are synthesized against a peptide homologous to the carboxy-terminus and would therefore bind completely formed proteins only, as is evidenced by the detection of only 2 bands for F344 rat protein (Figure 4.2.2). Additionally, bands reported by investigators as recorded in Table 4, Literature Review Section of this document are at 50 kD and greater and are the bands to which HK-2 bands will be compared. For all entries in Table 4, antibodies

were synthesized against peptides homologous to the carboxy-termini of the proteins.

The only human OAT1 Western blots reported in the literature were those of Cihlar et al. (1999) and Motohashi et al. (2002) who found bands at 80-90 kD and 84 kD, respectively. HK-2 blots performed for this study demonstrated bands at 80 (Figure 4.2.3) and 90 kD (Figures 4.2.1 and 4.2.2). Bands at 64 kD (Figure 4.2.1), 62 kD (Figure 4.2.2) and 65 kD (Figure 4.2.3) for HK-2 cells likely represent the nonglycosylated OAT1 proteins with MW near the predicted value of 61.8 kD (http://harvester.embl.de). Faint bands at 55.5 kD (Figure 4.2.1) and 54 kD (Figure 4.2.2) may represent lower MW isoform(s) of OAT1 whose molecular weights are predicted to be 55.6 and 57.4 kD (http://harvester.embl.de). The heaviest bands found in HK-2 cells for OAT1 are the 75 kD (Figures 4.2.1 and 4.2.2) and 80 kD bands (Figure 4.2.3) which likely represent glycosylated forms of the OAT1 isoforms. The 75 kD bands are nearest to the 77 kD bands reported by Ji et al. (2002) for rat OAT1. Collectively, the bands demonstrated for OAT1 in HK-2 cells are similar to those reported in the literature for both nonglycosylated and glycosylated proteins and, as such, are evidence of OAT1 expression in the HK-2 cell line.

The OAT1 bands demonstrated for F344 rat PTCs at 75 and 76 kD bands (Figures 4.2.1 and 4.2.2, respectively) are near the 77 kD band reported by Ji et al. (2002) for rOAT1 whereas the 61.3 and 60.4 kD bands (Figures 4.2.1 and 4.2.2) are likely the nonglycosylated protein forms.
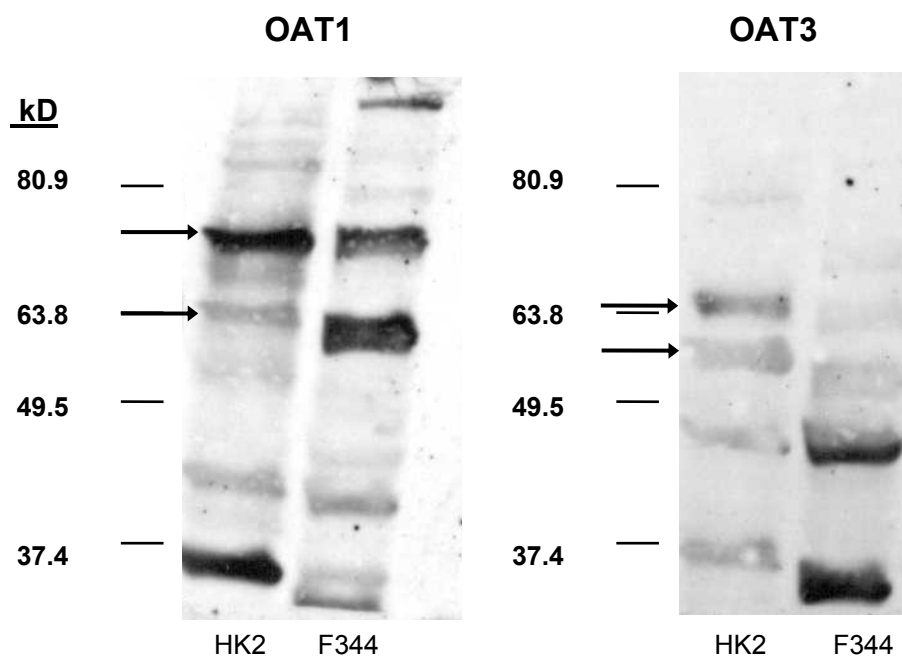
Figure 4.2.1. Western Blot Analysis for OAT1 and OAT3. Crude membrane fractions (250 µg protein/lane) isolated from HK-2 cells, passage 29, scraped from T75 flasks and from F344 rat PTCs were separated on a 12% polyacrylamide gel, blotted onto nitrocellulose then exposed to antibodies against OAT1 or OAT3. Bands were detected at 64 and 75 kD (arrows) with faint bands at 55.5, 69 and 90 kD for OAT1 in HK-2 cells. For OAT3 in HK-2 cells, bands were detected at 58 and 65 kD (arrows) with a faint band at 79 kD. In freshly isolated F344 PTCs, bands were detected at 61.3 and 75 kD for OAT1, and faint bands for OAT3 were detected at 54 and 63 kD.
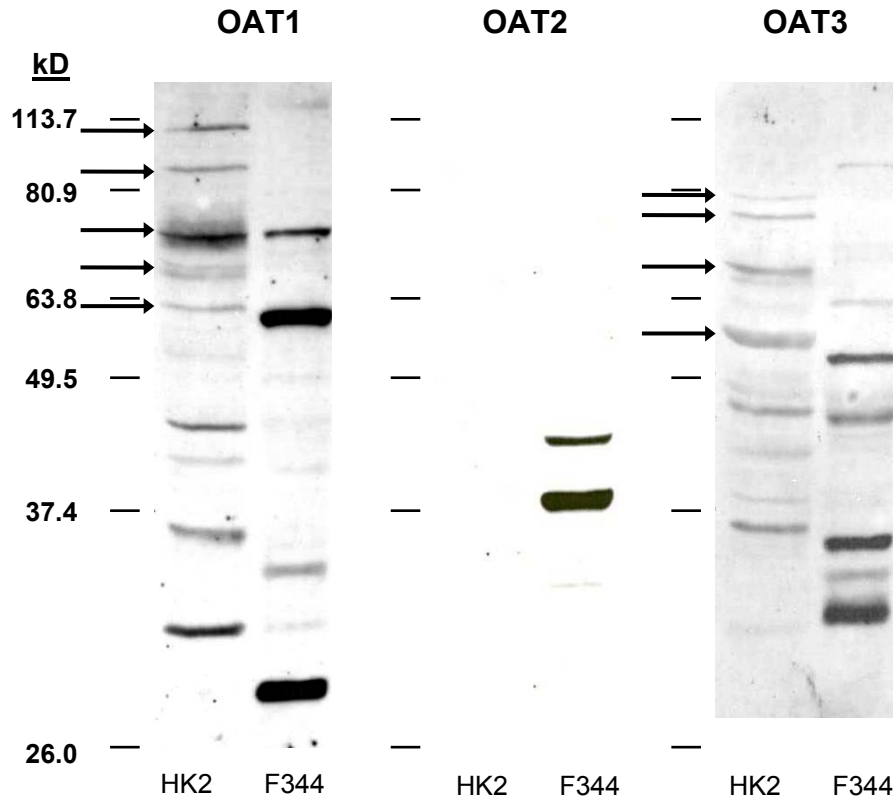
Figure 4.2.2. Western Blot Analysis for OAT1, OAT2 and OAT3. Crude membrane fractions (200 µg protein/lane) isolated from HK-2 cells, passage 20, scraped from T75 flasks and from freshly isolated F344 rat PTCs were separated on a 12% polyacrylamide gel, blotted onto nitrocellulose then exposed to antibodies against OAT1, OAT2 or OAT3. The heaviest band was detected at 75 kD with lighter bands at 62, 69, 90 and 107 kD (arrows) and a faint band at 54 kD for OAT1; and 57, 69, 77 and 80 kD (arrows) with a faint band at 63 kD for OAT3 in HK-2 cells. No bands were detected in HK-2 cells for OAT2. A heavy band was detected for freshly isolated F344 PTCs at 60.4 kD with a moderate weight band at 76 kD for OAT1. Bands were detected at 39 and 44 kD for OAT2 in F344 PTCs and at 54 kD with a lighter band at 63 kD for F344 OAT3.
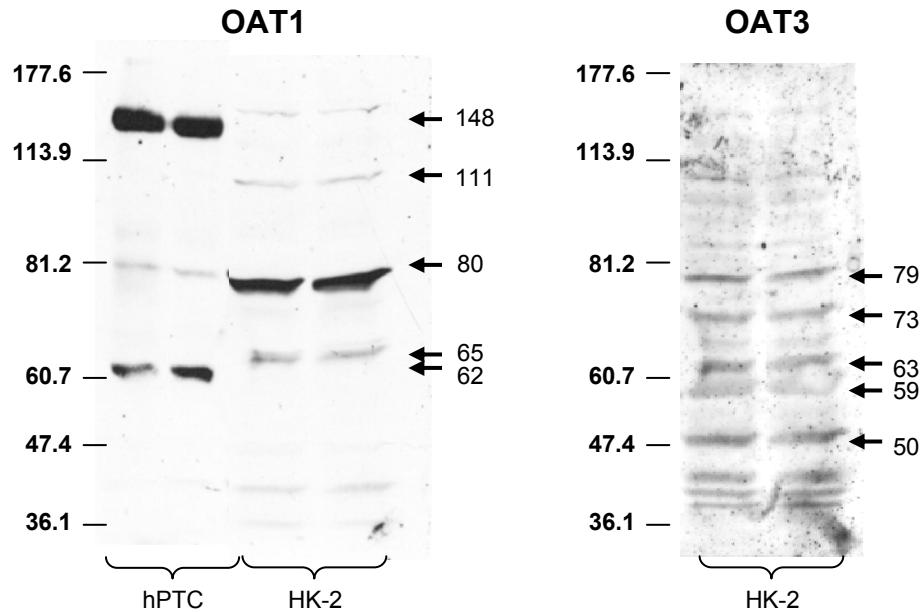
Figure 4.2.3. Western Blot Analysis for OAT1 and OAT3, Human vs. HK-2.
Plasma membrane fractions isolated from freshly isolated human renal proximal
tubule cells (hPTC; 63 µg protein/lane) or from HK-2 cells, passage 50, grown in
T75 flasks (200 µg protein/lane) were separated on an 8% polyacrylamide gel,
blotted onto nitrocellulose then exposed to antibodies against OAT1 or OAT3. For
the human cells, the strongest band was detected at 148 kD with a medium
density band at 62 kD and a lighter band at 81 kD for OAT1. Bands were detected
in HK-2 cells at 80 kD, a medium density band at 65 kD and faint bands at 111 and
148 kD for OAT1. For OAT3, bands for the HK-2 fractions were detected at 50,
59, 63, 73 and 79 kD. Because the quality of the blot was poor, lanes containing
human proteins are not displayed above, but bands were detected at 54 and 62 kD
for OAT3. For the OAT1 blot, lane 1 protein was denatured but not reduced; lane
2 was reduced; lane 3 proteins were incubated with a reducing agent and a
deglycosylating enzyme and lane 4 proteins were denatured but not reduced or
deglycosylated. For the OAT3 blot, lane 1 proteins were incubated with a reducing
agent and a deglycosylating enzyme and lane 2 proteins were denatured but not
reduced or deglycosylated.

Peptide alignment of the hOAT1 isoform b (550 aa) vs. isoform a (563 aa) shows an excision of residues 522-534 to form the splice variant, isoform b. The antibody produced by Cihlar et al. (1999) that demonstrated an 80-90 kD band which resolved to a 60 kD band upon deglycosylation was raised against a synthetic peptide of aa 515-528 of a 550 aa hOAT1. The antibodies likely would not bind to isoform a or isoform d since these latter isoforms contain a 13 aa sequence between residues 521 and 522 of isoform b, see Figure 4.2.4. It is also possible that the very broad band at 80-90 kD and also at 60 kD (deglycosylated) (Cihlar et al., 1999) are immunoreactive bands to multiple isoforms of hOAT1.
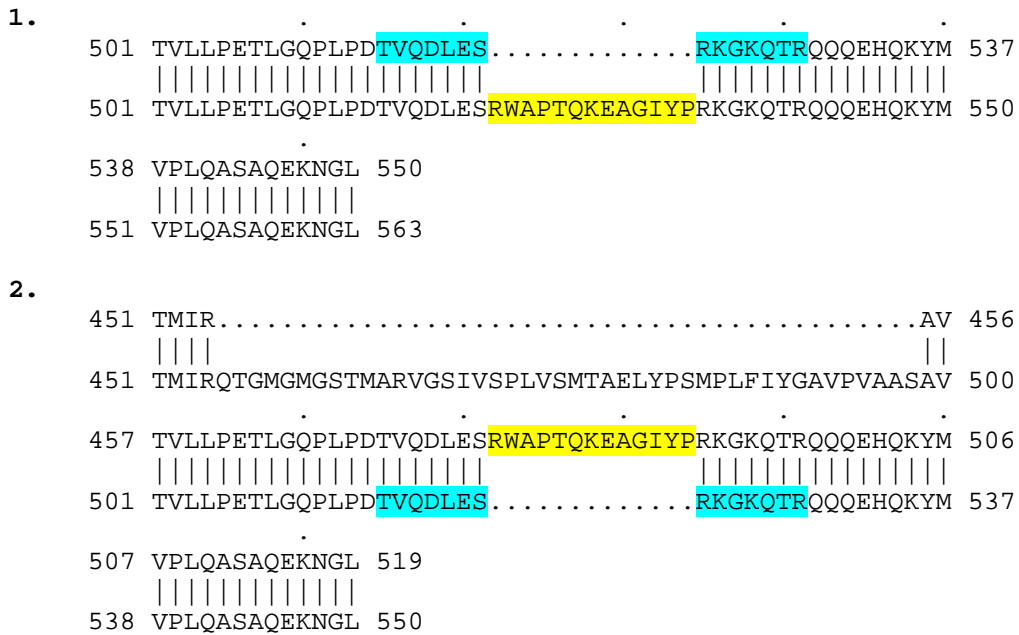
Figure 4.2.4. **Alignment of hOAT1 isoforms.** Alignment of hOAT1 isoform b (550 aa) with (1) isoform a (563 aa) and (2) isoform d (519 aa) demonstrates the existence of an sequence of 13 aa excised from isoform b between residues 521 and 522. Analyzed by accelrys SeqWeb version 2 web-based software.

The only known human Western blot for OAT 3 was performed by Motohashi et al. (2002) demonstrating a very broad band at 80 kD. The strongest most well defined band for the HK-2 plasma membrane proteins was at 80 kD (Figure 4.2.3). HK-2 crude membrane fractions demonstrated 79 kD bands (Figures 4.2.1 and 4.2.2). Each HK-2 blot had a band near the predicted MW for OAT3 (62 kD; http://harvester.embl.de) with bands at 65 kD (Figure 4.2.1) and 63 kD (Figures 4.2.2 and 4.2.3). Other bands found for OAT3, such as 58 kD (Figure 4.2.1), 57 kD (Figure 4.2.2) and 59 kD (Figure 4.2.3) may represent the lower MW isoform of OAT3 estimated to be at 59.9 kD (http://harvester.embl.de). The 69, 77 kD (Figure 4.2.2), 50 and 73 kD (Figure 4.2.3) bands demonstrated for HK-2 cells are similar to those reported for rat OAT3 (Table 4, Literature Review). Collectively, the bands demonstrated in HK-2 cells are similar to the bands reported in the literature or are near the predicted MW for OAT3 and, as such, are evidence of the expression of OAT3 in the HK-2 cell line.

The 54 and 63 kD OAT3 bands demonstrated for F344 rat PTCs (Figures 4.2.1 and 4.2.2) are identical to those reported in the literature (Table 4, Literature Review).

Again, as with OAT1, the OAT3 Western blot by Motohashi et al. (2002) may not detect all isoforms of OAT3. Alignment at the sequence used by Motohashi et al. (2002) to raise antibodies against the 568 aa hOAT3 reveals a 3 aa sequence at the beginning of the synthetic peptide that is absent from the shorter version of the protein (see Figure 4.2.5). It is possible then, that the Western analysis performed by Motohashi et al. (2002), which demonstrated a very broad band at 80 kD would not have demonstrated a band for the shorter isoform. It is also possible that the width of the band would encompass multiple isoforms.

```
495 TLNQP................LPETIEDLE.............NWSLRAKK 516
    ||| |                  |  :   |             .  |||||
493 TLNSPCQRRSKTWKTGQSLPLAPSVLLPGEAGLGPGLFLSSLSLGLRAKK 542

              .             .
517 PKQEPEVEKASQRIPLQPHGPGLGSS 542
    |||||||||||||||||||||||||
543 PKQEPEVEKASQRIPLQPHGPGLGSS 568
```

Figure 4.2.5. **Alignment of 568 aa vs. 542 aa hOAT3 sequences at the carboxy- termini.** The highlighted sequence represents the synthetic peptide sequence used by Motohashi et al. (2002) to raise antibodies against OAT3. The 3 aa residues at 509-511 of the 542 aa hOAT3 protein (upper sequence) represents an area of non-homology to the peptide sequence for the shorter isoform of OAT3. Analyzed by accelrys SeqWeb version 2 web-based software.

Toxicity Studies

Before transport studies were conducted, it was necessary to ensure that the model compound for transport studies, AG, was not toxic to the HK-2 cells. Toxicity studies were performed for AG and the parent compound acetaminophen (APAP) by measuring LDH release from the cells after incubating the cells in medium containing 200 µM and 500 µM AG (Figure 4.3.1) or APAP (Figure 4.3.2). It was determined that neither AG nor APAP caused an increase in the release of LDH, indicating no cytotoxicity from either compound for incubations up to 120 min. Parallel studies were conducted in our lab for freshly isolated PTCs from F344 rats with similar findings (unpublished data, Sarah Miles). Additionally, ATP studies were performed with freshly isolated F344 PTCs and no decrease in ATP levels was found at 200 or 500 µM AG or APAP incubation (unpublished data, Sarah Miles). It was, therefore, concluded that at 200 and 500 µM, neither APAP nor AG were cytotoxic to HK-2 or F344 PTCs for up to 120 min exposure.

Transport of organic anions is considered to be an energy consuming process. Toxicity to cells would, therefore, result in altered transport capability. Higher concentrations of AG (2.5 mM) were used in transport studies with no effect on the ability of the HK-2 cells to transport AG (uptake or transepithelial), thus, AG appears not to be cytotoxic at concentrations up to 2.5 mM for 5 min. Ninety min incubation with 20 µM resulted in an intracellular AG concentration much higher than that at 250 or 500 µM AG for 5 min and caused no alteration in the ability to transport. Therefore, there is additional evidence that AG is not cytotoxic to HK-2 cells when used for the time periods of this study.
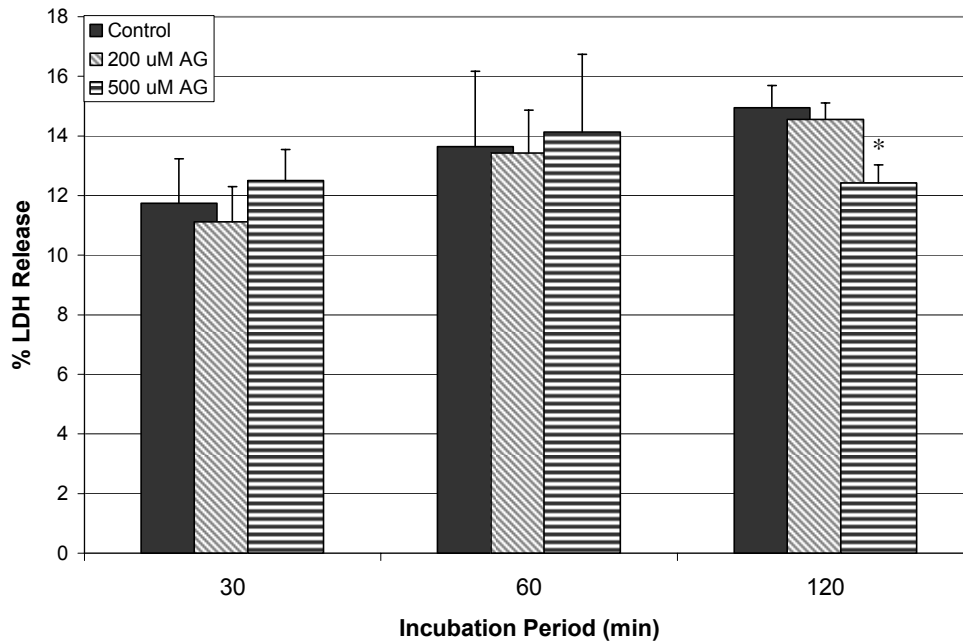
Figure 4.3.1. Percent LDH Release for AG Treated HK-2 Cells. To determine if AG is cytotoxic to HK-2 cells, 5-7 day old HK-2 monolayers grown on 35 mm plates were rinsed with incubation medium (phosphate buffered saline solution (PBS) with 5 mM glucose), then placed in incubation medium in the absence or presence of 200 µM or 500 µM AG for 30, 60 or 120 min. Separate plates were used for each incubation period. Upon expiration of the incubation period, medium from each plate was sampled and assayed for LDH activity. Cells were scraped from the plates, and solubilized in a 1% Triton-X100 solution and assayed for LDH. Each bar represents the LDH released from the cells into the medium expressed as a percent of the total LDH (remaining in the cells + released into the medium) +/- SEM for 4 HK-2 monolayers. There was no statistical difference for control vs. treated in LDH release at 30 or 60 min. *Percent LDH release for the 500 µM AG treatment at 120 min was significantly lower than control as analyzed by One Way ANOVA with Dunnett's Post Test, $p < 0.05$.
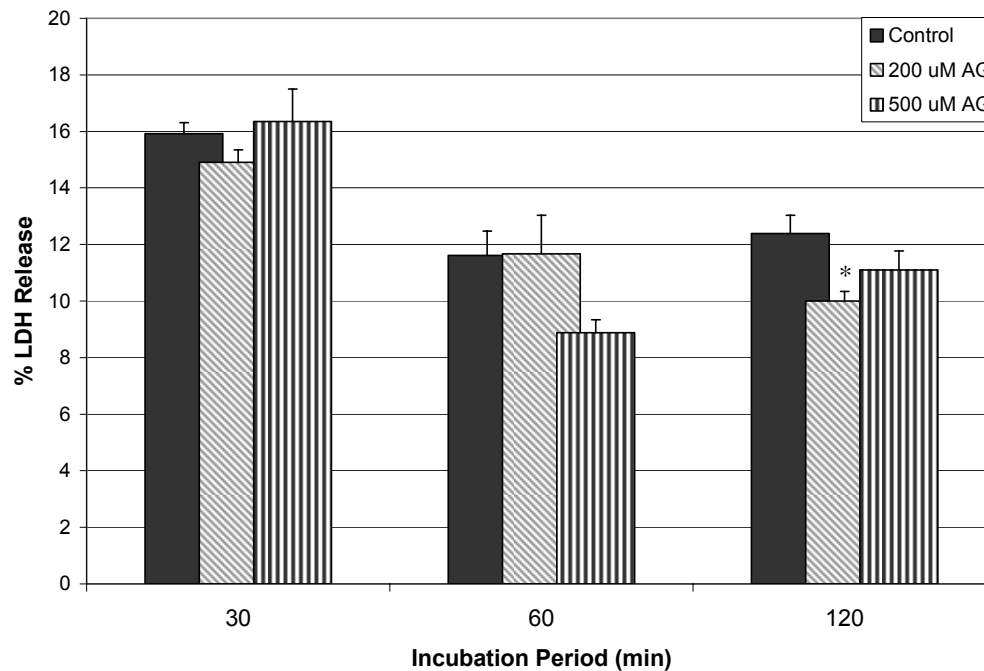
Figure 4.3.2. Percent LDH Release for APAP Treated HK-2 Cells. To determine if APAP is toxic to HK-2 cells, HK-2 monolayers grown on 35 mm plates were rinsed with incubation medium (phosphate buffered saline solution (PBS) with 5 mM glucose), then placed in incubation medium in the absence or presence of 200 µM or 500 µM APAP for 30, 60 or 120 min. Separate plates were used for each incubation period. Upon expiration of the incubation period, medium from each plate was sampled and assayed for LDH activity. Cells were scraped from the plates, and solubilized in a 1% Triton-X100 solution and assayed for LDH. Each bar represents the LDH released from the cells into the medium expressed as a percent of the total LDH (remaining in the cells + released into the medium) +/- SEM for 4 HK-2 monolayers. There was no statistical difference in LDH release for control vs. treated at 30 or 60 min. *Percent LDH release for the 200 µM AG treatment at 120 min was significantly lower than control as analyzed by One Way ANOVA with Dunnett's Post Test, $p < 0.05$.

Transport Studies

HK-2 Monolayer Confluence and FL Transport

HK-2 cells were first characterized for transport by determining their ability to form confluent monolayers such that transport processes were distinguishable from diffusion. Two different types of inserts were studied and several growth conditions were examined to determine optimal confluence and transport function. Transport models were selected based on the ability to form the most confluent monolayers as demonstrated by the lowest rate of FLD diffusion while also demonstrating polarization on the monolayer via vectorial transport of FL.

In the initial studies, HK-2 monolayers were seeded onto Millicell-PCF inserts for transport studies. These membranes were opaque and thus, visualization of the monolayer under microscopy was not possible. To study confluence of the monolayers, experiments were performed to determine FLD diffusion across the monolayers in comparison to diffusion on blank inserts (Figure 4.4.1). The FLD rate of diffusion for 5-10 day old monolayers was consistently lower than the diffusion rate on blank inserts from 15 to 120 mins. However, the rate of FLD diffusion across the monolayers was still high.

In an attempt to improve confluence (decrease diffusion), the Millicell-CM inserts were tested. These inserts are clear and permit visualization of the monolayer by phase contrast microscopy (Figure 4.1.2). It was noted that there was an acellular margin around the perimeter of the monolayer when the cells were grown on Millicell-CM inserts. Moreover, the Millicell-CM and the Millicell-PCF membranes appeared to be slightly concave which may have caused cells to drift to the center of the membrane before attaching, resulting in the high rate of diffusion. The cell morphology on the Millicell-CM inserts appeared more compact, round and with fewer cytoplasmic processes as compared to cells grown on culture flasks.

As an alternative to the Millicell inserts, the Transwell-Clear inserts were tested. Monolayers (Figure 4.1.3.) appeared to be uniformly distributed across the

74

membrane with cells extending to the insert housing, indicating improved confluence on the Transwell-Clear vs. the Millicell-CM inserts. A confluence study by FLD diffusion was conducted for the Transwell-Clear inserts (Figure 4.4.2.), indicating improved confluence relative to the Millicell-PCF inserts.

Clearance studies with the OAT1/OAT3 substrate FL demonstrated vectorial transport with BL-A clearance greater than A-BL for both monolayers grown on Millicell-PCF and Transwell-Clear inserts (Figure 4.4.3). The BL-A/A-BL clearance ratio was greater for the Millicell-PCF inserts. However, due to the improved confluence and the ability to visualize the cells under microscopy, it was decided that the Transwell-Clear inserts were a better choice for this study. For all studies involving the transport of FL, clearance rates are corrected for FLD diffusion.

To understand the differences in vectorial transport for the 2 models, directional diffusion of FL on blank Millicell-PCF vs. Transwell-Clear inserts was studied. It was demonstrated that on Transwell-Clear inserts, FL diffuses at nearly twice the rate in the A-BL direction than the BL-A direction vs. nearly the same rate in each direction on Millicell-PCF inserts (Figure 4.4.4). For both models, FL diffusion was greater than FLD diffusion. When corrected for FLD diffusion on the blank inserts, the ratio of A-BL/BL-A diffusion of FL was greater than unity (A-BL > BL-A) for Transwell-Clear inserts and less than unity (A-BL < BL-A) for Millicell-PCF inserts (Figure 4.4.5). These ratios suggest that the differences in diffusion rates of FL and FLD on Transwell-Clear vs. Millicell-PCF inserts may contribute to the difference in vectorial transport of FL for HK-2 monolayers on the respective inserts (Figure 4.4.3).

A time-dependent clearance study of FL by cells grown on Transwell-Clear inserts demonstrated a nearly linear clearance for FL with time. Kinetic analysis of the clearance of FL was best described by a rectangular hyperbolic regression with a first order term for diffusion (Figure 4.4.6). This analysis revealed that diffusion of FL across the monolayers increased with time to a greater extent than did transport of FL. A table is included in the figure listing the percent of FL clearance due to diffusion. As in all clearance studies, the FL clearance for the time-dependent

uptake was corrected for FLD diffusion. Thus, the rate of FL diffusion is greater than that of FLD across HK-2 monolayers seeded on Transwell-Clear inserts. High substrate diffusion has the effect of diminishing differences in clearance rates for control vs. treated experiments, such that, as diffusion increases, differences in protein-mediated processes are less evident and the clearance rate for treated cells when expressed as a percent of control approaches 100%.

To determine if increased oxygenation would improve confluence of the monolayers (Groves et al., 1999b), beginning the day after seeding, growth of monolayers placed on an orbital shaker vs. a stationary shelf were compared for diffusion of FLD and transport of FL (Figure 4.4.7). There was a slight increase in the diffusion of FLD on the shaker-grown monolayers suggestive of decreased confluence. There was no difference in the clearance of FL. Because ascorbic acid has been shown to improve monolayer confluence under shaking conditions (Nowak et al., 1996), the addition of ascorbate phosphate (AscP) to shaking monolayers was tested (Figure 4.4.8). No improvement in confluence was demonstrated by the addition of 100 µM AscP to shaking monolayers.

For studies on the Millicell-PCF inserts and early studies on the Transwell-Clear inserts, the seeding density was 4.0×10^5 cells/insert. The seeding density was increased to a superconfluent density of 1.41×10^6 cells/insert for later studies on the Transwell-Clear inserts and is indicated herein as superseeded (Whitin et al., 2002). When viewed under phase contrast microscopy, the superseeded monolayers appeared to form a much tighter monolayer as compared with the lower seeding density monolayers in which growth was required to attain confluence (Figure 4.1.4). The cells also displayed fewer cytoplasmic processes, which are thought to be responsible for cell migration. Diffusion of FLD also decreased for superseeded monolayers (Figure 4.4.9).

With cells seeded at superconfluence, growth of cells to form the monolayer is unnecessary. Thus, the absence of epidermal growth factor (EGF) in the culture medium was tested to determine the effect on transport (Figure 4.4.10). There was

no statistical difference in the clearance of FL for cells grown with vs. without EGF. It was, therefore, decided that EGF was not a necessary component of the media for superseeded cells and EGF was excluded from the culture media for superseeded monolayers.

To summarize the model-selection criteria: Initial studies were performed on Millicell-PCF inserts. Although FLD diffusion rates were determined to be higher for blank inserts than those with HK-2 monolayers, concern of incomplete confluence across the insert leading to high diffusion and inability to visualize the monolayers led to the search for another insert. Comparison of diffusion for monolayers seeded on Millicell-PCF inserts vs. those seeded on Transwell-Clear inserts prompted selection of the latter for future studies even though vectorial transport of FL by monolayers seeded on the Millicell-PCF was higher than that of the Transwell-Clear inserts. Differences in directional diffusion of FL for Transwell-Clear inserts (A-BL > BL-A) but similar directional diffusion of FL on the Millicell-PCF inserts as well as differences in FL vs. FLD diffusion on the 2 insert types may contribute to the differences in vectorial FL transport between the insert types. Regression analysis of a time-course study of FL transport for monolayers seeded on Transwell-Clear inserts revealed that the rate of FL diffusion was greater than FLD diffusion and, over time, exceeded the rate of FL transport. This finding could also be explained by an increased rate of apical efflux of FL over time. Addition of AscP to the medium and/or use of an orbital shaker to increase aeration during cell growth did not significantly affect confluence of the monolayers. Superseeding resulted in slightly decreased FLD diffusion with improvement in the tightness of the monolayer with fewer cytosolic processes as judged by phase contrast microscopy, and, therefore, was selected as the preferred seeding density for subsequent studies. Use of EGF as a media supplement to superseeded monolayers was determined to be unnecessary as there was no significant difference in transport of FL with vs. without supplementation. Therefore, subsequent studies with superseeded monolayers were grown in medium without EGF.

Diffusion of Fluorescein-Dextran for Millicell-PCF Inserts
Blank Inserts vs. 4-10 day old HK-2 Monolayers
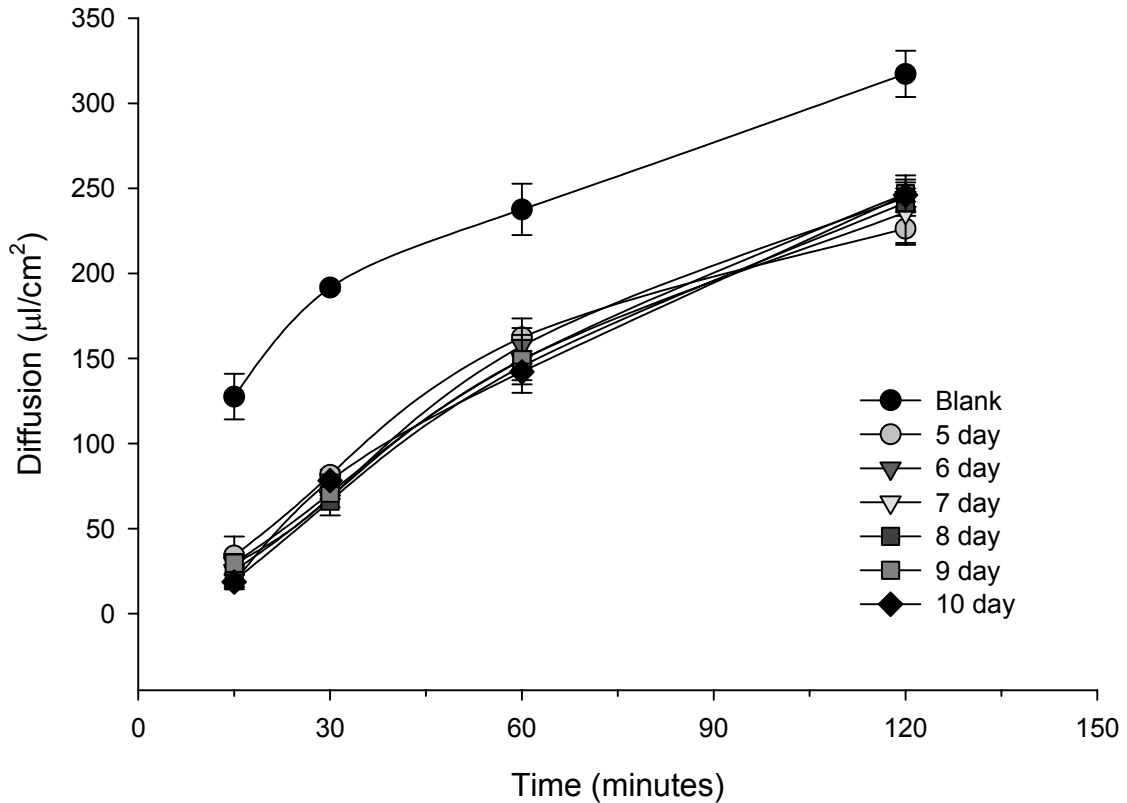
Figure 4.4.1. HK-2 Monolayer Confluence Study on Millicell-PCF Inserts. Confluence of 5 to 10 day old HK-2 monolayers seeded on Millicell-PCF inserts was evaluated by comparing BL to A FLD diffusion across the monolayer vs. BL to A FLD diffusion across blank (no cells) inserts. Monolayers were equilibrated in TM, aspirated, placed in TM to which FLD was added basolaterally and incubated for the respective period at 37°C, 5% CO_2/95% air, as described. Parallel inserts were used for each incubation period. Aliquots (100 µl) from each compartment were assayed in triplicate for fluorescence. For each incubation period, the diffusion for the blank inserts is significantly greater than that of all other groups, as analyzed by One-Way ANOVA followed by Tukey's All-Pairwise Comparison Test, $p < 0.05$. Each data point represents the mean diffusion ± SEM for 3 inserts.

Diffusion of Fluorescein-Dextran for Transwell-Clear permeable membranes
Blank inserts vs. HK-2 cell monolayers grown for 3 to 7 days
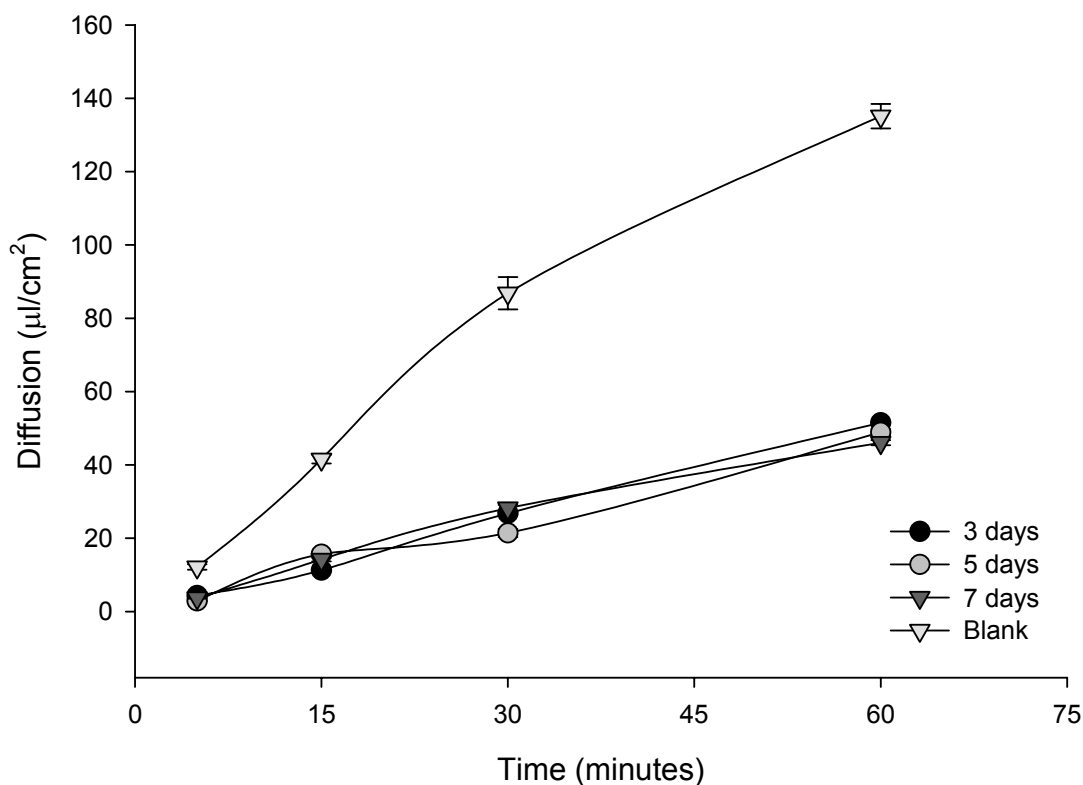
Figure 4.4.2. HK-2 Monolayer Confluence Study on Transwell-Clear Inserts.
Confluence of 3, 5 and 7 day old HK-2 monolayers seeded on Transwell-Clear inserts was evaluated by comparing BL to A FLD diffusion across the monolayer vs. BL to A FLD diffusion across blank (no cells) inserts. Monolayers were equilibrated in TM, aspirated, placed in TM to which FLD was added basolaterally and incubated for the respective period at $37^{o}C$, 5% CO_2/95% air, as described. Parallel inserts were used for each incubation period; n = 3 per group. Aliquots (100 µl) from each compartment were assayed in triplicate for fluorescence. Diffusion is expressed in µl/cm^2 for each incubation period. The increased diffusion for the blank inserts is significantly greater, per incubation period, than diffusion for the corresponding groups, as analyzed by One-Way ANOVA followed by Tukey's All-Pairwise Comparison Test within a 95% confidence interval.

A **Fluorescein Clearance on Millicell-PCF inserts**

B **Fluorescein Clearance on Transwell-Clear inserts**

	BL-A / A-BL ratio
Millicell-PCF	3.47
Transwell Clear	1.67
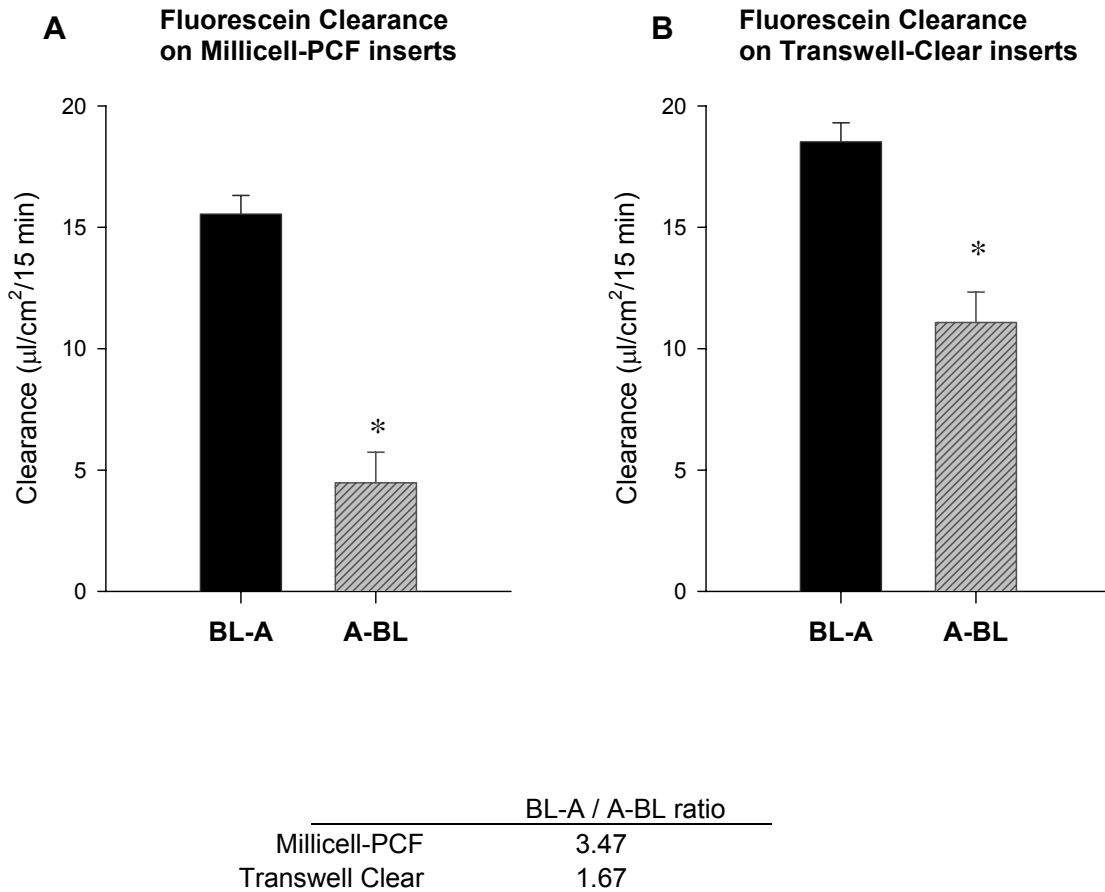
Figure 4.4.3. Vectorial Transport of FL on Millicell-PCF vs. Transwell-Clear Inserts. Directional transport of FL was determined for Millicell-PCF and Transwell-Clear inserts. Five day old HK-2 monolayers seeded onto respective inserts were equilibrated for 10 min in TM at 37°C, 5% CO_2/ 95% air, aspirated of media, placed in TM with 4 µM FL added basolaterally or apically, and incubated for 15 min at 37°C, 5% CO_2/ 95% air on an orbital shaker at 60 cycles/min. Compartmental samples were collected, aliquots (100 µl) were assayed for fluorescence and clearance rates calculated. *A-BL clearance was significantly less than BL-A clearance for both insert types as determined by Student's t-Test per insert type, $p < 0.05$, n = 3 per group. The BL-A vs. A-BL ratio of FL for Millicell-PCF was twice that for Transwell-Clear inserts.

Fluorescein Diffusion on blank plates
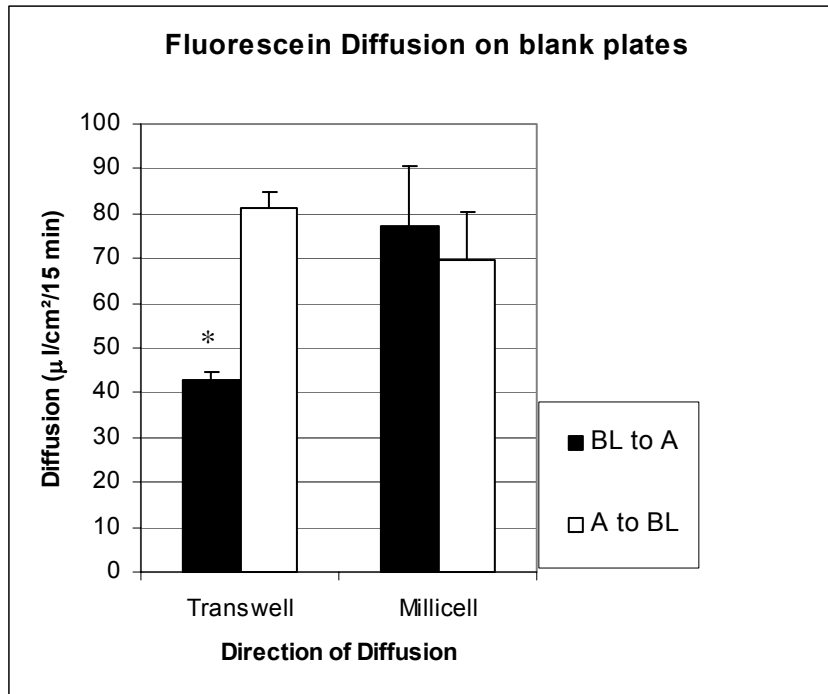
| | A-BL / BL-A ratio | |
	FL	FLD
Millicell-PCF	1.18	2.65
Transwell-Clear	1.88	4.87

Figure 4.4.4.   Diffusion of FL on Blank Inserts: Transwell vs. Millicell. Directional diffusion of FL across blank (no cells) Transwell-Clear inserts and Millicell-PCF inserts was determined by incubating inserts in TM with 4 µM FL in the A vs. BL compartment for 15 min on an orbital shaker at 60 cycles/min at $37^{o}C$, 5% CO2/95% air. *BL-A diffusion of FL is significantly less than A-BL FL diffusion on Transwell-Clear inserts and than BL-A or A-BL FL diffusion on Millicell-PCF inserts.   There is no significant difference in the directional diffusion of FL on Millicell-PCF inserts.   Statistics: One Way ANOVA with Tukey All Pairwise Comparison for Multiple Groups, $p < 0.05$; n = 2 per group. Additionally, the ratio of A-BL vs. BL-A FL diffusion for each insert type was calculated with A-BL diffusion nearly double that of BL-A for the Transwell-Clear inserts vs. nearly equal directional diffusion for the Millicell-PCF inserts.

FL - FLD Diffusion on Blank Inserts
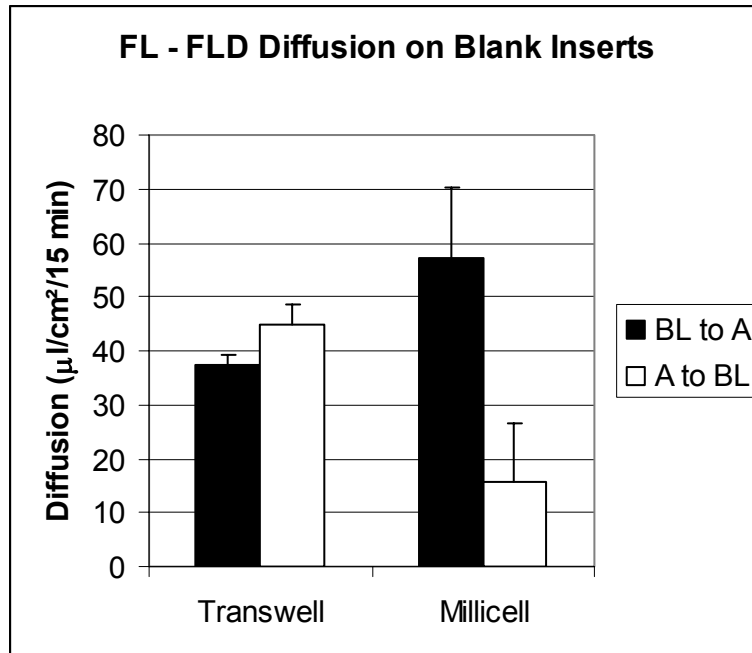
A-BL/BL-A
FL Diffusion Ratio

Millicell-PCF	0.28
Transwell-Clear	1.20

Figure 4.4.5. Comparison of Directional FL Diffusion Corrected for FLD Diffusion on Blank Millicell-PCF vs. Transwell-Clear Inserts. To compare the directional rates of diffusion of FL minus FLD, blank Millicell-PCF and Transwell-Clear inserts were incubated for 15 min in TM containing 100 μM FLD or 4 μM FL on an orbital shaker at 60 cycles per min at 37°C, 5% CO_2, 95% air. Samples were taken from both compartments per insert, 100 μl aliquots were assayed for fluorescence and diffusion rates were calculated. FL diffusion rates were corrected for FLD diffusion by calculating their difference, FL - FLD diffusion. The A-BL/BL-A ratios of the diffusion rates of FL corrected for FLD were then calculated for both insert types. There was no statistical difference in the FL - FLD diffusion in the A-BL direction than BL-A direction for Transwell-Clear or Millicell-PCF blank inserts as determined by Student's t-Test, $p < 0.05$. Each bar represents mean diffusion +/- SEM of 2 inserts (3 for Transwell-Clear FL diffusion).
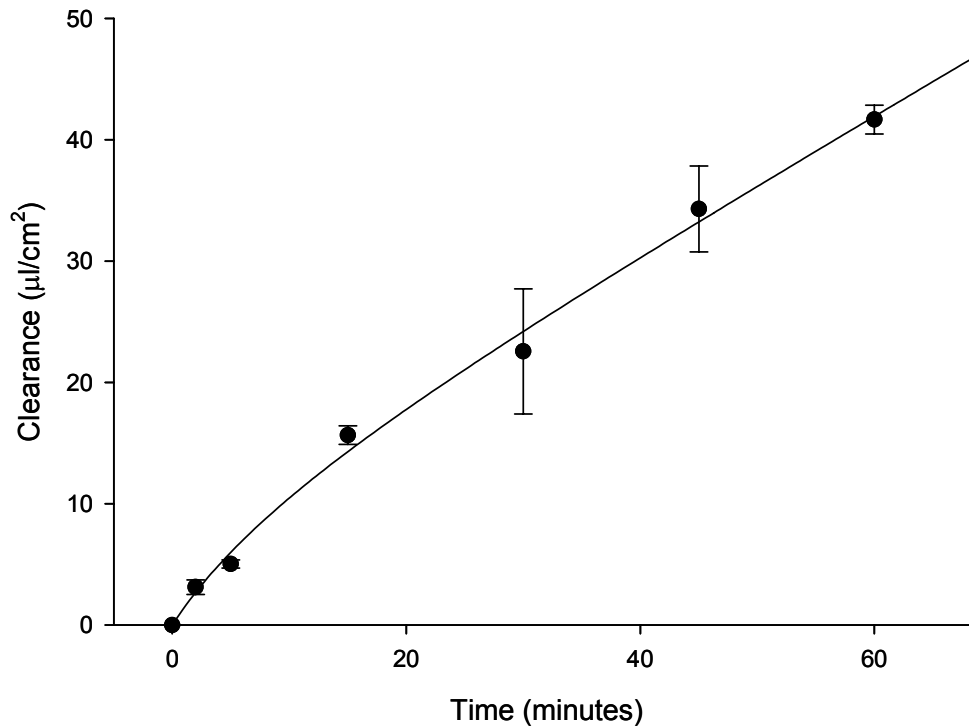
Computed Values from Regression Analysis		
Time (min)	FL Clearance ($\mu l/cm^2$)	% of clearance due to diffusion
5	6.0	46
15	14.3	58
60	41.9	79

Figure 4.4.6.   Time-Course of Clearance of 4 μM FL.   The time-course clearance for 4μM FL was performed on parallel five day-old HK-2 monolayers grown of Transwell-Clear inserts. HK-2 monolayers were equilibrated in TM for 10 min.   FL (4 μM final concentration) was added to the BL compartments and monolayers were incubated on an orbital shaker at 60 cycles/min at 37°C, 5% CO_2/95% air. Samples were withdrawn from the BL and A compartments at time 2, 5, 15, 30, 45 and 60 min. Aliquots (100 μl) were assayed for fluorescence and clearance rates determined. Each data point represents the mean clearance for 3 monolayers +/- SEM. Linear regression yields R^2 = 0.987 whereas a rectangular hyperbolic regression yields an R^2 of 0.996 such that the clearance (Cl) at any time (t) can be calculated by the equation: Cl = (10.62 * t)/(11.4 min + t) + 0.55 * t.

A

**Fluorescein-Dextran Diffusion for
Shaker vs. Stationary-grown Cells**

B

**Fluorescein Clearance for
Shaker vs. Stationary-grown Cells**
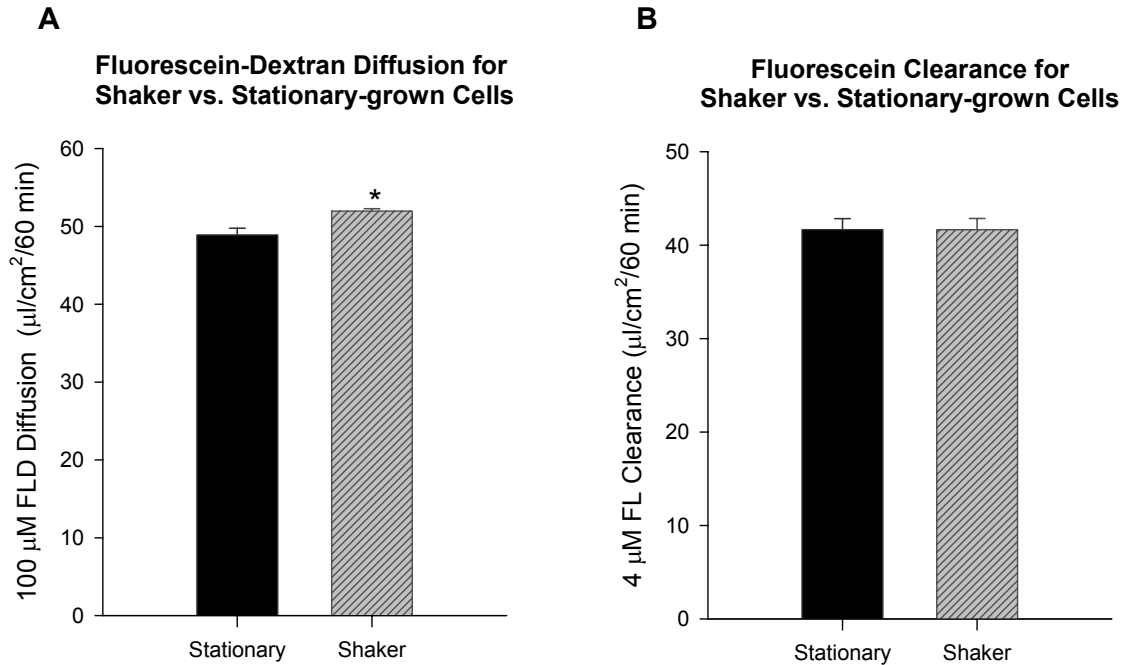
Figure 4.4.7. The Effects of Shaker-Grown vs. Stationary-Grown Monolayers on Confluence and Transport. HK-2 monolayers seeded on Transwell-Clear inserts were grown in an incubator at 37°C, 5% CO_2/95% air. Beginning on the day after seeding, 6 monolayers were grown on an orbital shaker at 60 cycles/min and 6 monolayers remained on a stationary shelf. Five day old monolayers were equilibrated in TM for 10 min on the shaker at 60 cycles per min, aspirated, placed in TM with 100 µM FLD or 4 µM FL added to the BL compartment. All monolayers were incubated at 37°C, 5% CO_2/95% air for 60 min on an orbital shaker at 60 cycles/min. Samples were collected from both compartments of the inserts and 100 µl aliquots were assayed for fluorescence. (A) No significant difference was demonstrated in FLD diffusion for control vs. shaker-grown cells (Student's t-Test, $p < 0.05$, n = 3 per group). (B) No difference was seen for control vs. shaker-grown cells for the clearance of FL when corrected for diffusion (n = 3 per group). Each bar represents mean clearance +/- SEM.
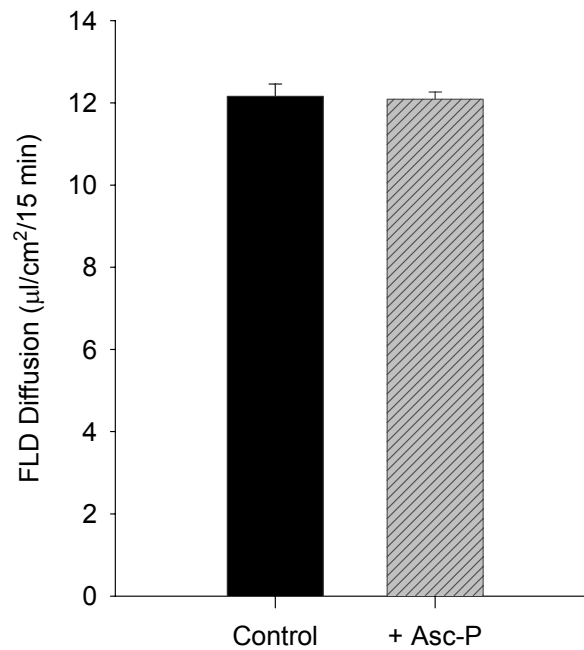
Figure 4.4.8. The Effects of Ascorbate Phosphate in Shaker-Grown Monolayers on Confluence. HK-2 monolayers seeded on Transwell-Clear inserts were grown in an incubator at 37°C, 5% CO_2/95% air. Beginning on the day after seeding, 6 monolayers were grown on an orbital shaker at 60 cycles/min, 3 of which received 100 µM AscP daily. Five day old monolayers were equilibrated in TM for 10 min on the shaker at 60 cycles per min, aspirated, placed in TM with 100 µM FLD added to the BL compartment. Monolayers were incubated at 37°C, 5% CO_2/95% air for 15 min on an orbital shaker at 60 cycles/min. Samples were collected from both compartments of the inserts and 100 µl aliquots were assayed for fluorescence. There is no statistical difference in the diffusion of FLD for the 2 groups. Each bar represents the mean diffusion +/- SEM for 3 monolayers.
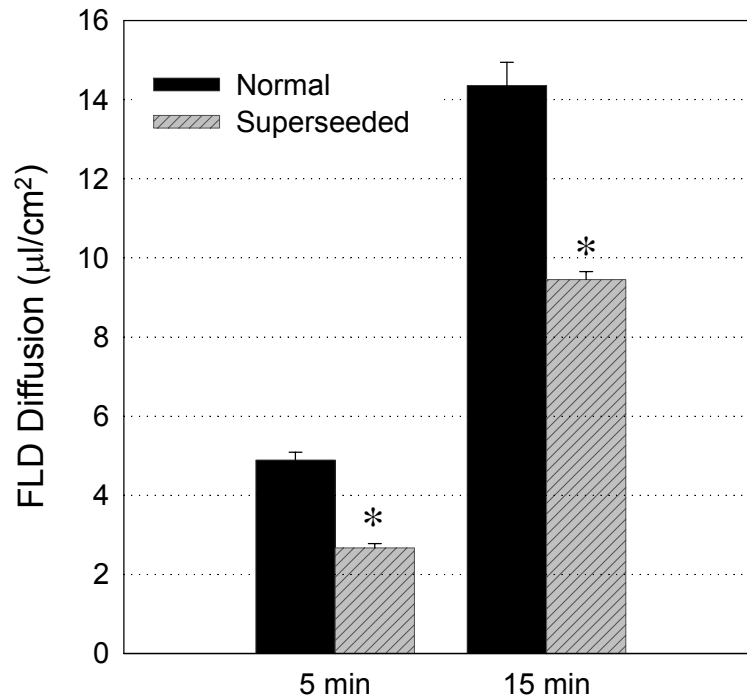
Figure 4.4.9. FLD Diffusion for Normal vs. Superseeded Monolayers. The FLD diffusion rates calculated for various transport studies by 5 to 7 day old HK-2 monolayers seeded at 4.0 X 10^5 cells/insert or superseeded at 1.41 X 10^6 cells/insert on Transwell-Clear inserts were compared. The diffusion rates were determined by incubation of monolayers for 5 or 15 min in 100 μM FLD. The media from each compartment per insert was sampled, aliquots (100 μl) were assayed for fluorescence and diffusion rates calculated. *For 5 and 15 min incubation periods, the rate of FLD diffusion for the superseeded monolayers was statistically lower than that of the normally seeded monolayers. Data was analyzed by Student's t-Test per incubation period, $p < 0.01$; n = 3 for normally seeded; n = 2 for superseeded monolayers. Each bar represents mean diffusion +/- SEM.

A

FLD Diffusion

B
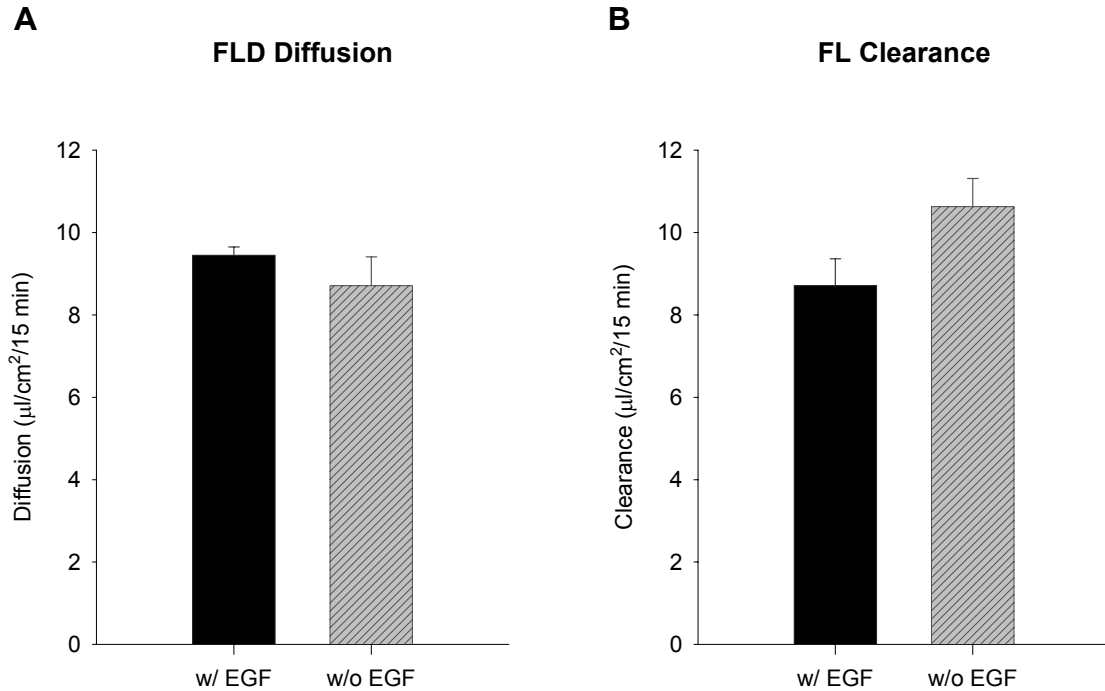
FL Clearance

Figure 4.4.10.   The Effect of Epidermal Growth Factor (EGF) in Culture Medium on FLD Diffusion and FL Clearance. To compare the effects of cells grown in culture medium with or without EGF supplementation, cells superseeded on Transwell-Clear inserts were cultured and maintained in standard culture medium with (standard) or without EGF (5 ng/ml) supplementation. Five day old monolayers were equilibrated for 10 min in TM, aspirated, then placed in TM with 100 µM FLD (A) or 4 µM FL (B) added to the BL compartment and incubated at 37°C, 5% CO_2/95% air for 15 min on an orbital shaker at 60 cycles/min. Samples were taken from both compartments and diffusion or clearance rates determined as described. A) EGF in the culture medium had no effect on the rate of FLD diffusion. B) There was a 22% increase in the clearance of FL for the cells grown without EGF supplementation that was statistically insignificant by Student's t-Test at a 95% confidence interval. Each bar represents the mean clearance +/- SEM for 2 monolayers for the FLD diffusion study and 3 monolayers for the FL clearance study.

Characterization of FL Transport

HK-2 monolayers seeded or superseeded on Transwell-Clear inserts, as indicated per study, were used to study FL transport and those factors that affect FL transport. To determine if the transport of FL across the HK-2 monolayer was a protein-mediated process, temperature-dependent transport was evaluated by comparing FL clearance at $37^{o}C$ vs. $4^{o}C$ (Figure 4.5.1). The significant reduction in transport at $4^{o}C$ is consistent with transport mediated by a protein such as an organic anion transporter.

To demonstrate that the cells are polarized on the membranes of the Transwell-Clear inserts, uptake of FL from the BL vs. A compartment was performed (Figure 4.5.2). Uptake is significantly higher from the A compartment than from the BL. This demonstrates polarization of the monolayer and is consistent with higher permeability of the BBM to FL (Dantzler, 2002).

Because sodium butyrate has been demonstrated to upregulate expression of the organic anion transporters (Sugiyama et al., 2001), 24 hour pretreatment of HK-2 cells with sodium butyrate was tested. Although the addition of 5 mM sodium butyrate to the culture medium 24 hours prior to experimentation caused a significant increase in FL clearance at 15 and 30 min (Figure 4.5.3), the difference was only minor in this model and, therefore, was not adapted as a standard procedure.

The cardiac glycoside ouabain, which inhibits the Na/K-ATPase, and thus, Na^{+}-dependent OAT1-mediated transport, was used to study OAT1-mediated FL transport. Differing effects on the transport of FL were observed for monolayers that were preincubated with ouabain compared to monolayers with no pretreatment. For monolayers coincubated only, the effect of ouabain on FL transport was determined for 2, 5 and 15 min (Figure 4.5.4, A). For the 2 and 5 min incubation periods, the trend was a decreasing inhibitory effect of ouabain on FL clearance with time. By 15 min, there was no difference in FL clearance for

treated vs. control. To determine long term effects of ouabain on FL transport, monolayers were first preincubated with or without ouabain prior to the addition of FL. For these monolayers, preincubated for 30 min with 100 μM ouabain, then coincubated with 4 μM FL, the 15 min clearance of FL increased compared to control (Figure 4.5.4, B). Thus, the acute effect of ouabain on FL clearance is inhibitory, diminishing with time, whereas, the long term effect appears to be stimulatory. The acute, inhibitory effect of ouabain is consistent with FL transport by OAT1, but the long term effect suggests that there are compensatory effects that increase FL transport. For subsequent studies, a shorter incubation period may be favorable to minimize compensatory effects.

The OAT1/OAT3 exchange substrate αKG and the OAT1/OAT3 inhibitor probenecid were found to effect transport of FL (Figure 4.5.5). Cells preloaded with the dicarboxylate showed increased FL clearance suggestive of trans-stimulation of FL uptake. Coincubation of FL with probenecid resulted in inhibition of FL clearance. Both results are consistent with transport of FL by an organic anion exchanger such as OAT1 and possibly OAT3.

Inhibition studies of FL transport by the OAT1/OAT3 substrate PAH and the OAT3 substrate DHEAS demonstrated no statistical difference in the 15 min clearance of FL by PAH (Figure 4.5.6) and a 10% decrease in the 15 min clearance of FL by DHEAS (Figure 4.5.7).

To summarize characterization of FL transport by HK-2 monolayers seeded or superseeded on Transwell-Clear inserts: Temperature-dependent clearance of FL indicated that transport of FL is protein-mediated. Greater uptake of FL from the A vs. BL compartment is consistent with a polarized monolayer exhibiting higher permeability of FL at the BBM. Preincubation of HK-2 monolayers with sodium butyrate for 24 hours slightly increased FL transport, but not enough to warrant incorporation of this step into standard procedure. Consistent with transport by OAT1 and/or OAT3, FL clearance was increased by preincubation with αKG and

decreased by coincubation with probenecid, DHEAS and ouabain. Possible distortion of modulatory effects due to the high rate of diffusion and the potential for compensatory effects as shown in the ouabain study led to the decision to conduct subsequent studies for substrate uptake rather than clearance and over a shorter incubation period.

FL Clearance
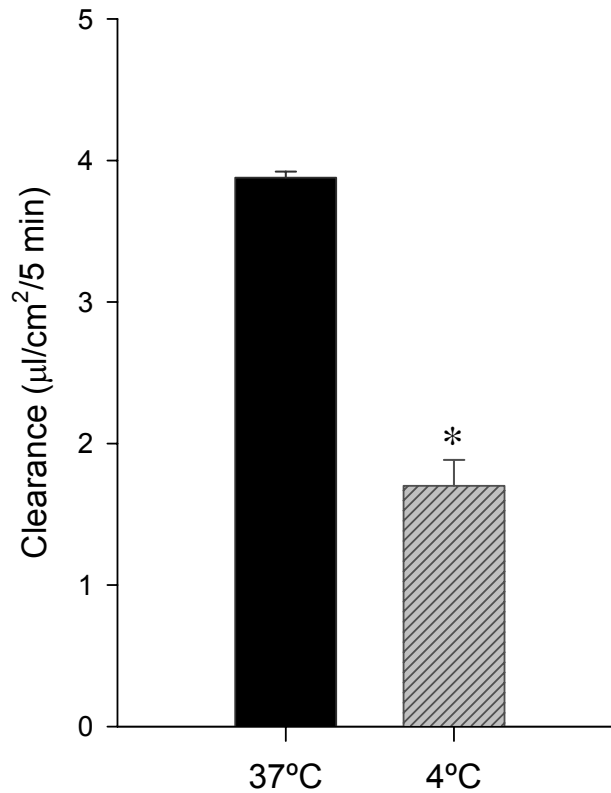
Figure 4.5.1. Temperature-Dependent Clearance of FL. A comparison of FL clearance at $4^{\circ}C$ vs. $37^{\circ}C$ was performed. Three day old HK-2 monolayers were equilibrated for 10 min in TM at $37^{\circ}C$, 5% CO_2/ 95% air, aspirated, placed in ice-cold TM or in $37^{\circ}C$ TM, both with 4 µM FL in the BL compartment. Monolayers were incubated for 5 min at $4^{\circ}C$ on an orbital shaker at 60 cycles/min or in a $37^{\circ}C$ shaking water bath. Samples were taken from both compartments and 100 µl aliquots were assayed for fluorescence. A parallel procedure was conducted for FLD diffusion and FL clearance was corrected for diffusion as described. Clearance of 4 µM fluorescein was significantly lower at $4^{\circ}C$ vs. $37^{\circ}C$. The difference in clearance was statistically analyzed by Student's t-Test, $p < 0.05$; n = 3 and 4 for $37^{\circ}C$ and $4^{\circ}C$ treatments, respectively.
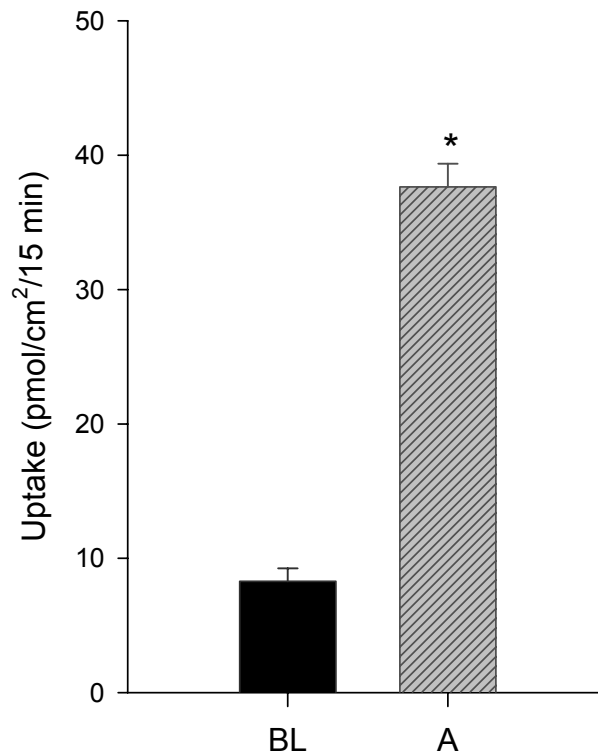
Figure 4.5.2. BL vs. A Uptake of FL. The rate of FL uptake from the BL vs. the A compartment was studied by incubating five day old HK-2 monolayers seeded onto Transwell-Clear inserts in TM containing 4 µM FL in the BL vs. the A compartment. Monolayers were equilibrated in TM for 10 min, aspirated and placed in TM containing 4 µM FL in the BL or in the A compartments. Monolayers were incubated for 15 min on an orbital shaker at 60 cycles per min, $37^{\circ}C$, 5% CO_2, 95% air. After 15 min, monolayers were rinsed twice in ice-cold TM, lysed in 0.1 N NaOH and assayed for fluorescence. There is a 4.5-fold greater uptake of FL from the A vs. the BL compartment. *The difference is statisically significant by Student's t-Test, p = 0.0001. Each bar represents the mean uptake +/- SEM for 3 monolayers.
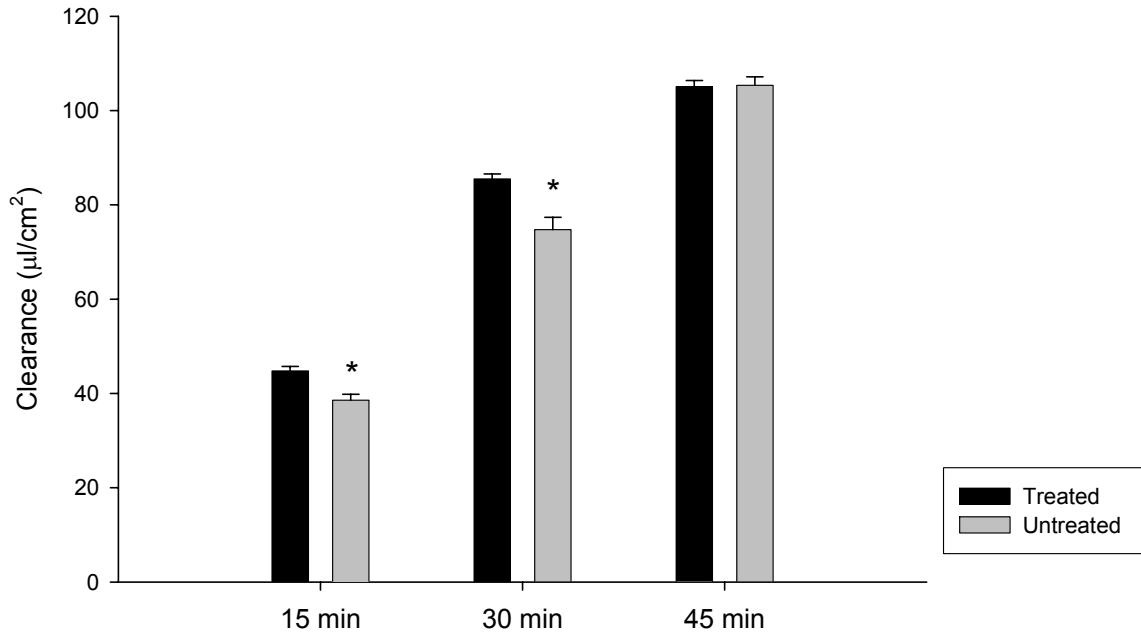
Figure 4.5.3. The Effects of Sodium Butyrate on FL Transport. To determine the effect of sodium butyrate on FL clearance, 5 mM sodium butyrate was added to the culture media of 3 HK-2 monolayers per incubation period 24 hours before transport studies were conducted. Monolayers grown on Transwell-Clear inserts were equilibrated for 10 min in TM, aspirated and placed in TM containing 4 µM FL for 15, 30 or 45 min. Upon expiration of the incubation period, media was sampled from both compartments per insert, 100 µl aliquots were assayed for radioactivity and clearance rates were calculated. *The differences in clearance are statistically significant as determined by Student's t-Test, $p < 0.05$. Each bar represents the mean clearance +/- SEM for 3 monolayers.
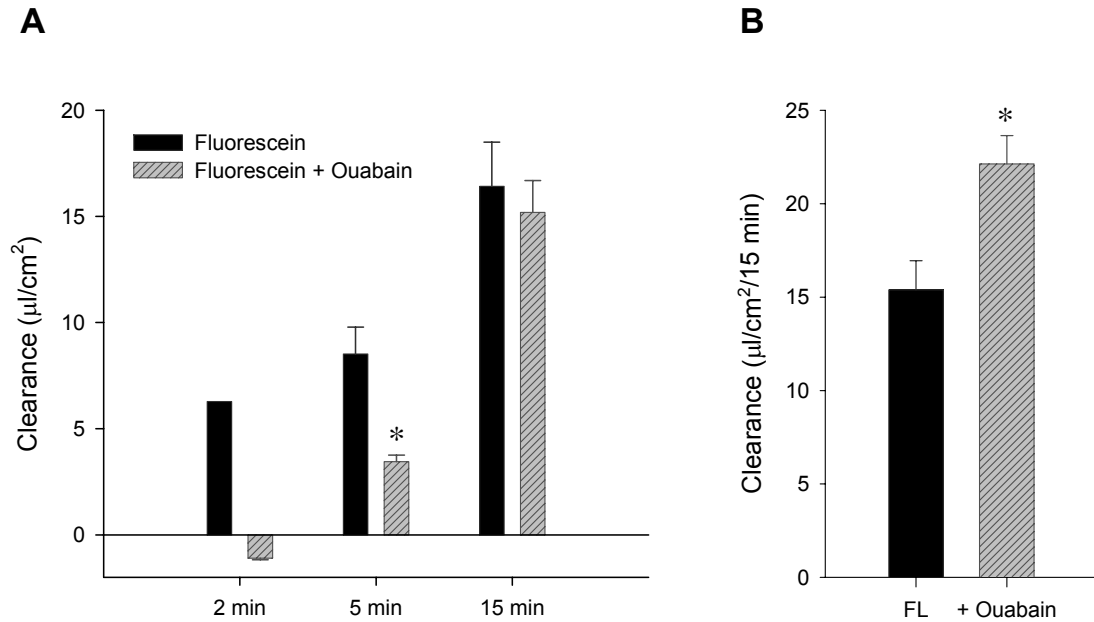
Figure 4.5.4. The Effect of Ouabain on FL Clearance. A) To determine the acute effects of ouabain on FL transport, 8 day old HK-2 monolayers were equilibrated for 10 min TM, aspirated, then incubated for 2, 5 or 15 min in 4 µM FL ± 100 µM ouabain on an orbital shaker at $37^{o}C$, 5% CO_2/95% air. Coincubation vs. control resulted in inhibition of FL clearance that diminished with time. There was no significant difference in FL clearance at 15 min; n = 3 treated, n = 2 for control. *At 5 min, ouabain significantly inhibited the clearance of FL; Student's t-Test, $p < 0.05$, n = 3 per group. The 2 min data was not statistically analyzed (n = 3 for treated, n = 1 for control); however, the control value was within range of prior 2 min clearance rates for FL. B) To determine the long term effects of ouabain on FL clearance, 7 day old HK-2 monolayers were preincubated for 30 min in TM with or without 100 µM ouabain. FL was then added to the BL compartment of each insert and monolayers were incubated for 15 min on an orbital shaker at $37^{o}C$, 5% CO_2/95% air. Aliquots from both compartments per insert were analyzed for fluorescence and the clearance, corrected for FLD diffusion, was determined. Preincubation with ouabain significantly increased the 15 min clearance of FL as analyzed by Student's t-Test, $p = 0.021$, n = 4 per group.
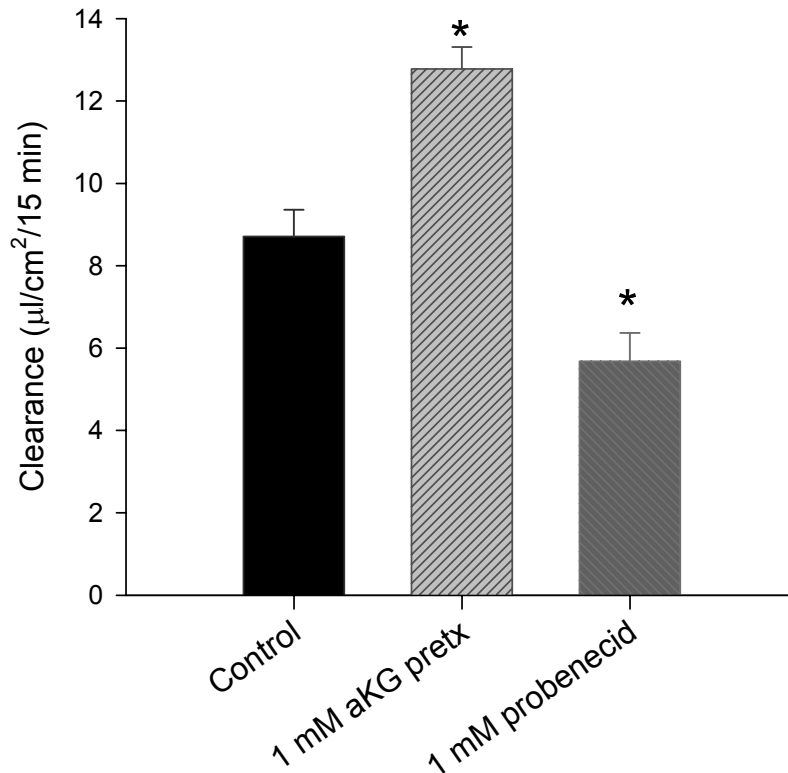
Figure 4.5.5. Effects of αKG Preincubation and Probenecid Coincubation on the Clearance of FL. A comparison of the FL clearance rates for HK-2 monolayers preincubated in αKG or coincubated in probenecid vs. control was performed on 5 day old HK-2 monolayers superseeded on Transwell-Clear inserts. All monolayers (3 per group) were aspirated and equilibrated in TM with or without αKG (1 mM) for 15 min. Monolayers were rinsed twice in TM and placed in TM with 4 μM FL with or without 1 mM probenecid in the BL compartments. After 15 min on an orbital shaker at 60 cycles/min, 37°C, 5% CO_2/95% air, samples were taken from both compartments per insert and 100 μl aliquots were assayed for fluorescence. Clearance of FL was corrected for FLD diffusion on parallel inserts. Preincubation with αKG resulted in a 47% increase and coincubation with probenecid resulted in 35% decrease in clearance of FL. *Differences in clearance were significantly different for treated vs. control as analyzed by One-Way ANOVA followed by a Dunnett's Test for Multiple Comparison vs. Control, $p < 0.05$.
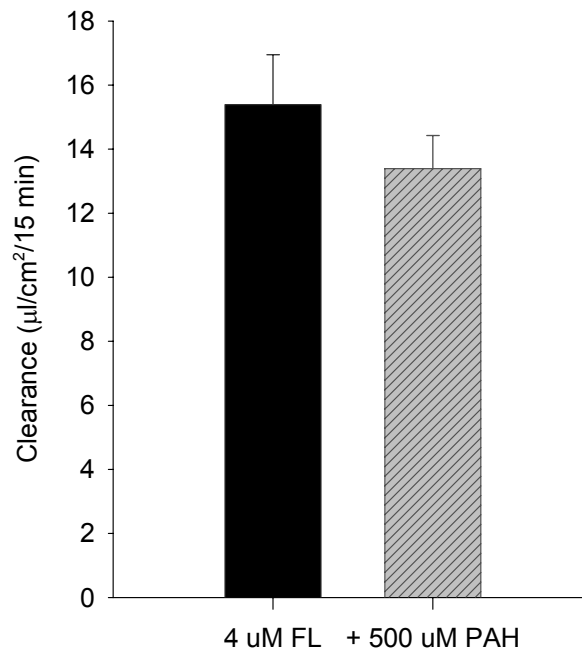
Figure 4.5.6. The Effect of PAH on the Clearance of FL. The effect of 500 μM PAH on the clearance of 4 μM FL was determined. Seven day old HK-2 monolayers grown on Transwell-Clear inserts (3 per group) were equilibrated for 10 min in TM, aspirated then placed in TM with 4 μM FL in the absence or presence of 500 μM PAH in the BL compartment. After 15 min on an orbital shaker at 60 cycles/min, 37^oC, 5% CO_2/95% air, samples were taken from both compartments per insert and 100 μl aliquots were assayed for fluorescence. Clearance rates were corrected for FLD diffusion on parallel inserts. PAH did not significantly decrease the clearance of FL at 15 min. The data were analyzed by Student's t-Test.
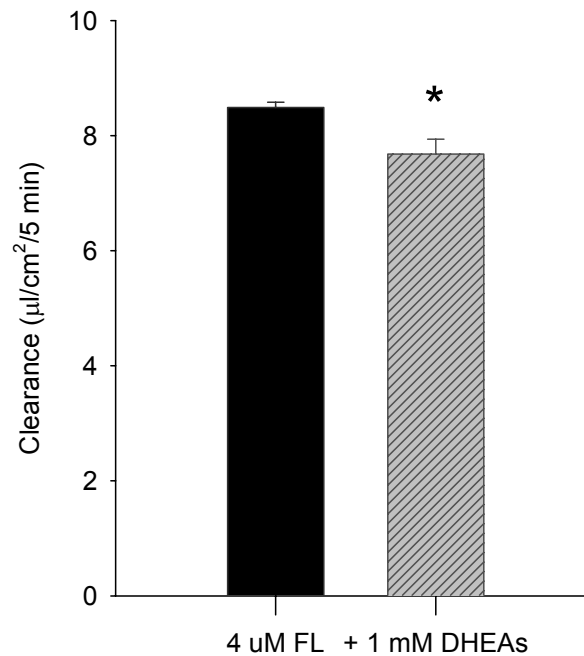
Figure 4.5.7. The Effect of DHEAS on the Clearance of FL. The effect of 1 mM DHEAS on the clearance of 4 µM FL was determined. Five day old HK-2 monolayers grown on Transwell-Clear inserts were equilibrated for 10 min in TM, aspirated then placed in TM with 4 µM FL in the absence or presence of 1 µM DHEAS in the BL compartment. After 15 min on an orbital shaker at 60 cycles/min, 37°C, 5% CO_2/95% air, samples were taken from both compartments per insert and 100 µl aliquots were assayed for fluorescence. Clearance rates were corrected for FLD diffusion on parallel inserts. DHEAS caused a slight (10%) but significant decrease in the clearance of FL at 15 min as indicated by the asterisk (*). The data were analyzed by Student's t-Test, $p < 0.05$, n = 2 per group.

Transport of OAT1 and OAT3 Substrates

The uptake and/or clearance of PAH as the model OAT1 substrate and DHEAS and ES as the model OAT3 substrates were studied. The ability of a substrate to inhibit its own uptake (labeled vs. addition of unlabeled), demonstrates a competitive, protein-mediated, uptake process. This was demonstrated for all three substrates, PAH, ES and DHEAS.

PAH

To determine if PAH transport is protein-mediated, unlabeled PAH was coincubated with labeled PAH and the uptake determined. The addition of 1 mM PAH to 4.2 μM [^{14}C]PAH inhibited the uptake of [^{14}C]PAH by 50% (Figure 4.6.1).

The OAT1 trans-stimulatory substrate αKG showed inhibitory rather than stimulatory effects on the uptake and clearance of 70 μM PAH when preloaded into HK-2 monolayers (Figure 4.6.2). The αKG effects on PAH clearance were not as great as the effects on uptake (59% decrease in uptake vs. 22% decrease for clearance). Although the preloaded monolayers were rinsed twice with TM before incubating in PAH, the results are consistent with inhibitory uptake by αKG and may be due to residual dicarboxylate on the BLM of the cells. In the same figure, 1 mM probenecid was shown to inhibit the uptake of 70 μM PAH by 73% and the clearance of PAH by 15%. Diminished differences in clearance than uptake are likely due to paracellular diffusion of substrate across the monolayer.

Because the αKG results were inhibitory rather than stimulatory, as expected, a subsequent experiment was performed with another dicarboxylate, glutarate, in a shorter incubation period. Similar inhibitory effects were seen for 5 min uptake of 4 μM PAH by monolayers preloaded with glutarate or coincubated with 1 mM probenecid (Figure 4.6.3). As with the αKG experiment, the preloaded monolayers were rinsed twice before the incubation. However, these results also suggest inhibition of uptake by residual dicarboxylate.

In summary for PAH transport: Transport of PAH demonstrates self-inhibition in the HK-2 model, consistent with protein-mediated transport. PAH transport was inhibited by probenecid and by preloaded dicarboxylates.

ES

Uptake of the prototypical OAT3 substrate [^{3}H]ES (3.6 nM) in the presence of unlabeled ES (100 µM) was inhibited by 50% compared to control (Figure 4.6.4 A) whereas the OAT3 substrate E$_2$17βG (100 µM) had no effect on ES uptake (Figure 4.6.4B). The inability of E$_2$17βG to inhibit uptake of ES is not surprising in that the affinity of ES for OAT3 is reported to be very high (K$_m$ = 3 µM; Cha et al., 2001). Low solubility of E$_2$17βG prohibited experimentation with a high concentration, such as 1 mM E$_2$17βG.

Probenecid caused a greater inhibitory effect on the clearance of ES than on the uptake of ES (Figure 4.6.5). This finding suggests a decreased permeability of the BBM to ES relative to control, such that probenecid inhibits both the uptake and efflux of ES. The inhibitory effect of probenecid at the BBM would create an increased steady state concentration of ES intracellularly, such that the true inhibitory effect at the BLM is not reflected in net accumulation of ES. This is a confounding problem inherent in systems with both BLM and BBM transporters, unlike the single transporter transfectant models.

In summary for ES: Transport of ES exhibits self-inhibition consistent with a protein-mediated process. E$_2$17βG (100 µM) shows no inhibitory effect on uptake of ES whereas probenecid inhibits both uptake and, to a greater extent, clearance of ES.

DHEAS

Transport of the OAT3 substrate DHEAS (2.2 nM) was inhibited to a greater extent by unlabeled DHEAS (100 µM) than by equimolar ES (Figure 4.6.6; 45%

99

inhibition for DHEAS vs. no significant inhibition for ES). This experiment suggests that DHEAS has a higher affinity for the transporter than does ES and/or that the substrates are transported by multiple transporters that do not transport the other substrate or that display noncompetitive transport of both substrates.   Higher affinity of DHEAS than ES for OAT3 is consistent with the findings of Cha et al. (2001).
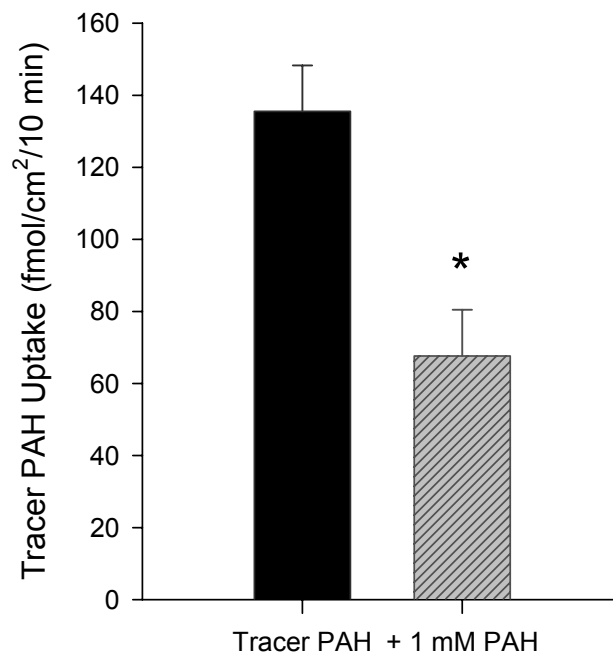
Figure 4.6.1. The Effect of Unlabeled PAH on the Uptake of [^{14}C]PAH. The effect of unlabeled PAH on the uptake of radiolabeled PAH was determined. Six - 9 day old HK-2 monolayers superseeded on Transwell-Clear inserts were rinsed with WBTM then placed in WBTM containing 4.2 µM [^{14}C]PAH with or without 1 mM unlabeled PAH in the BL compartments. Monolayers were incubated in a shaking water bath at 37°C. After 10 min, uptake was terminated by immersing the inserts into ice-cold WBTM. Inserts were rinsed with ice-cold WBTM and aspirated. Cells were lysed and assayed for radioactivity to determine uptake. The 50% decrease in the uptake of [^{14}C]PAH in the presence of unlabeled PAH was statistically significant as determined by One-Way ANOVA for Repeated Measures, $p < 0.05$, n = 5 per group.

A   Uptake of 70 μM PAH   **B**   Clearance of 70 μM PAH
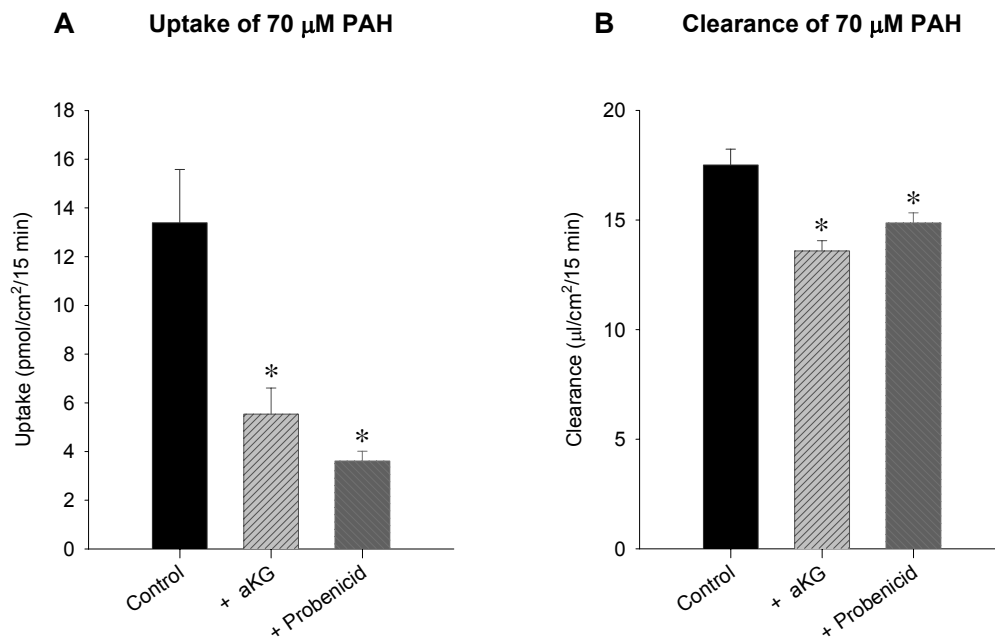
Figure 4.6.2.   The Effects of αKG Preincubation and Probenecid Coincubation on PAH Transport.   To determine the effects of αKG preincubation and probenecid coincubation on the uptake and clearance of PAH, nine day old HK-2 monolayers superseeded on Transwell-Clear inserts were equilibrated in TM with or without 1 mM αKG for 15 min.   Monolayers were then rinsed 2 x with TM and placed in TM containing 70 μM PAH (~ 4 μM [^{14}C]PAH) with or without 1 mM probenecid in the BL compartments.   After 15 min on an orbital shaker at 60 cycles/min, 37°C, 5% CO_2/95% air, samples were taken from the A and BL compartments, the inserts were placed into ice-cold TM and rinsed 2 x with ice-cold TM.   Cells were lysed with 0.1 N NaOH, assayed for radioactivity and uptake was calculated.   Aliquots (30 μl) of the BL and A media were assayed for radioactivity and clearance rates were determined.   Both treatments resulted in a significant decrease in uptake and clearance of PAH as indicated by the asterisk (*).   For both uptake and clearance the data were analyzed by One-Way ANOVA followed by Dunnett's Test for Multiple Comparisons vs. Control, $p < 0.05$, n = 3 per treatment.   The αKG and probenecid treatments resulted in 59% and 73% decreases in the uptake and 22% and 15% decreases in the clearance of PAH, respectively.
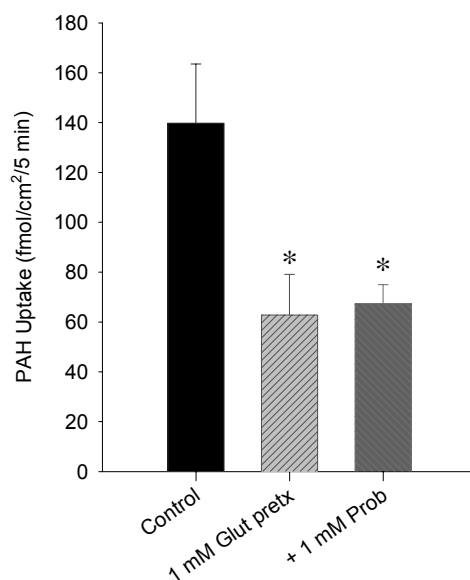
Figure 4.6.3. **The Effects of Glutarate Preincubation and Probenecid Coincubation on PAH Transport.** To determine the effects of glutarate preincubation and probenecid coincubation on the uptake of PAH, glutarate (final concentration, 1 mM) or an equivolume of WBTM was added to the culture media of both BL and A compartments of 5 day old HK-2 monolayers superseeded on Transwell-Clear inserts. After a 30 min preincubation period on an orbital shaker at 60 cycles/min, 37°C, 5% CO_2/95% air, inserts were rinsed X 2 with WBTM then placed in WBTM containing 4 µM [^{14}C]PAH with or without 1 mM probenecid in the BL compartments. Monolayers were incubated in a shaking water bath at 37°C. After 5 min, uptake was terminated by immersing the inserts in ice-cold WBTM. Inserts were rinsed with ice-cold WBTM, aspirated, and cells were lysed in 1% SDS/0.1N NaOH then assayed for radioactivity to determine uptake. *A significant decrease in mean uptake of PAH was found for both treated groups by One-Way ANOVA with Dunnett's Post Test for Multiple Comparison vs. Control, $p < 0.05$. n = 3 per treatment.

A

B
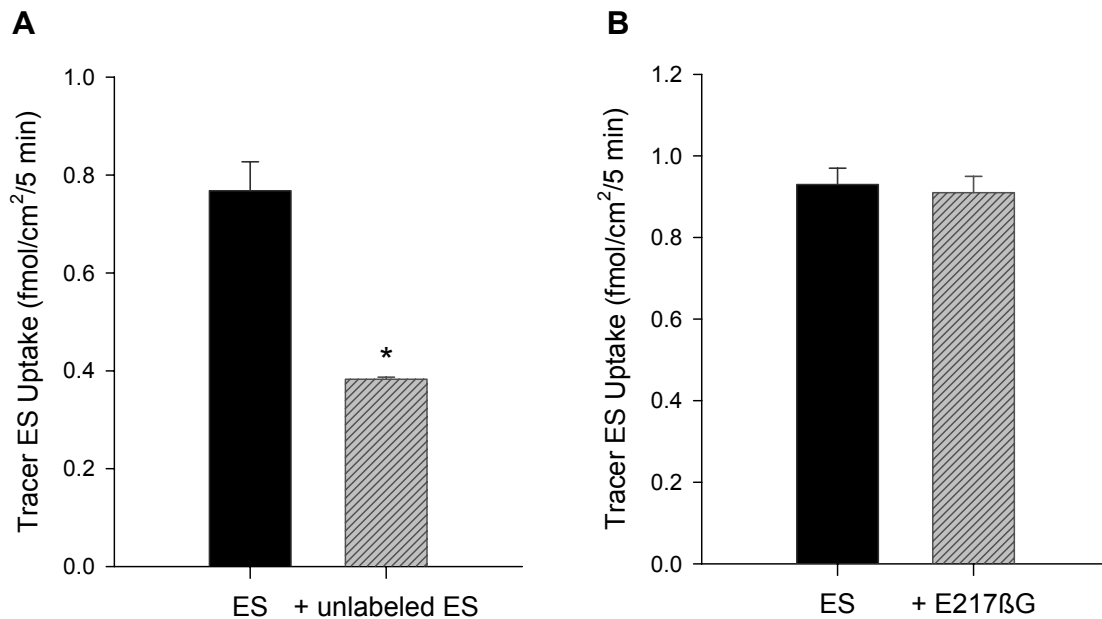
Figure 4.6.4. The Effects of Unlabeled ES and $E_2 17\beta G$ on the Uptake of ES.
In separate studies, the uptake of $[^3H]ES$ was determined in the presence or absence of unlabeled ES and $E_2 17\beta G$. HK-2 monolayers superseeded on Transwell-Clear inserts were rinsed with WBTM then placed in WBTM containing 3.6 nM $[^3H]ES$ with or without 50 µM unlabeled ES (A) in the BL compartments; or 4 nM $[^3H]ES$ with or without 100 µM $E_2 17\beta G$ (B), in the BL compartments. Monolayers were incubated in a shaking water bath at $37^o C$. After 5 min, uptake was terminated by immersing the inserts into ice-cold WBTM. Monolayers were rinsed with ice-cold WBTM and aspirated. Cells were lysed in 1% SDS, 0.1 N NaOH and assayed for radioactivity to determine uptake. The 50% decrease in the uptake of $[^3H]ES$ in the presence of unlabeled ES by 8 day old monolayers was statistically significant as determined by Student's t-Test, $p < 0.05$; n = 3 per group. $E_2 17\beta G$ had no effect on the uptake of $[^3H]ES$ by 5 day old monolayers, n = 3 per group.
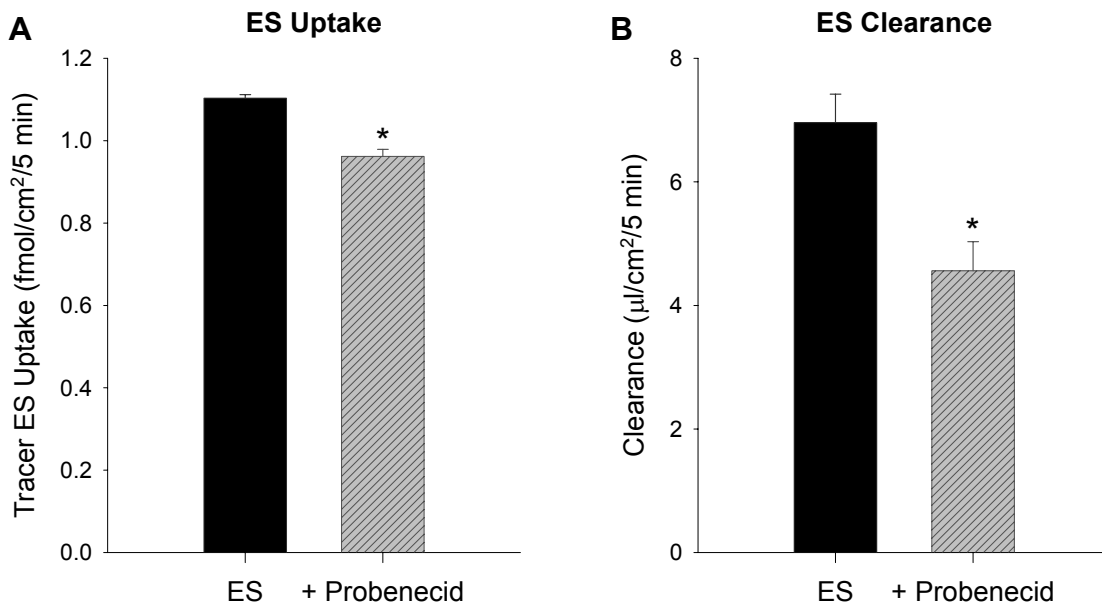
Figure 4.6.5. The Effect of Probenecid on the Transport of Estrone Sulfate. To study the uptake and clearance of ES in the absence or presence of probenecid, 4 day old HK-2 monolayers superseeded on Transwell-Clear inserts were rinsed with WBTM then placed in WBTM containing 3.6 nM [^{3}H]ES with or without 1 mM probenecid in the BL compartments. Monolayers were incubated in a shaking water bath at 37°C. After 5 min, uptake was terminated by transferring the inserts into ice-cold WBTM. Monolayers were rinsed with ice-cold WBTM and aspirated. Cells were lysed in 1% SDS, 0.1 N NaOH and assayed for radioactivity to determine uptake. The uptake of ES was inhibited only 13%, whereas, the clearance was decreased by 44% in the presence of probenecid. *Both decreases were significant as determined by Student's t-Test, $p < 0.05$. Each bar represents the mean uptake $\pm$ SEM (A) or the mean clearance $\pm$ SEM (B); n = 2 for uptake control; n = 3 for uptake treated, clearance control and treated.

**Effects of Unlabeled DHEAs and ES
on the Uptake of 2.2 nM DHEAs**
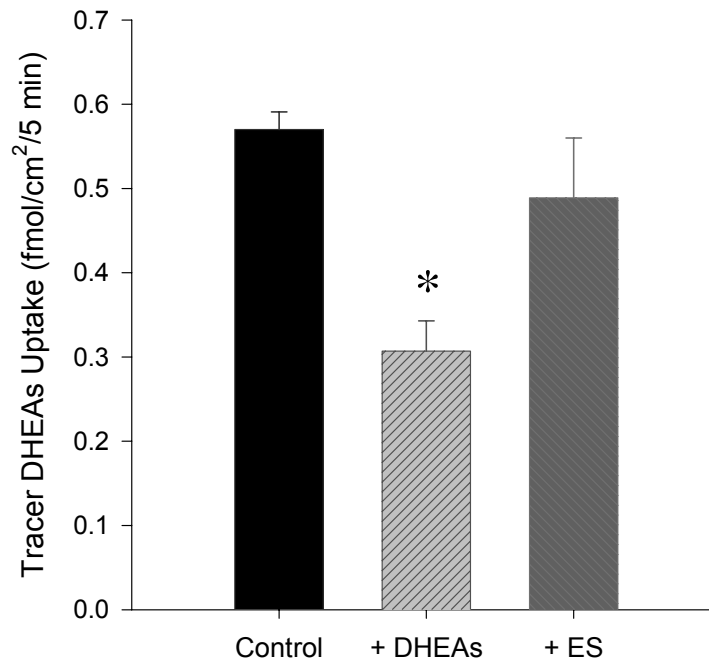
**Figure 4.6.6.   The Effects of Unlabeled DHEAS and ES on the Uptake of
[³H]DHEAS.**   To determine the effects of DHEAS and ES on the uptake of
DHEAS, 8 day old HK-2 monolayers superseeded on Transwell-Clear inserts were
rinsed in WBTM then placed in WBTM with 2.2 nM [³H]DHEAS +/- 100 µM DHEAS
or 100 µM ES added to the BL compartments. Monolayers were incubated for 5
min at 37°C in a shaking water bath, transferred to wells containing ice-cold TM,
rinsed in ice-cold TM, lysed with 1% SDS/0.1 N NaOH and assayed for
radioactivity. [³H]DHEAS uptake was statistically inhibited by 46% in the presence
of 100 µM unlabeled DHEAS. The 14 percent inhibition demonstrated by 100 µM
ES was not significant.   Each bar represents the mean uptake + SEM for 3
monolayers. Statistics were analyzed by One-Way ANOVA with Dunnett's Test for
Multiple Comparisons vs. Control, $p < 0.05$.

AG Transport by HK-2 Cells

Initial AG transport studies were conducted at 15 min. After performing the time-course uptake study, it was decided to decrease the incubation period to 5 min to minimize compensatory effects in the system and work within the linear phase of uptake. Initial AG transport studies were also conducted with relatively high concentrations of AG (50-100 µM). Later studies were conducted with tracer AG only (4-9 µM) to maximize modulatory effects on AG transport. The results presented below are grouped by modulator rather than chronologically such that sections may contain data with varying incubation periods or AG concentration levels.

The time-course uptake of AG exhibited slightly biphasic uptake with nearly linear uptake from 2 to 10 min then rapid decline in rate of uptake between 10 to 15 min (Figure 4.7.1). The uptake was best fit to a single rectangular hyperbolic regression without a zero or first order term for nonspecific binding and/or diffusion. When a nonspecific term was included in the regression, the term constant was negative suggesting a reabsorptive process or an increase in the rate of apical efflux with time. A correlation coefficient, R^2 = 0.99, for the regression without the nonspecific term was greater than that for the regression with the nonspecific term (0.95, first order; 0.94, zero order); thus, the regression excluding a nonspecific term as shown in Figure 4.7.1 is the best fit.

Because uptake was nearly linear from 2 to 10 min, an intermediate time, 5 min was selected for the concentration-dependent study. Concentration-dependent uptake of AG also displayed biphasic kinetics (Figure 4.7.2). At high concentrations (> 1 mM), net intracellular accumulation of labeled AG no longer decreased, but rapidly increased. This finding is consistent with that of AG disposition in the dog with net reabsorption at high concentrations of AG (Duggin and Mudge, 1975). Analysis of the concentration-dependent uptake of AG for concentrations up to 1 mM unlabeled AG fit a Michaelis-Menten regression with

$R^2 = 0.959$, $K_m = 260$ µM and $V_{max} = 27.2$ pmol/cm^2/5 min. These data, however, would not fit to a Berteloot regression.

Because the activity measured for the uptake of AG in the previous study was so close to background and the data failed to fit a Berteloot regression analysis, additional concentration-dependent studies were performed using a higher concentration of [^{14}C]AG with unlabeled concentrations of AG up to 1 mM. Figure 4.7.3 represents the combined data from 2 experiments. These data fit both a Berteloot ($R^2 = 0.863$) and a Michaelis-Menten ($R^2 = 0.995$) regression analysis (Figure 4.7.3, graph A and B, respectively). The Berteloot regression yields a K_m of 326 µM, V_{max} of 6.1 pmol/cm^2/5 min vs. a K_m of 1.44 mM, V_{max} of 16.4 pmol/cm^2/5 min for the Michaelis-Menten regression. Together, the regression analyses indicate low affinity transport of AG.

To determine if the increase in intracellular [^{14}C]AG accumulation when challenged with high concentrations of unlabeled AG occurred by reabsorption at the BBM, a dynamic study was performed in which the apical medium was continuously exchanged for fresh medium (Figure 4.7.4). It was found that AG effluxed into the apical medium had no effect on the net accumulation of intracellular AG, supporting mechanisms other than reuptake at the BBM to explain the increasing intracellular accumulation of AG at higher concentrations of AG in the BL medium.

To determine the effect of intracellular AG on AG uptake and clearance, HK-2 monolayers were preloaded with unlabeled AG or [^{14}C]AG by incubation in equimolar AG or [^{14}C]AG medium for 90 min. Each group was then rinsed and placed in equimolar labeled AG for the unlabeled preloaded cells or unlabeled AG for the preloaded [^{14}C]AG cells, such that each group was the exact complement to the other. A control group with no preloading was run on parallel monolayers (Figure 4.7.5). Neither uptake nor clearance of [^{14}C]AG were significantly altered for the preloaded AG group compared to control. Because these effects were not

significant, no conclusions can be made, however, had there been a significant increase in transport, it could be explained by a trans-stimulation of AG uptake at the BLM with or without an upregulation of efflux and/or uptake transporters. What can be concluded is that intracellular AG does not inhibit the uptake or the efflux of AG. Comparison of A vs. BL efflux of the [^{14}C]AG preloaded cells reveals that A efflux was 1.46 times greater than BL efflux suggestive of net secretion of AG. Comparison of A vs. BL uptake demonstrates greater uptake from the A vs. the BL compartment (Figure 4.7.6). Higher efflux and greater uptake from the BBM indicate polarization of the monolayers and suggest greater permeability of the BBM vs. BLM to AG such that transport at the BLM is the rate limiting step in transepithelial transport of AG.

Temperature-dependent transport was demonstrated by total inhibition of AG clearance at 4°C, yet only a tendency toward lower net AG accumulation was suggested (Figure 4.7.7). Net accumulation at low temperature could be explained by nonspecific binding or by uptake processes (gradient-dependent) that are less sensitive than are efflux processes (ATP-dependent) to temperature. A greater effect on efflux than on uptake would increase the net intracellular accumulation of AG, thus, masking the effect of decreased uptake. This study indicates that AG transport is protein-mediated.

To study the effects of OAT1 and/or OAT3 modulation on the transport of AG, studies with ouabain, probenecid and the prototypical substrates were conducted. AG/ouabain coincubation resulted in a 2.5-fold increase in the 15 min AG BL-A clearance vs. no significant effect in A-BL clearance compared to the AG treatments (Figure 4.7.8 A). Since the expected ouabain effect for OAT1-mediated transport would be decreased BL-A clearance, this experiment suggests AG uptake at the BLM mediated by transporter(s) other than OAT1 with a possible upregulation of transporters at the BLM or BBM rather than inhibition by ouabain. The effect of preincubation and coincubation with ouabain had no significant effect on AG transport (Figure 4.7.8 B).

To determine the effect of OAT1/OAT3 inhibition on AG transport, 15 min probenecid and AG coincubation experiments were performed. Probenecid (1 mM) was found to cause a significant decrease in the net accumulation of tracer AG (4 µM) while it tended to cause an increase in AG clearance (Figure 4.7.9). Although there was no significant effect of probenecid on AG clearance, that the efflux did not instead decrease in proportion to the net accumulation implies that the permeability of the BBM was increased. An increase in permeability at the BBM is quantitatively demonstrated by a permeability-surface area product (PSa) 2.4 times greater than control. The effect of probenecid, then, may be at the BBM with little or no effect at the BLM.

To determine if probenecid had similar effects from the A vs. BL compartment, 1 mM probenecid was added to the A or to the BL compartment with 50 µM AG in the BL compartment (Figure 4.7.10 A). Probenecid in the BL compartment caused a decrease in net accumulation of AG. However, when probenecid was added to the A compartment, there was no significant effect on net AG accumulation from the BLM compared to control. AG uptake from the BBM (Figure 4.7.10 B) demonstrates that probenecid plays no inhibitory role on BBM uptake transporters when coincubated with AG in the A compartment.

At higher concentrations of AG (100 µM), 1 mM probenecid had no significant effect on 5 min BL-A AG clearance (Figure 4.7.11).

To determine if a dicarboxylate exchange mechanism is involved in the transport of AG, glutarate preloading experiments were run. Glutarate (90 min preincubation) caused no significant increase in either uptake or clearance of 8 µM AG compared to control (Figure 4.7.12).

PAH and FL were coincubated with AG to demonstrate OAT1 and/or OAT3 interactions. AG (200 µM) was found to have a stimulatory effect on the 15 min clearance of 4 µM FL (Figure 4.7.13) whereas no effect was found for AG on the 5 min clearance of 4 µM PAH (Figure 4.7.14 B). The differences in effect may be

due to differences in transport of FL vs. PAH or it may be due to an upregulation in transporters with time. Interestingly, the net intracellular accumulation of PAH was decreased by AG suggesting possible inhibitory effects at OAT1 or OAT3, or stimulatory effects of PAH efflux at the BBM (Figure 4.7.14 A).

ES was used to explore inhibitory effects at OAT3. AG (1 mM) had no effect on the uptake of 4 nM ES (Figure 4.7.15), whereas 100 µM ES caused a 32% decrease in the net accumulation of AG (Figure 4.7.16) and tended to decrease AG clearance. ES is the prototypical substrate for OAT3 and, therefore, would likely inhibit the BL uptake of AG, if AG is an OAT3 substrate. If AG and ES are competitive for the same sites on the transporter and OAT3 is the sole transporter available to both substances, one would expect mutual inhibition of transport. Recalling that 100 µM ES inhibited low concentration uptake of ES by 50% in this model and the K_m for AG is approximately 300-1000 µM, inhibition of 9 µM AG much greater than 50% would be expected with the addition of 100 µM ES and tracer ES uptake should be inhibited by about 50% by 1 mM AG. Assuming transport of ES by OAT3 in this model, unless the substrates bind at different sites on the transporter or multiple transporters are responsible for ES and AG uptake, OAT3 transport of AG is likely very low in HK-2 cells. ES uptake mediated by multiple transporters is supported by the study of Sweet et al. (2002) which demonstrated that uptake of ES in mouse renal cortical slices was inhibited 56% by probenecid and was transported at 53% of rates of wild-type control in renal cortical slices of Oat3-knockout mouse.

The effects of the OAT3 substrate DHEAS on the transport of AG are AG concentration- and/or time-dependent. At 5 min, 1 mM DHEAS caused a 42% decrease in the clearance of 100 µM AG (Figure 4.7.17). To minimize possible upregulation of BLM or BBM transporters, the DHEAS (1 mM) and PAH (1 mM) study was conducted at 2 min. The AG concentration was increased to 20 µM to ensure readings were well above background. At 2 min, neither 1 mM PAH nor 1 mM DHEAS had an effect on the uptake or the clearance of 20 µM AG (Figure

4.7.18). This study indicates that primary uptake of AG is not likely mediated by OAT1 nor OAT3 unless AG binds at different sites on the transporters than do PAH and DHEAS.

To assess the long term effects of DHEAS on AG transport, monolayers were treated for 24 hours with 1 mM DHEAS (Figure 4.7.19). A 76% significant increase in AG transport was shown for DHEAS preincubated monolayers, implying upregulation of BLM and possibly BBM transporters. This effect could also be explained by trans-stimulation from preloaded DHEAS.

The effects of the glucuronide conjugates, MUG and $E_2 17\beta G$, on the transport of AG were studied as presented in Figure 4.7.20. No significant effect in net accumulation or transepithelial transport was demonstrated for either glucuronide. Lack of inhibition of AG uptake by $E_2 17\beta G$, a substrate for OAT3, is consistent with the results of the ES and DHEAS studies indicating that AG is likely not a good substrate for OAT3, multiple transporters are involved, or that AG binds at a different site on the transporter than does $E_2 17\beta G$.

In summary for AG transport: HK-2 cells exhibit biphasic transport for both time- and concentration-dependent uptake. The increasing rate of intracellular accumulation of AG at concentrations above 1 mM is consistent with reabsorption of AG as reported by Duggin and Mudge (1975). Temperature-dependent studies indicate that AG movement across the HK-2 monolayer is transporter-mediated. The BBM of HK-2 cells is more permeable to AG than is the BLM as evidenced by higher uptake from the A vs. BL compartment and higher BBM vs. BLM efflux from preloaded cells. Lack of inhibition of AG uptake by intracellular AG and greater AG efflux across the BBM than the BLM were demonstrated in cells preloaded with AG. A tendency for increased AG clearance when coincubated with ouabain or probenecid suggests possible upregulation of transporters whereas decreased clearance rates at high concentrations of AG suggest that probenecid may inhibit BLM uptake and/or BBM efflux. ES results suggest possible low affinity AG

transport by OAT3; however, PAH and DHEAS studies suggest uptake of AG primarily by transporters other than OAT1 or OAT3. Furthermore, DHEAS studies also indicate modulatory effects over time with decreased transepithelial transport of AG at higher concentrations of AG and DHEAS. The glucuronides, MUG and $E_2$17βG, caused no significant effect on net AG accumulation or clearance. No inhibition at the BLM by $E_2$17βG also suggests a noncompetitive process or little to no transport of AG by OAT3.
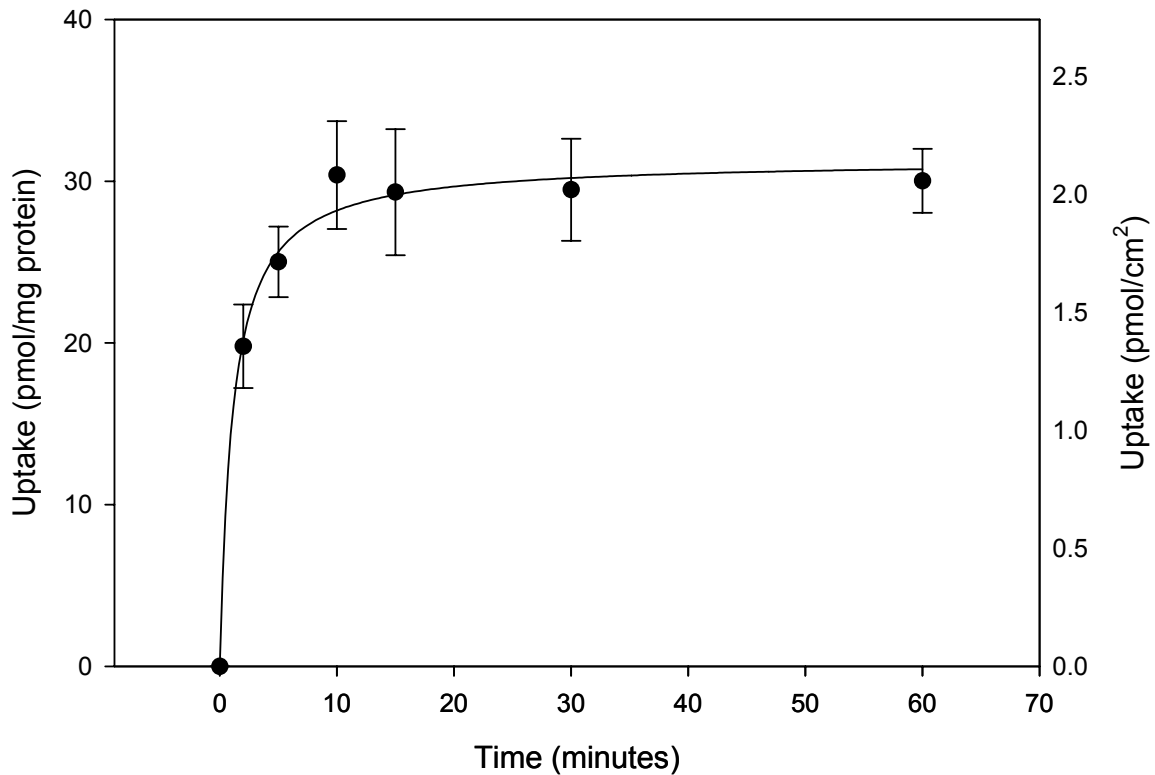
Figure 4.7.1. Time Course Uptake of 50 µM AG. The uptake of 50 µM AG was performed by incubating 6-7 day old HK-2 monolayers superseeded on Transwell-Clear inserts for 2, 5, 15, 30 and 60 min in WBTM containing 50 µM AG in the BL compartments. After 5 min in a shaking water bath at 37°C, inserts were transferred to ice-cold TM, rinsed with ice-cold TM, lysed in 0.1 N NaOH and assayed for radioactivity. Parallel monolayers were used for protein determination. Each data point represents the mean AG uptake +/- SEM for 3 monolayers. The plot includes a single rectangular hyperbolic regression of the data that can be expressed by the equation: Uptake = (3.131 pmol/mg protein x time)/(1.11 + time); $R^2 = 0.99$.
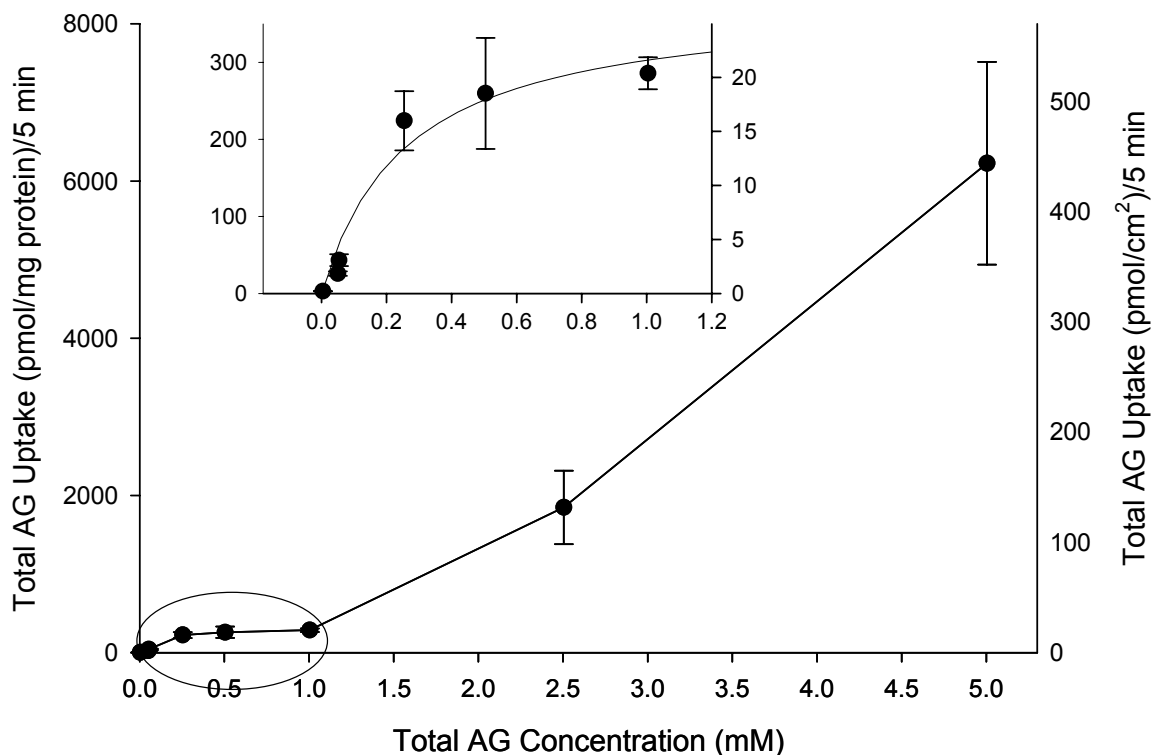
Figure 4.7.2. Biphasic Concentration-Dependent AG Uptake - Study I. A concentration-dependent study was conducted using 4 μM [^{14}C]AG (tracer) in the presence of 0, 0.046, 0.05, 0.25, 0.5, 1, 2.5 and 5 mM unlabeled AG. Seven day old HK-2 monolayers superseeded on Transwell-Clear inserts were rinsed in WBTM then placed in WBTM containing tracer and unlabeled AG in a 37°C shaking water bath. After 5 min, inserts were transferred to ice-cold TM, rinsed with ice-cold TM, lysed in 0.1 N NaOH, assayed for radioactivity and uptake was calculated. Parallel inserts were used for protein determination. Each data point represents the mean total AG uptake +/- SEM for 3 monolayers. The plot depicts total AG uptake vs. total AG concentration indicating a biphasic accumulation of intracellular AG which first plateaus with increasing concentration of AG in the incubation medium, then rapidly rises at the highest concentrations tested. The inset depicts the first 6 data points and includes a Michaelis-Menten regression curve. The regression analysis yields V_{max} = 27.2 pmol/cm^2/5 min or 381.6 pmol/mg/5 min and K_m = 260 μM with an R^2 = 0.959.
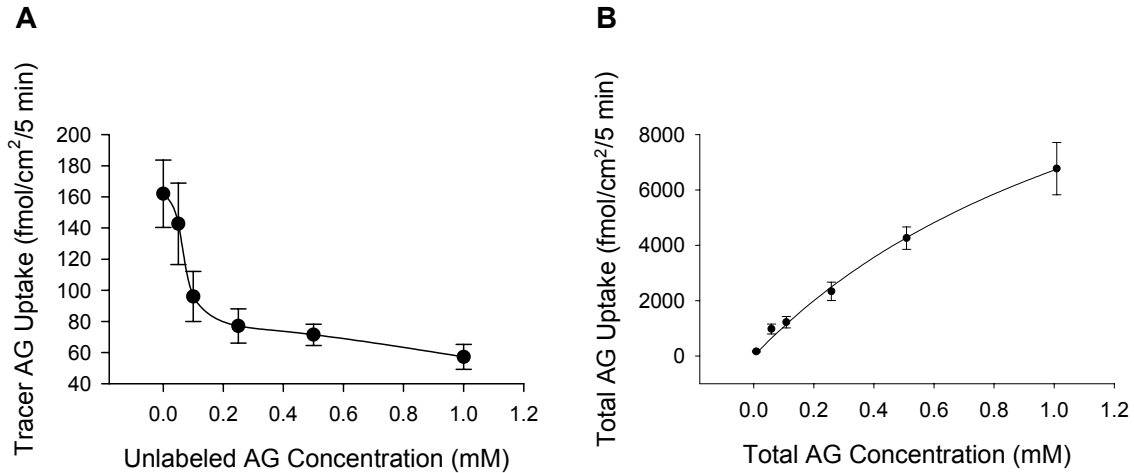
Figure 4.7.3. Concentration Dependent Uptake of AG - Study II. The concentration-dependent uptake for AG was evaluated using 8.5 µM [^{14}C]AG (tracer) in the presence of 0, 0.05, 0.1, 0.25, 0.5, and 1 mM unlabeled AG. Five to 7 day old HK-2 monolayers superseeded on Transwell-Clear inserts were rinsed in WBTM then placed in WBTM containing tracer and unlabeled AG in a 37°C shaking water bath. After 5 min, inserts were transferred to ice-cold TM, rinsed with ice-cold TM, lysed in 1%SDS/0.1 N NaOH and assayed for radioactivity from which uptake was calculated. Both graphs represent the same data, but expressed as tracer and unlabeled AG (A) or total AG (B). Each data point represents the mean AG uptake +/- SEM for 7 monolayers. Graph A is a plot of the uptake of tracer AG vs. unlabeled AG concentration. A Berteloot regression analysis for this data yields the kinetic constants, V_{max} = 6.1 pmol/cm^2/5 min and K_m = 326.3 µM AG with an R^2 = 0.863. Graph B is a plot of total AG uptake vs. total AG concentration and includes a Michaelis-Menten regression curve. Michaelis-Menten regression analysis gives V_{max} = 16.4 pmol/cm^2/5 min) and K_m = 1.44 mM with an R^2 = 0.995.
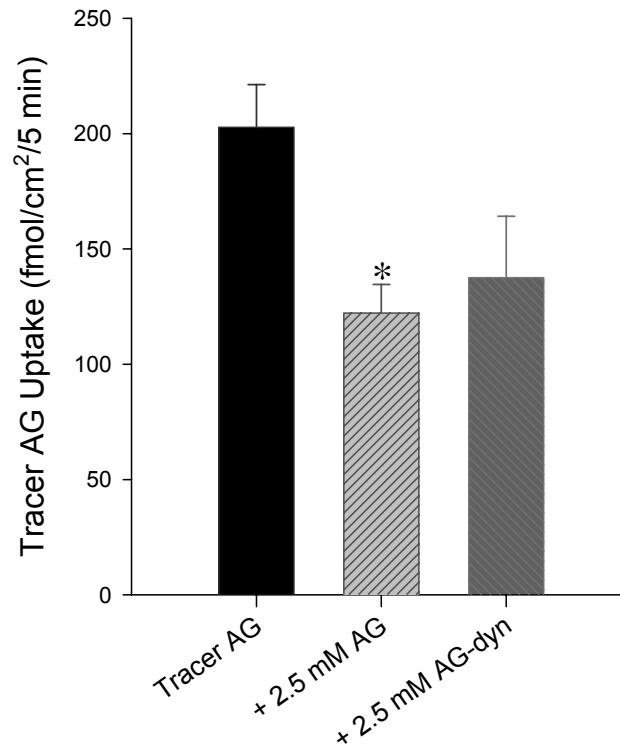
Figure 4.7.4. The Effects of Unlabeled AG on the Uptake of [^{14}C]AG - Dynamic vs. Static Apical Compartment. The uptake of 9 μM [^{14}C]AG (tracer) in the presence or absence of a high concentration of unlabeled AG (2.5 mM) was determined using 5 day old HK-2 monolayers superseeded on Transwell-Clear inserts. Monolayers were rinsed in WBTM then placed in WBTM containing tracer +/- unlabeled AG in the BL compartments and incubated in a 37°C shaking water bath for 5 min. For the dynamic (dyn) group, the medium in the A compartment was continuously exchanged for fresh WBTM. The monolayers were placed in ice-cold TM, rinsed with ice-cold TM, lysed in 1%SDS/0.1 N NaOH and assayed for radioactivity. *Tracer AG uptake was significantly inhibited by the presence of 2.5 mM AG as analyzed by a Student's t-Test, p = 0.022. Data failed to achieve significance by One-Way ANOVA for the 3 groups. Each bar represents the mean uptake +/- SEM for 3 monolayers.

117
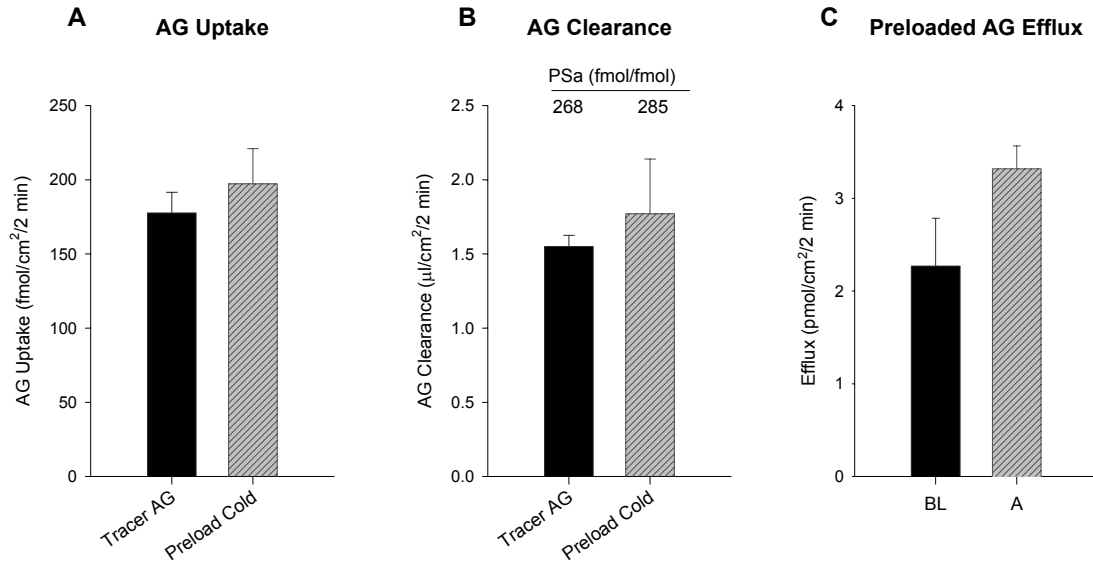
Figure 4.7.5. The Effects of Preloaded AG on AG Transport. To determine the effects of preloaded AG on the transport of AG, 5 day old HK-2 monolayers superseeded on Transwell-Clear inserts were preloaded by 90 min incubation in WBTM containing 20 μM [^{14}C]AG or 20 μM unlabeled AG on an orbital shaker at 60 cycles/min at 37°C, 5% CO_2/95% air. Monolayers were rinsed in WBTM, placed in WBTM with the BL compartments containing either 20 μM unlabeled AG, for monolayers preloaded with radiolabeled AG; or 20 μM [^{14}C]AG (tracer), for control monolayers and monolayers preloaded with unlabeled AG. After 2 min in a 37°C shaking water bath, media was sampled from both compartments per insert and the monolayers were placed into ice-cold TM, rinsed with ice-cold TM, lysed with 1% SDS/0.1 N NaOH and assayed for radioactivity. Uptake was then calculated. Aliquots (50 μl) of the BL and A compartments were assayed for radioactivity and the clearance rates and efflux were calculated. There was no significant difference in the uptake (A) or the clearance (B) of tracer AG for control vs. preloaded monolayers. (A) Each bar represents the mean of uptake +/- SEM for 4 control monolayers and 3 monolayers preloaded with unlabeled AG. (B) Each bar represents the mean clearance +/- SEM for 3 control and 4 monolayers preloaded with unlabeled AG. (C) Their was no statistical significance for A vs. BL efflux of preloaded tracer AG. Each bar represents the mean efflux +/- SEM for 4 monolayers.

118

A

AG Uptake

B

AG Clearance
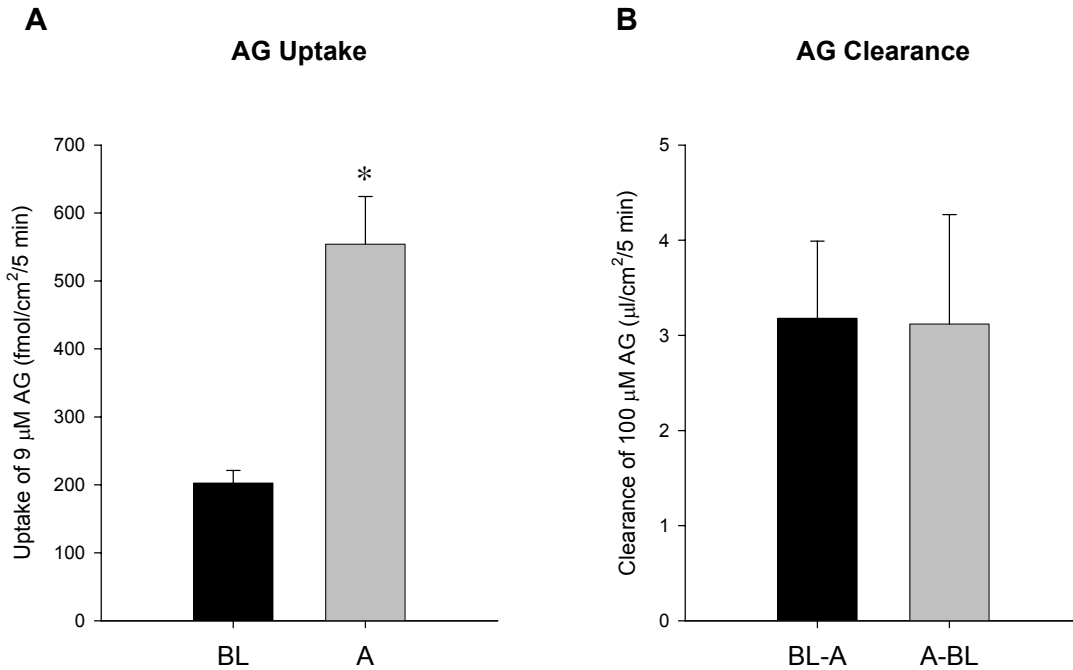
Figure 4.7.6. BL vs. A Uptake of AG. A) To determine the BL vs. A uptake of AG, 5 day old HK-2 monolayers superseeded on Transwell-Clear inserts were rinsed with WBTM, placed in WBTM containing 9 µM AG in the BL or A compartments and incubated in a 37°C shaking water bath.   After 5 min, monolayers were transferred to ice-cold TM, rinsed with ice-cold TM, lysed with 1%SDS, 0.1 N NaOH and assayed for radioactivity. The uptake rates were then calculated. Uptake of AG was significantly greater from the A vs. BL compartment as analyzed by Student's t-Test, $p < 0.01$. Each bar represents the mean uptake +/- SEM for 3 monolayers. B) To determine the BL-A vs. A-BL clearance of 100 µM AG, 3 day old HK-2 monolayers grown on Transwell-Clear inserts were equilibrated in TM at 37°C, 5% CO_2, 95% air for 10 min, aspirated, placed in TM containing 100 µM AG in the BL or A compartments and incubated in the same atmosphere for 5 min. Samples were taken from the BL and A media, aliquots (100 µl) were assayed for radioactivity and clearance rates were calculated. There was no difference in the BL-A vs. A-BL clearance of AG. Each bar represents the mean clearance +/- SEM for 2 monolayers.

AG Uptake   **AG Clearance**
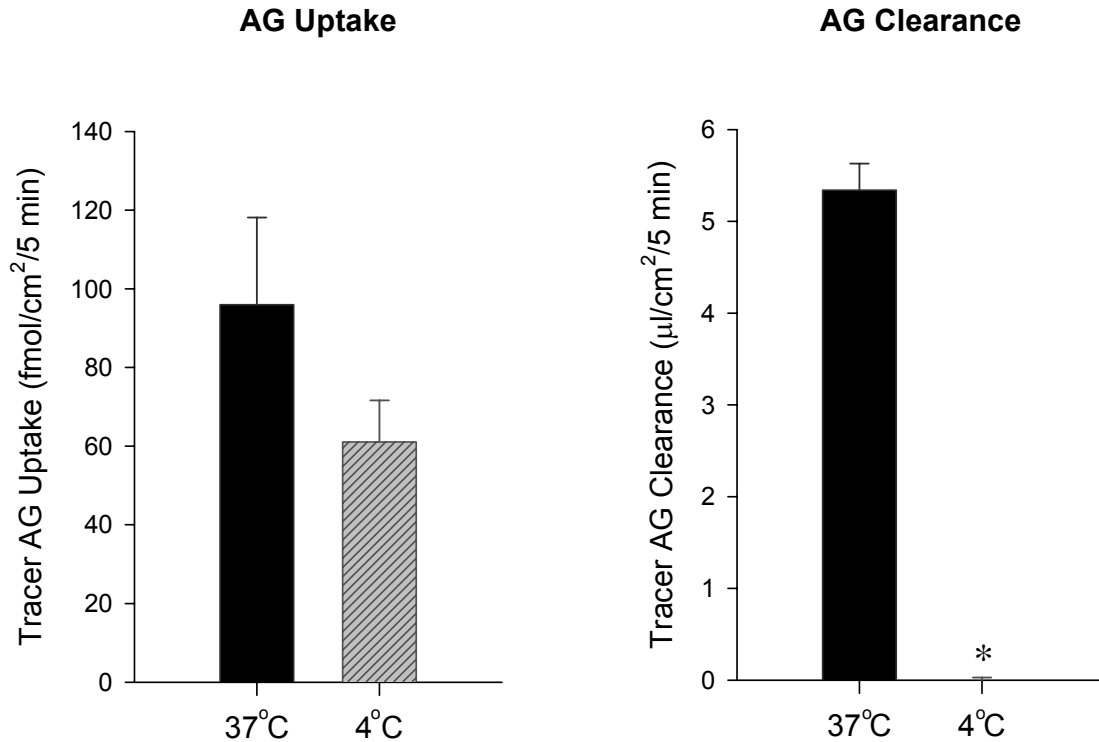
Figure 4.7.7.   Temperature-Dependent Transport of AG.   The uptake and clearance of 9 µM AG were examined at 37°C vs. 4°C using 5 and 7 day old HK-2 monolayers superseeded on Transwell-Clear inserts. Monolayers were rinsed with WBTM, placed in WBTM containing 9 µM AG in the BL compartments and incubated in a 37°C or 4°C shaking water bath. After 5 min, samples were taken from both compartments per insert and the inserts were placed in ice-cold TM, rinsed with ice-cold TM, lysed with 1%SDS, 0.1 N NaOH and assayed for radioactivity. The uptake rates were then calculated. Aliquots (100 µl) of BL and A media were assayed for radioactivity and the clearance rates were calculated. The decrease in uptake at 4°C vs. 37°C was statistically insignificant whereas the clearance of AG was abolished at 4°C. Each bar represents the mean uptake +/- SEM for 6 monolayers or the mean clearance +/- SEM for 3 monolayers. *Data was analyzed by Student's t-Test, $p < 0.001$.

A **Effect of Ouabain Cotreatment on AG Clearance**

B **Effect of Ouabain Pretreatment and Cotreatment on AG Clearance**
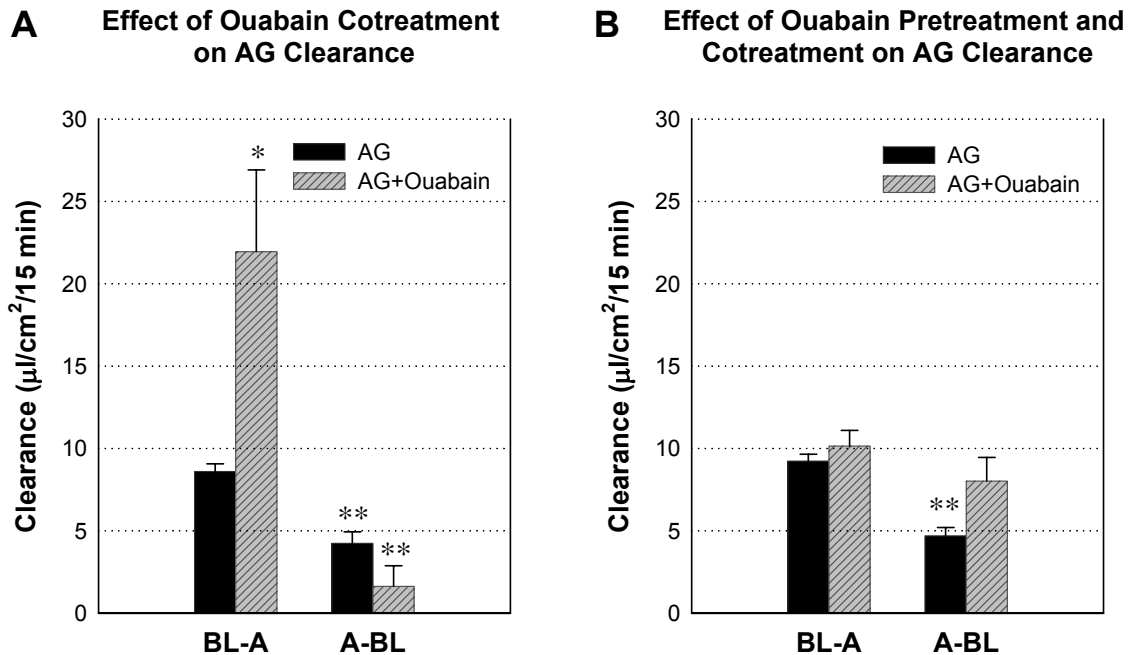
Figure 4.7.8. The Effects of Ouabain on AG Clearance. To determine the effects of (A) ouabain coincubation or (B) ouabain preincubation and coincubation on the clearance of AG, 4-7 day old HK-2 monolayers seeded on Transwell-Clear inserts were (A) equilibrated in TM for 10 min or (B) equilibrated in TM +/- 100 μM ouabain for 30 min, then aspirated and placed in TM containing 200 μM AG +/- 100 μM ouabain in the BL or A compartments. After 15 min at 37°C, 5% CO_2, 95% air on an orbital shaker at 60 cycles/min, 1 ml samples were taken from both compartments per insert and the AG concentrations were determined by HPLC. A) *The difference in BL-A AG clearance for control vs. ouabain cotreated monolayers was statistically significant by Student's t-Test, p=0.011. **The difference in BL-A vs. A-BL AG clearance for like treatments was statistically significant by Student's t-Test, p<0.02. Each bar represents the mean clearance +/- SEM for 5 monolayers for control (AG-treated) and 3 monolayers for the AG+ouabain cotreated monolayers. B)**The difference in BL-A vs. A-BL AG clearance was statistically significant by Student's t-Test, p=0.006. Each bar represents the mean clearance +/- SEM for 3 monolayers, except control A-BL, 2 monolayers.

AG Uptake
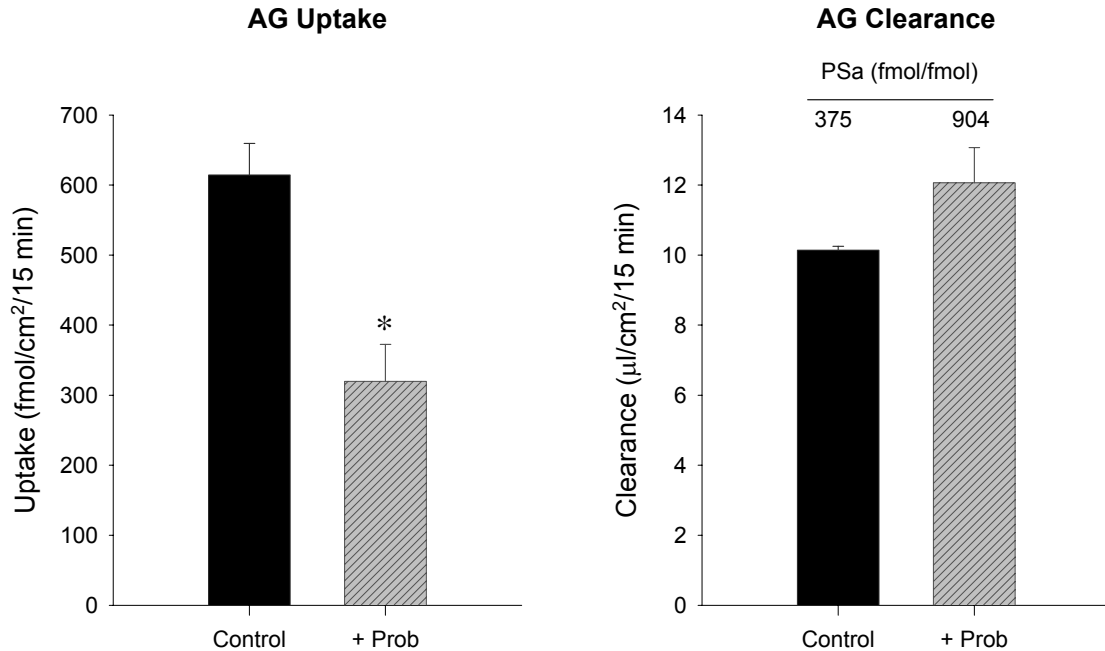
AG Clearance

Figure 4.7.9. The Effect of Probenecid on AG Transport. The uptake and clearance of 4 µM AG were examined in the absence and presence of 1 mM probenecid using 7 day old HK-2 monolayers superseeded on Transwell-Clear inserts. Monolayers were equilibrated in TM for 10 min at 37°C, 5% CO_2, 95% air, aspirated then placed in TM containing 4 µM AG +/- 1 mM probenecid in the BL compartments and incubated for 15 min as above. Samples were taken from both compartments per insert and the inserts were placed in ice-cold TM, rinsed with ice-cold TM, lysed with 0.1 N NaOH and assayed for radioactivity. Uptake was then calculated. Aliquots (100 µl) of BL and A media were assayed for radioactivity and the clearance rates were calculated. Probenecid caused a significant decrease (52% x control) in the net accumulation of intracellular AG. The clearance rate increased by 19%, but this difference was not statistically significant. The PSa for the probenecid treated cells was 2.4 times that of control indicating an increase in BBM permeability. Each bar represents the mean uptake or clearance +/- SEM for 3 monolayers. *Data was analyzed by Student's t-Test, $p < 0.002$.

A

Effects of BL vs. A Probenecid on the BL Uptake of AG

B

BL vs. A Uptake of AG +/- Probenecid
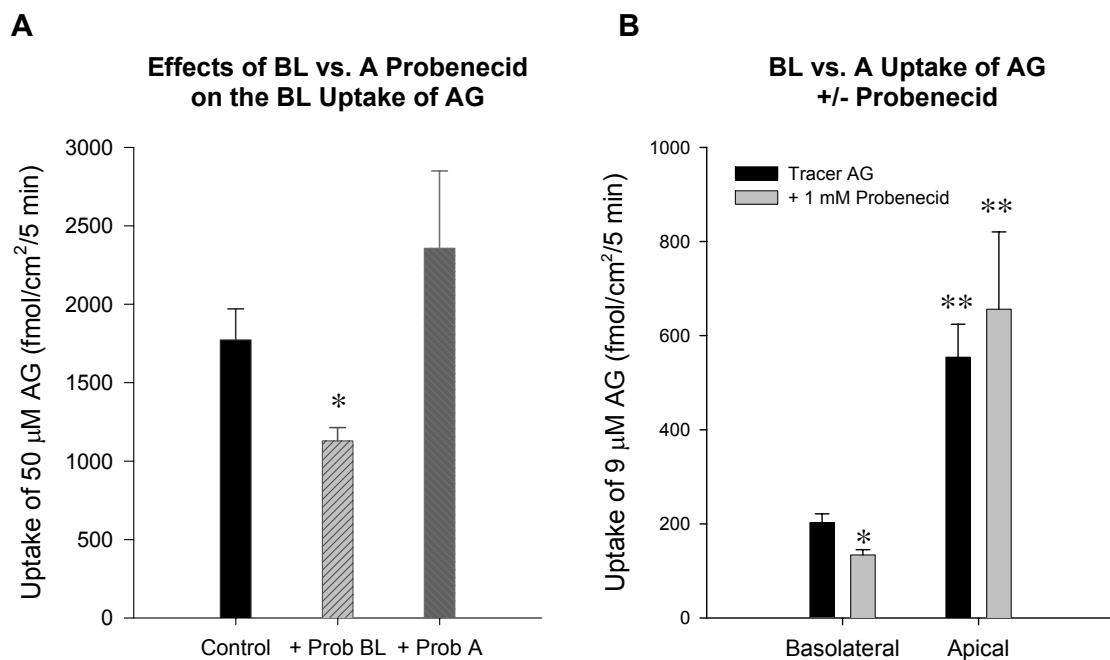
Figure 4.7.10. The Effects of BL vs. A Probenecid on the Uptake of AG. To determine the A vs. BL effect of probenecid on the uptake of AG, 5 and 6 day old HK-2 monolayers superseeded on Transwell-Clear inserts were rinsed with WBTM and placed in WBTM containing 50 µM AG in the BL compartments in the absence or presence of 1 mM probenecid in the BL or A compartments (A) or 9 µM AG in the A or BL compartments in the absence or presence of 1 mM probenecid in the same compartment (B). Monolayers were incubated in a 37° C shaking water bath. After 5 min, they were transferred to ice-cold TM, rinsed with ice-cold TM, lysed with 0.1 N NaOH and assayed for radioactivity. The uptake rates were then calculated. Each bar represents the mean uptake +/- SEM for 3 monolayers. *Probenecid caused a significant decrease in the uptake of AG when coinincubated in the BL compartment. A) Probenecid in the A compartment had no significant effect on BL AG uptake. Data analyzed by One-Way ANOVA with Dunnett's post test, $p < 0.05$. B) ** There is a statistical difference in like treatments for BL vs. A uptake. Probenecid had no significant effect on the uptake of AG from the A compartment. Data analyzed by Student's t-Test per comparison, $p < 0.05$.
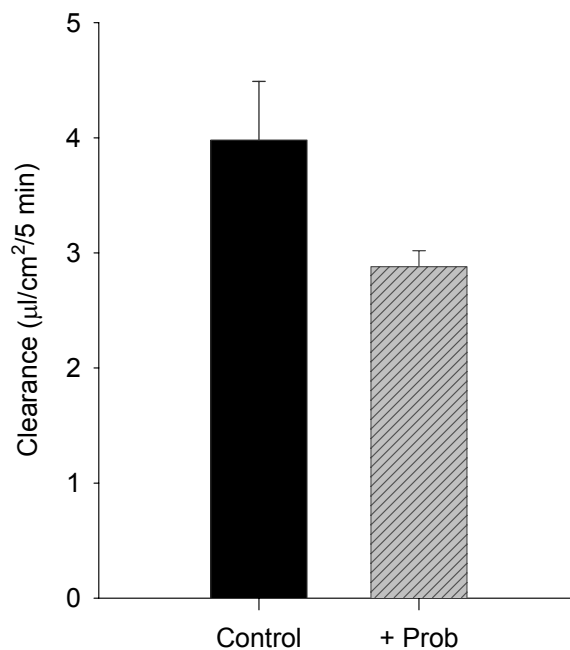
Figure 4.7.11. The Effect of Probenecid on the Clearance of AG. To determine the effect of probenecid on the clearance AG, 3 and 4 day old HK-2 monolayers grown on Transwell-Clear inserts were equilibrated in TM at 37°C, 5% CO_2, 95% air for 10 min, aspirated, placed in TM containing 100 µM AG +/- 1 mM probenecid in the BL compartments and incubated in the same atmosphere for 5 min. Samples were taken from the BL and A media, aliquots (100 µl) were assayed for radioactivity and clearance rates were calculated. The decreased clearance of AG for the probenecid treatment was not significant by Student's t-Test at a 95% confidence interval. Each bar represents the mean clearance +/- SEM for 4 monolayers.

A   AG Uptake   **B**   AG Clearance
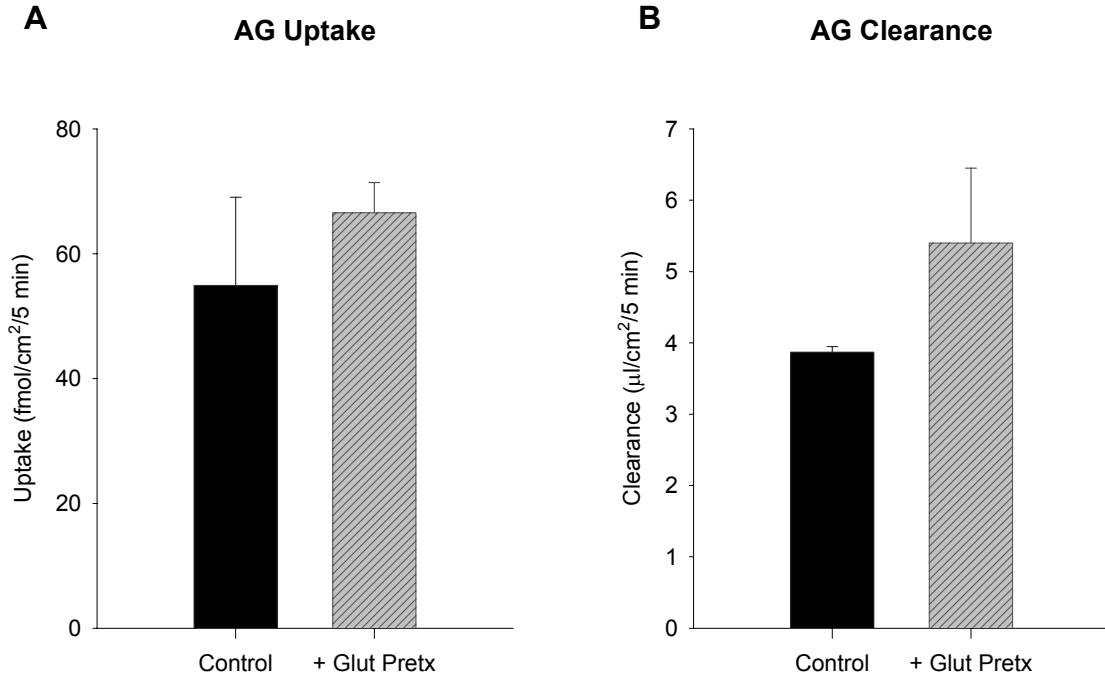
Figure 4.7.12. The Effects of Glutarate Preincubation on AG Transport. To determine the effects of glutarate preincubation on AG transport, 8 day old HK-2 monolayers superseeded on Transwell-Clear inserts were incubated for 90 min in culture media containing 1 mM glutarate. Preincubated and control monolayers were then rinsed twice with WBTM, placed in WBTM containing 7.9 µM AG in the BL compartments and incubated at 37°C in a shaking water bath. After 5 min, media samples were removed from each compartment per insert and monolayers were placed into ice-cold TM, rinsed with ice-cold TM, lysed in 1% SDS, 0.1 N NaOH and assayed for radioactivity. Uptake rates were then calculated. Aliquots (50 µl) of the BL and A media were assayed for radioactivity and the clearance rates determined. The glutarate preincubation caused an increase in both uptake and clearance of AG, yet both were insignificant by Student's t-Tests. Each bar represents the transport mean +/- SEM for 3 monolayers.

FL Clearance
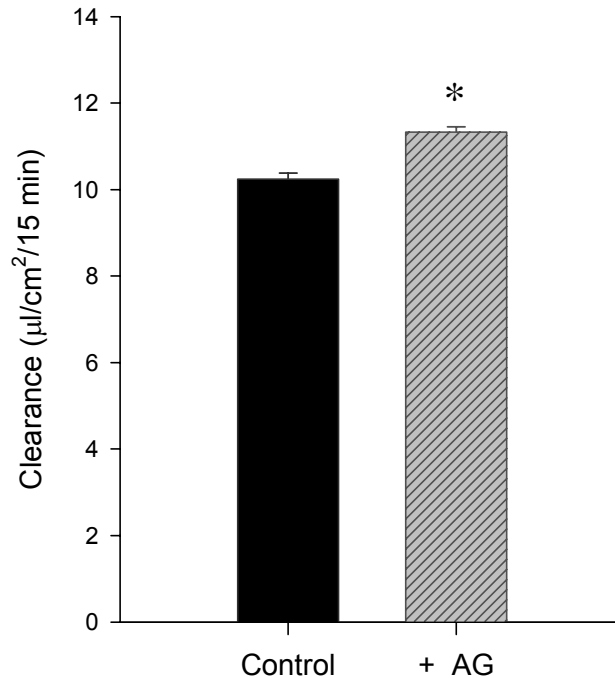
Figure 4.7.13. The Effect of AG on the Clearance of FL. The clearance of 4 µM FL in the presence of 200 µM AG was determined using 6 day old HK-2 monolayers seeded on Transwell-Clear inserts. Monolayers were first equilibrated for 10 min in TM at 37°C, 5% CO_2, 95% air on an orbital shaker at 60 cycles/min before a 15 min incubation period in TM containing 4µM FL +/- 200 µM AG in the BL compartment under the same conditions. Aliquots (100 µl) of the media from both compartments per insert were assayed for fluorescence and the clearance rates determined. A slight increase in FL clearance which was statistically significant by Student's t-Test, $p < 0.05$, resulted from coincubation with AG when compared to control. Each bar represents the mean clearance +/- SEM for 3 monolayers.

A   **PAH Uptake**
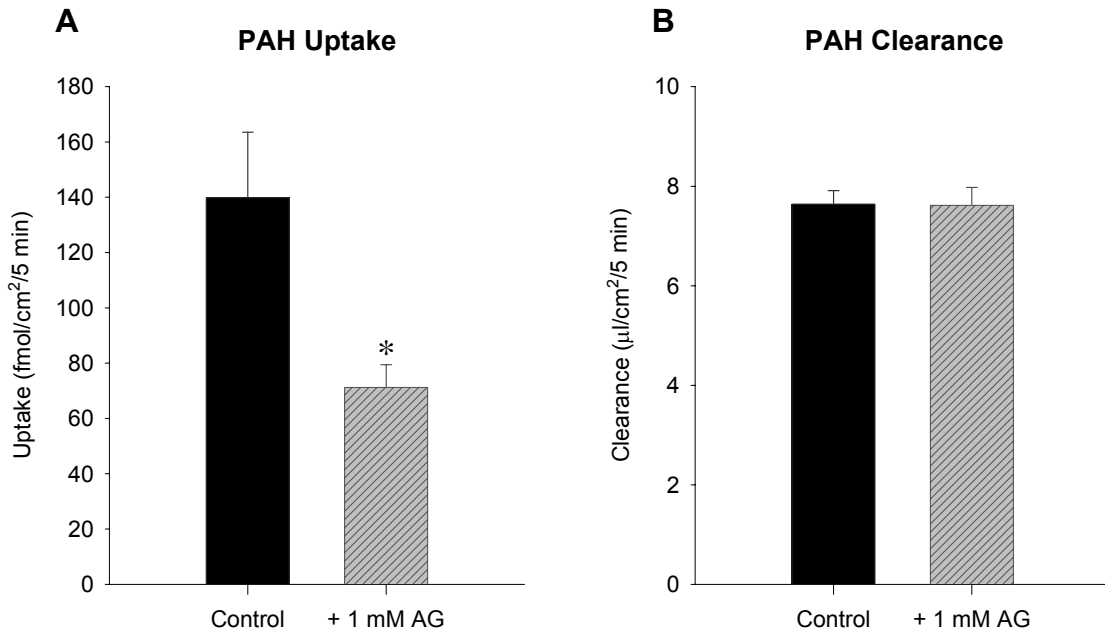
B   **PAH Clearance**

Figure 4.7.14. The Effect of AG on the Transport of 4 µM PAH. To determine the effect of AG on the uptake and clearance of PAH, 5 day old HK-2 monolayers superseeded on Transwell-Clear inserts were rinsed with WBTM, placed in WBTM containing 4 µM PAH +/- 1 mM AG in the BL compartments and incubated at 37°C in a shaking water bath. After 5 min, media samples were taken from BL and A compartments and uptake was terminated by placing the monolayers into ice-cold TM. Monolayers were rinsed in ice-cold TM, lysed in 1%SDS/0.1 N NaOH, assayed for radioactivity and the uptake rates calculated. Aliquots (50 µl) of the BL and A media were assayed for radioactivity and the clearance rates were calculated. A) *AG coincubation with PAH resulted in a 49% inhibition of PAH uptake compared to control as analyzed by Student's t-Test, $p < 0.05$. B) AG had no effect on the clearance of PAH. Each bar represents the mean uptake +/- SEM or the mean clearance +/- SEM for 3 monolayers.
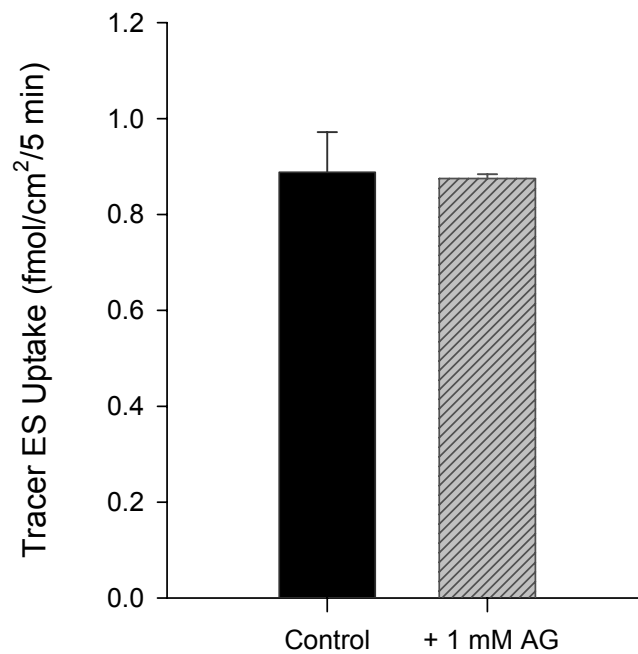
Figure 4.7.15. The Effect of AG on ES Uptake. To determine the effects of AG on ES uptake 7 day old HK-2 monolayers superseeded on Transwell-Clear inserts were rinsed in WBTM and placed in WBTM with 4 nM ES +/- 1 mM AG added to the BL compartments. Monolayers were incubated at 37°C in a shaking water bath. After 5 min, uptake was terminated with ice-cold TM and monolayers were rinsed with ice-cold TM. Cells were lysed in 1% SDS/0.1 N NaOH, assayed for radioactivity and the uptake rates were calculated. The addition of 1 mM AG to 4 nM ES had no effect on the uptake of ES; n = 3 per group. Each bar represents the mean uptake +/- SEM.

A AG Uptake
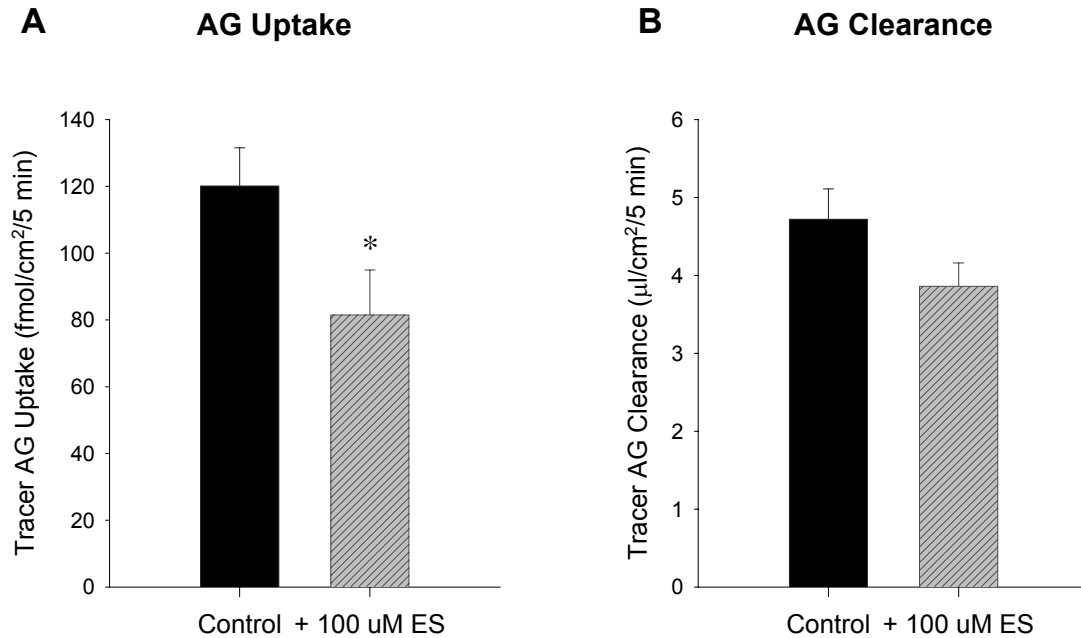
B AG Clearance

Figure 4.7.16. The Effect of ES the Uptake and Clearance of AG. To determine the effects of ES on AG transport, 5 and 7 day old HK-2 monolayers superseeded on Transwell-Clear inserts were rinsed in WBTM and placed in WBTM with 9 µM ES +/- 100 µM ES added to the BL compartments. Monolayers were incubated at 37°C in a shaking water bath. After 5 min, media samples were taken from the BL and A compartments. Uptake was terminated with ice-cold TM and monolayers were rinsed with ice-cold TM. Cells were lysed in 1% SDS/0.1 N NaOH, assayed for radioactivity and the uptake rates were calculated. Aliquots (50 µl) of media were assayed for radioactivity and clearance rates were calculated. A) ES (100 µM) inhibited the uptake of 9 µM AG by 32%. *The difference was statistically significant as analyzed by paired T-Test; $p < 0.05$; n = 9 for control, n = 7 for the + 100 µM ES treatment. B) There was no statistical significance in the clearance between groups. n = 6 per group. Each bar represents the mean uptake or clearance +/- SEM.

129

**Effect of 1 mM DHEAs on
the Clearance of 100 μM AG**
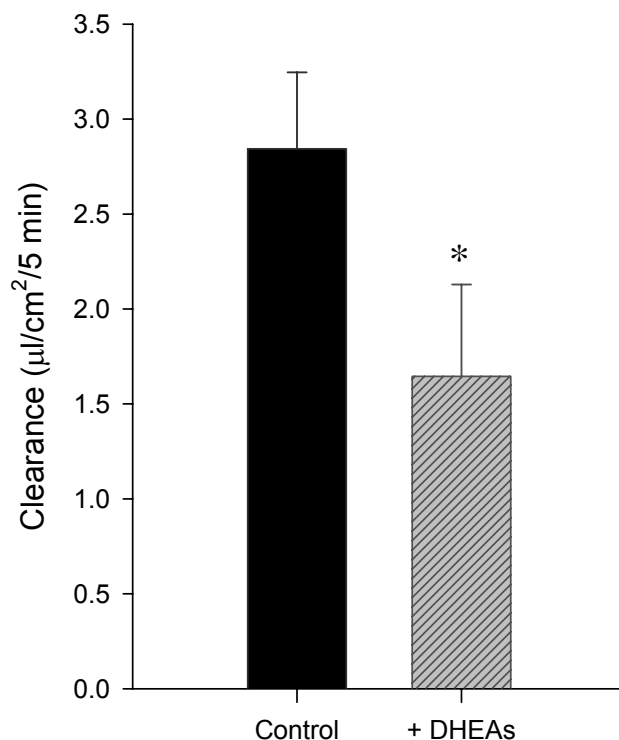
Figure 4.7.17. The Effect of DHEAS on the Clearance of AG. To determine the effects of DHEAS on the clearance of AG, 3 and 4 day old HK-2 monolayers superseeded on Transwell-Clear inserts were equilibrated in TM for 10 min on an orbital shaker at 60 revolutions/min, 37°C, 5% CO_2/95% air, aspirated, transferred to TM containing 100 μM AG +/- 1 mM DHEAS in the BL compartments and returned to the same conditions. After 5 min, media samples were taken from A and BL compartments per insert. Aliquots (100 μl) were assayed for radioactivity and clearance rates determined. DHEAS caused a 42% reduction in clearance of AG. This difference was statistically significant from control as analyzed by One-Way ANOVA for Repeated Measures, $p < 0.05$. Each bar represents the mean clearance +/- SEM for 6 monolayers.

AG Uptake
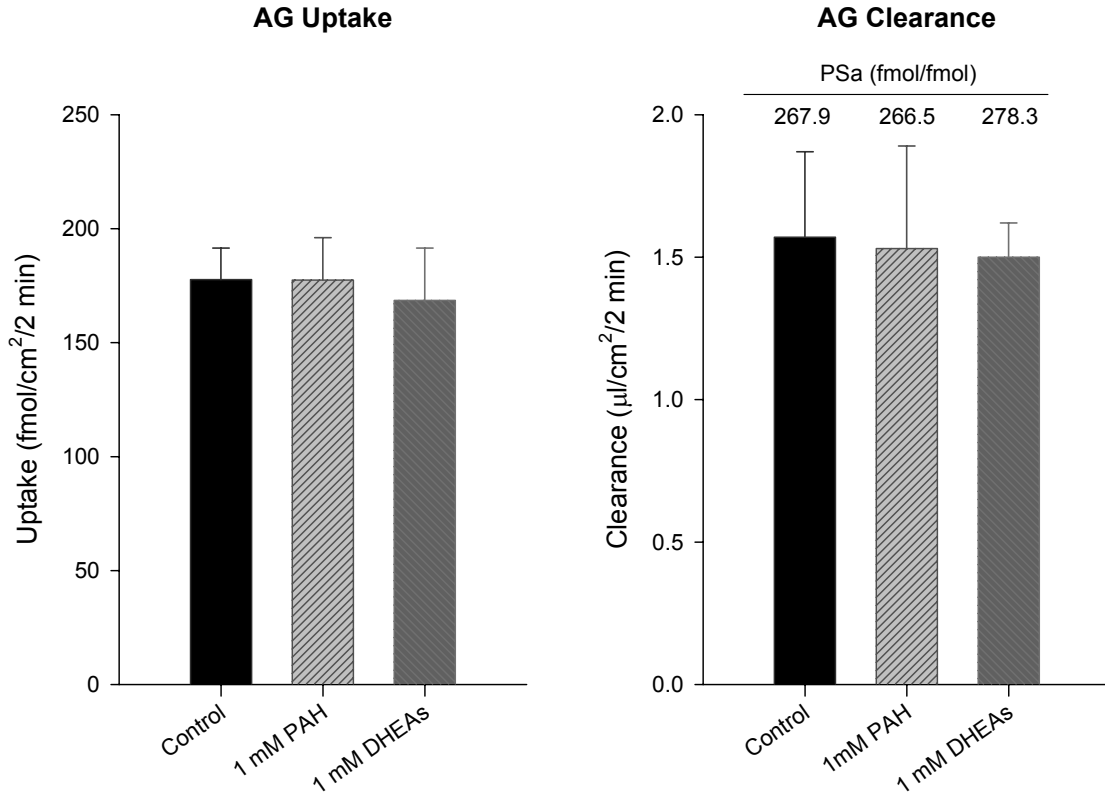
AG Clearance

Figure 4.7.18. The Effects of PAH and DHEAS on the 2 min Transport of AG.
The uptake and clearance rates for AG in the absence or presence of PAH and
DHEAS were determined using 5 day old HK-2 monolayers superseeded on
Transwell-Clear inserts. Monolayers were rinsed with WBTM, placed in WBTM
containing 20 μM AG +/- 1 mM PAH or 1 mM DHEAS in the BL compartments and
incubated at 37°C in a shaking water bath. After 5 min, media was sampled from both
compartments per insert and uptake was terminated by placing the inserts into ice-
cold TM. Cells were rinsed with ice-cold TM, lysed in 1% SDS, 0.1 N NaOH, assayed
for radioactivity and the uptake rates were determined. Aliquots (50 μl) of the media
samples were assayed and the clearance rates were determined. There was no
difference in the uptake or the clearance rates for either +PAH or +DHEAS vs. control.
This is reflected in the PSa values indicating no change in the BBM permeability in
response to PAH or DHEAS. Each bar represents the mean uptake +/- SEM or the
mean clearance +/- SEM for 5 control monolayers and 4 monolayers for both PAH and
DHEAS treated.

131
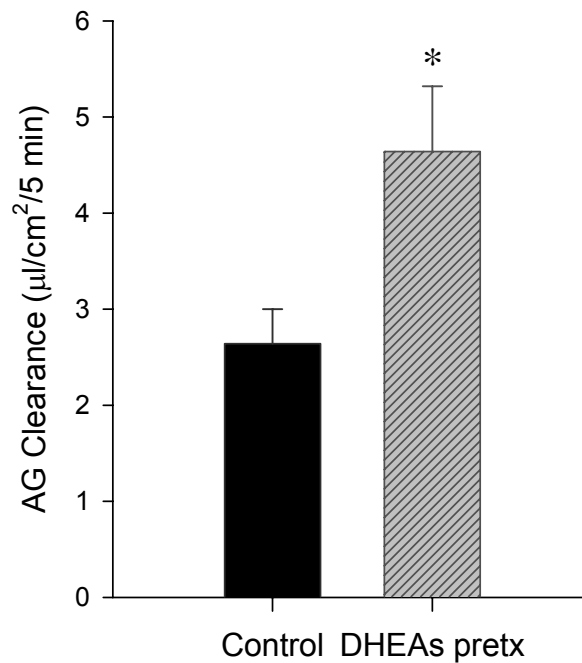
Figure 4.7.19.   The Effect of 24 Hour Pretreatment with DHEAS on the Clearance of AG.   To determine the effects of DHEAS pretreatment on the clearance of AG, 8 day old HK-2 monolayers seeded on Transwell-Clear inserts were incubated for 24 hours in culture medium with or without 1 mM DHEAS. Monolayers were rinsed twice with TM then equilibrated in TM for 10 min on an orbital shaker at 60 revolutions/min, 37°C, 5% CO_2/95% air, aspirated, transferred to TM containing 100 µM AG in the BL compartments and returned to the same conditions. After 5 min, media samples were taken from A and BL compartments per insert.   Aliquots (100 µl) were assayed for fluorescence and clearance rates determined.   DHEAS 24 hour preincubation caused a 76% increase in clearance of AG.   This difference was statistically significant from control as analyzed by Student's t-Test, $p < 0.05$. Each bar represents the mean clearance +/- SEM for 3 monolayers.

AG Uptake
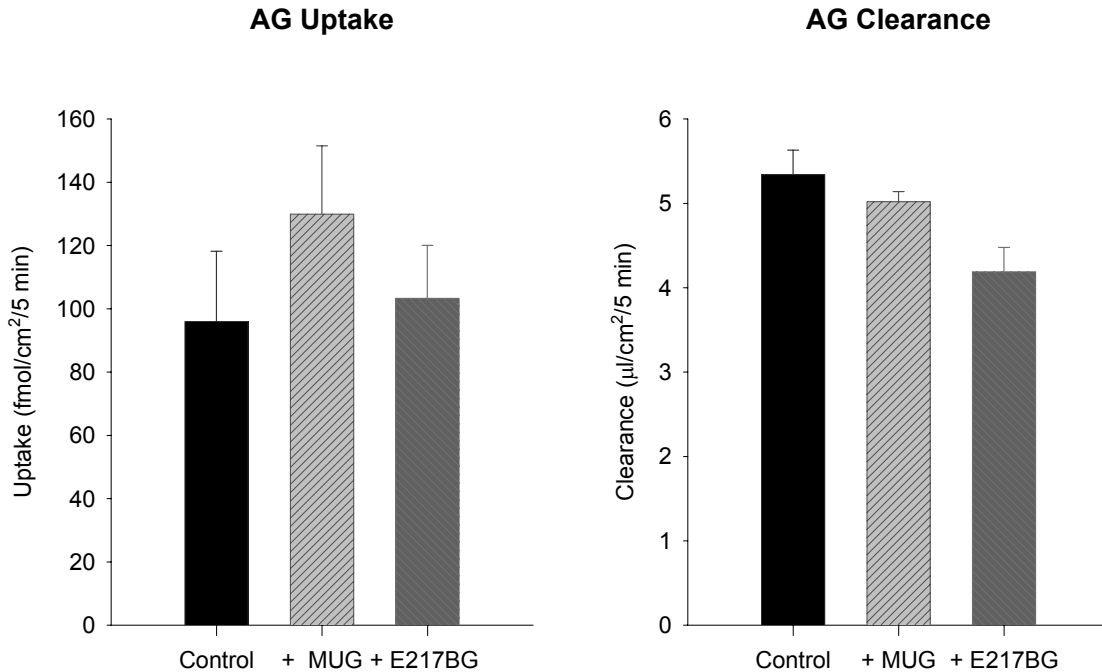
AG Clearance

Figure 4.7.20. The Effect of MUG and E$_2$17βG on the Transport of AG. The uptake and clearance rates for AG in the absence or presence of MUG and E$_2$17βG were determined using 5 and 7 day old HK-2 monolayers superseeded on Transwell-Clear inserts. Monolayers were rinsed with WBTM, placed in WBTM containing 9 μM AG +/- 100 μM MUG or 100 μM E$_2$17βG in the BL compartments and incubated at 37°C in a shaking water bath. After 5 min, media was sampled from both compartments per insert and uptake was terminated by placing the inserts into ice-cold TM. Cells were rinsed with ice-cold TM, lysed in 1% SDS, 0.1 N NaOH, assayed for radioactivity and the uptake rates were determined. Aliquots (50 μl) of the media samples were assayed and the clearance rates were determined. There was no difference in the uptake for either +MUG or +E$_2$17βG vs. control as analyzed by One-Way Repeated Measures ANOVA. The difference in clearance for E$_2$17βG vs. Control is statistically significant by One-Way ANOVA followed by Dunnett's Test for Multiple Comparisons vs. Control, $p < 0.05$. The clearance for E$_2$17βG was calculated using the BL concentrations for the MUG data because sampling problems due to viscosity of E$_2$17βG made the BL concentrations artificially low and was apparent by media sticking to the pipet tips. Sticking did not occur for the lower concentration of E$_2$17βG of the A compartment. MUG and E$_2$17βG medium were prepared from the same batch of AG WBTM. Each bar represents the mean uptake +/- SEM for 6 monolayers or the mean clearance +/- SEM for 3 control monolayers.

133

CHAPTER V

Discussion

Development of the HK-2 cell line as a Model for Transport Studies

Development of the HK-2 model utilized for organic anion transport in these studies involved several phases including PTC marker identification, optimization of growth conditions, OAT immunoblot analysis, and verification of cell polarization. Because HK-2 cells are an established human renal proximal tubule cell line, little characterization was necessary. Assay values for GGT and hexokinase and positive staining for AP were consistent with expected results for the enzymes in a proximal tubule cell line.

Growth conditions were optimized for protein, rate of growth, adherence and confluence of the monolayer. Growth of cells in flasks was optimal for protein and rate of growth when cultured in KSFM with 40 ng/ml BPE, 5 ng/ml EGF and supplemented with 2% FBS. This medium was initially used for cells grown on porous membranes, but was modified when cells were superseeded. Cells seeded at superconfluence (superseeded = 1.41×10^6 cells/4.7 cm^2 insert) onto Transwell-Clear membranes demonstrated the highest level of confluence as determined by phase contrast microscopy and FLD diffusion. Because growth of superseeded cells was not required to achieve confluence, use of EGF in the culture medium was not necessary and was omitted from the culture media. Cell adhesion was superior for inserts coated with human placental Type IV collagen (25 µg/insert).

To validate the HK-2 cell line as an appropriate model to study BL organic anion transport, evidence of transporter expression was sought. OAT1 and OAT3, known to be expressed in the BLM of human renal PTCs, were detected by

Western blot analysis of HK-2 cell membrane fractions using antibodies purchased from Alpha Diagnostics International, Inc.. An aberrant banding pattern was found for both transporters, suggestive of varying levels of glycosylation of transporter isoforms. The heaviest bands for OAT1 were 75 and 80 kD and for OAT3 were 79-80 kD. These bands are consistent with findings in the literature and likely represent glycosylated proteins. Lower MW bands, 62-65 kD for OAT1 and 63-65 kD for OAT3 are near the predicted MW for both transporters and thus would likely represent the nonglycosylated proteins. Bands found in this study are consistent with findings in the literature, and are thus, evidence of OAT1 and OAT3 expression in the HK-2 cell line.

Polarization of the HK-2 monolayer on Transwell-Clear membranes was demonstrated by FL and AG studies, both of which indicated higher permeability of the BBM vs. BLM per substrate. These results represent an expected finding for FL (Dantzler, 2002) and provide evidence of polarization for the HK-2 cell model. With polarization of the HK-2 monolayer, one can expect transport measurements to reflect net uptake across the BLM when substrate is added to the BL compartment of the Transwell insert.

Despite polarization and apparent confluence of the monolayers, high FL diffusion, greater than that of FLD diffusion, was suggested by regression analysis of a time-course study of FL clearance. This analysis indicated that diffusion represented an increasing percentage of total clearance of FL with time. This effect could also be explained by upregulation of transporters with time, however, with upregulation, one would expect to find magnified differences in clearance corresponding to longer incubation periods for control vs. treated experiments. This was not seen. Instead, a high rate of diffusion would diminish differences in clearance rates with rates for treated groups approaching 100% of control. Results of FL clearance experiments should be interpreted with this effect of diffusion in mind, particularly for those experiments conducted over 5 min. It was for this reason

as well as evidence of compensatory mechanisms over time that shorter incubation periods (5 min or less) were preferred.

OAT1 and OAT3 Studies

Time- and temperature-dependent transepithelial flux of FL demonstrated that FL movement across the HK-2 monolayer is a transporter-mediated process. Competitive self-inhibition of BL uptake of PAH, ES and DHEAS also supported transporter-mediated transport. Furthermore, because FL and PAH are the prototypical substrates for OAT1, as is ES for OAT3, the results suggest that these transporters are functional in the HK-2 model. Trans-stimulation of FL clearance by the dicarboxylate αKG, ouabain inhibition of FL clearance, and probenecid inhibition of FL, PAH and ES transport further support functionality of OAT1 and OAT3 in this model. However, because of substrate specificity overlap, probenecid sensitivity and recent evidence of similar mechanisms of action for OAT1 and OAT3, one cannot definitively state that OAT1 is functional in this model. That is, FL and PAH are reported to be substrates of OAT3 as well as OAT1; probenecid inhibits both OAT1- and OAT3-mediated transport; and OAT3 has been shown to act as an exchanger for dicarboxylates, as does OAT1 (Sweet et al., 2003).

The self-inhibition studies in this project demonstrated 50% inhibition of 4 µM [^{14}C]PAH by 1 mM PAH, 50% inhibition of 4 µM [^{3}H]ES by 100 µM ES and 45% inhibition of 2.2 nM [^{3}H]DHEAS by 100 µM DHEAS. For each of these substrates, a higher inhibition was expected due to the high affinity of these substrates for OAT1 and/or OAT3 as reported in the literature (Table 6, p. 35). These results suggest considerable nonspecific binding of substrate to the membrane support. The greatest inhibitory effect by probenecid for OAT1 and/or OAT3 substrates was found to be 73% inhibition of PAH uptake by 1 mM probenecid. Greater inhibitory effects were expected based on literature results. This, too, is thought to be attributed to nonspecific binding of substrate to the membrane support. Unlike

136

most renal PTC cell monolayers, HK-2 monolayers do not form domes which are indicative of tight junction formation (Kim et al., 2002). Thus, in the HK-2 cell model, substrates may have greater access to the membrane support resulting in high levels of nonspecific binding and high rates of diffusion across the membrane.

<u>AG Transport</u>

Studies with AG strongly support transporter-mediated uptake of AG across the BLM. Time-, concentration- and temperature-dependent uptake of AG were demonstrated in the HK-2 cell model. Time- and concentration-dependent studies revealed biphasic transport. The time-course was nearly linear for 10 min, then rapidly leveled off. This uptake was closely fit (R^2=0.99) to a single rectangular hyperbolic regression. Concentration-dependent uptake demonstrated typical kinetics of transporter-mediated uptake at low concentration and a nearly linear, increased rate of uptake at high concentrations (above 1 mM AG). Although these studies are referred to as uptake studies, the measurements are of net intracellular accumulation and are thus representative of uptake and efflux processes. Thus, the increased rate of uptake at high concentrations of AG may be due to increased uptake at the BLM, reuptake at the BBM, or decreased efflux at the BBM. Reuptake at the BBM was tested and determined not to occur. Decreased efflux at the BBM is suspected and is discussed in the next section.

Concentration-dependent uptake of AG up to 1 mM was analyzed by both Berteloot and Michaelis-Menten regressions yielding K_m values of 326 μM and 1.44 mM with correlation coefficients R^2 = 0.863 and 0.995, respectively. By formulation, a Berteloot regression is performed on the actual tracer uptake data as opposed to the total substrate uptake calculated from tracer and unlabeled substrate as required for a Michaelis-Menten regression. For this reason, a Berteloot regression is thought to be more reflective of the system. Thus, despite a lower correlation coefficient, the Berteloot analysis is likely a closer approximation of the kinetics of the system. Additionally, the initial Michaelis-

Menten analysis from earlier data yielded a K_m of 260 µM, closer to the Berteloot K_m. Together, these analyses suggest low affinity BL transport of AG in the HK-2 cell line with an approximate K_m of 330 µM.

Coincubations of AG with OAT1 substrates FL and PAH and OAT3 substrates DHEAS, $E_2 17\beta G$ and ES suggest a strong noncompetitive component to uptake at the BLM for these substrates with AG. The most convincing support for possible OAT3-mediated AG uptake is the ES study, which demonstrated a 32% inhibition of AG net accumulation with a decrease, although insignificant, in AG clearance (9 µM AG, 100 µM ES). A purely competitive process would have yielded a much greater inhibition of AG transport. Decreased clearance of 100 µM AG when coincubated with 1 mM DHEAS also suggests possible OAT3-mediated AG transport.

Additional support of possible OAT3- and/or OAT1-mediated transport of AG includes, a slight, but insignificant increase in 8 µM AG transport with preloaded glutarate, and a decrease in clearance of 100 µM AG when coincubated with probenecid. However, 2 min coincubation of monolayers with 20 µM AG and 1 mM PAH or 1 mM DHEAS resulted in no change in AG uptake or clearance. Longer incubation periods yielded varying results that are discussed in the section below. AG (1 mM) inhibition studies of 4 µM FL and 4 µM PAH demonstrated lack of inhibition of FL or PAH clearance across the monolayer. AG (1 mM) had no effect on 5 min, 4 nM ES uptake. The glucuronide conjugates $E_2 17\beta G$, an OAT3 substrate, and MUG, both at 100 µM, had no significant effect on the uptake or clearance of 9 µM AG, but tended to cause a slight increase in intracellular accumulation and a slight decrease in clearance suggestive of inhibition of efflux at the BBM as opposed to uptake at the BLM. Lack of inhibition of low concentrations of AG clearance by probenecid also supports uptake at the BLM by transporter(s) other than OAT1 or OAT3. However, the experiments of Takeda et al. (2002) should be considered when evaluating the inhibitory effects of substrates/inhibitors on low affinity substrate transport. Takeda and colleagues

found that the low affinity (K_m = 342 µM) hOAT1-mediated transport of acyclovir was only weakly inhibited by probenecid (~20% inhibition) vs. strong inhibition (~80-90%) of hOAT1-mediated PAH transport by probenecid found in earlier studies (Takeda et al., 2001). Thus, the prototypical substrate/inhibitor transport studies may not be predictive of the degree of inhibition for other low affinity substrates such as AG.

Due to overlap in OAT1/OAT3 substrate specificity, it is difficult to evaluate purely OAT1-mediated transport in a multiple transporter system. However, in that ES is an OAT3 and not an OAT1 substrate, it is thought that AG transport is more likely OAT3- rather than OAT1-mediated. OAT1-mediated AG transport is also less likely according to the findings of Ullrich et al. (1990) that glucuronidation of substrates reduces or abolishes the interaction with the PAH transporter.

<u>Evidence of Transporter Regulation</u>

Although the primary focus of this project was organic anion transport across the BLM, results of many of the studies made it difficult to ignore BBM transporters, some which have been shown to be highly regulated over time. Glucuronides are known substrates of the BBM transporters MRP2, MRP4 and NPT1. Little is known about the regulation of MRP4 or NPT1, however, MRP2 is regulated by insertion and retrieval into the membrane, as well as at the level of transcription and translation. For example, rapid retrieval and retargeting of MRP2 from the canalicular membrane to the BLM in hepatocytes in response to activation by PKC was reported to occur within 30 min (Kubitz et al., 2001). $E_2 17\beta G$ has been shown to affect endocytic retrieval of MRP2 (Mottino et al., 2003), whereas cAMP has been shown to cause insertion (Gerk and Vore, 2002). This regulation occurs within min (Gerk and Vore, 2002). Bile flow, a process involving MRP2-mediated efflux, was inhibited by 85% in 10 min by $E_2 17\beta G$ in rat (Mottino et al., 2002). Short incubation periods are ideal to limit these effects, however, the amount of tracer substrate required to attain intracellular radioactivity

levels well above background for short incubation periods was cost prohibitive in the HK-2 cell line. Additionally, probenecid (Bodo et al., 2003b) and ES (Sasaki et al., 2002) have been shown to cause stimulation of MRP2-mediated transport. Therefore, it became apparent that the BBM transporters must be considered when interpreting the results of several experiments, with concern of insertion or retrieval of transporters for studies with incubation periods of 5 min or longer.

Studies of PAH and AG, known substrates of MRP2, suggested possible upregulation or stimulation of apical transporters resulting in a diminished decrease or a net increase in transepithelial transport in the presence of decreased net intracellular accumulation of substrate when coincubated with other compounds. For example, PAH uptake was decreased 73% vs. 15% decreased clearance (a diminished decrease) when coincubated with probenecid. While diffusion of PAH likely contributed to the diminished effect of probenecid on PAH clearance, stimulation of the MRP2 transporter in the BBM by probenecid (Bodo et al., 2003b) may have resulted in increased apical efflux since PAH is a known substrate of MRP2 (Leier et al., 2000).

Similar results occurred with coincubation of AG and probenecid, showing decreased net accumulation of tracer AG, but no significant effect on the BL-A clearance. Since inhibition at the BLM would cause decreased clearance as well as accumulation, these results may best be explained by stimulation of BBM-mediated transport (such as MRP2) by probenecid resulting in greater efflux of AG with resultant lower intracellular AG. Because the amount of AG effluxed into the A compartment is on the order of 400 to 900 times that accumulated intracellularly, significant decreases in accumulation due to BBM efflux may not cause significant increases in clearance. Lack of decreased clearance of AG when coincubated with probenecid is also in line with the finding by Duggin and Mudge (1975) that probenecid does not inhibit the transport of AG. Even at a higher concentration of AG (100 µM), probenecid had no significant effect on AG clearance.

The opposite effect was seen for probenecid inhibition of ES transport, with a greater decrease (44%) in clearance than in net accumulation (13%). This finding is likely attributed to probenecid inhibition of both OAT3-mediated uptake at the BLM and OAT4-mediated efflux at the BBM (Cha et al., 2000) resulting in a net accumulation greater than would be expected with uninhibited apical efflux. ES is not a substrate of MRP2 (Sasaki et al., 2002).

Assuming expression of the human renal BBM transporters in the HK-2 cell line, the effects of probenecid at the BBM would be to inhibit efflux via MRP4 and NPT1 but to stimulate efflux via MRP2. These differing effects may also contribute to the results found for AG/probenecid coincubation. Results suggest the possibility of time-dependent and possibly concentration-dependent effects. At 15 min, 1 mM probenecid caused a decrease in intracellular accumulation of AG with no significant effect on clearance of 4 µM AG. If probenecid had inhibited uptake at the BLM, the clearance rate should also have been decreased. Thus, stimulation of AG efflux at the BBM best explains these results and is suggestive of MRP2-mediated efflux. However, at 5 min, 1 mM probenecid tended to cause a *decrease* in clearance of 100 µM AG. This discrepancy between these two experiments can be attributed to regulatory mechanisms or simply to a greater inhibitory than stimulatory effect at the higher concentration of AG resulting in decreased clearance. Two alternative explanations support regulation: 1. upregulation of MRP2 by insertion into the BBM over the longer incubation period and, therefore, greater efflux via MRP2 than inhibition of MRP4- or NPT1-mediated transport; 2. downregulation in MRP2 affected by the high concentration of AG resulting in primarily inhibitory effects of probenecid at MRP4 or NPT1.

The effects of DHEAS, a high affinity substrate of MRP4, on the transport of AG also appear to be time- and/or concentration-dependent. At 5 min, 1 mM DHEAS caused a 42% decrease in the clearance of 100 µM AG suggestive of inhibition of OAT3-mediated uptake and/or MRP4-mediated efflux. DHEAS is not a substrate of MRP2, but is a high affinity substrate for MRP4. Since no effect on uptake or

clearance was seen at 2 min for 20 µM AG coincubated with 1 mM DHEAS, a regulatory process is supported. Upregulation of MRP4 or NPT1 by higher concentrations of AG or DHEAS over the 5 min incubation period would explain these results. Alternatively, downregulation of MRP2 by the higher concentration of AG over the longer incubation period in conjunction with inhibition of MPR4 by DHEAS would also affect decreased clearance of AG compared to control. Thus, BBM transporter inhibition and regulation can explain the effects of DHEAS on the transport of AG.

Yet another study supports AG concentration-dependent efflux pump down-regulation. The biphasic concentration-dependent AG uptake study demonstrated a sharp increase in net intracellular accumulation of AG at concentrations above 1 mM. Downregulation of MRP2 by retrieval from the membrane, as affected by $E_2$17βG, was demonstrated by Mottino et al. (2002). Downregulation of MRP2 by high concentrations of AG would explain the biphasic results of the concentration-dependent study in HK-2 cells and the findings of Duggin and Mudge (1975) that AG is reabsorbed at high concentrations in the dog. Thus, 3 studies with HK-2 cells suggest that AG may downregulate MRP2.

The effects of ouabain on FL and AG transport are also best explained by regulatory mechanisms. Dickinson et al. (1979) demonstrated that ouabain stimulates bile flow. Because MRP2 is the primary canalicular pump responsible for efflux of bile acid conjugates, it is likely that ouabain stimulates MRP2-mediated transport. In the HK-2 model, ouabain affected an increase in 15 min AG BL-A clearance vs. no significant effect on A-BL clearance. For FL, coincubation with ouabain caused inhibition of transport at 2 and 5 min, but the effect was lost after 15 min. Reversal of the acute effects of ouabain was seen for both the FL and AG studies when monolayers were preincubated for 30 min with or without ouabain. In the preincubation studies, subsequent coincubation of substrate with ouabain vs. control caused no significant effect on AG clearance, but caused increased FL clearance. This 30 min preincubation period is adequate to allow regulatory

effects by retrieval or insertion as described by Kubitz et al. (2001), who found that retrieval and retargeting of MRP2 from the canalicular to the BLM in hepatocytes in response to activation by PKC occurred within 30 min.

<u>Project Appraisal</u>

Evidence of BLM transporters responsible for the initial step of renal excretion of numerous anions as shown by Western blot analysis and functional studies of OAT1 and OAT3 suggest the HK-2 cell line has considerable potential for organic anion transport studies. Determination of the presence of known renal PTC transporters would increase the usefulness of this cell line and eliminate much of the confusion in interpreting transport study results.

It is possible that the findings attributed to regulation of the BBM transporters could be overcome by selectively inhibiting those transporters. Because we chose not to focus on the apical transporters, this was not attempted. The inhibitors of MRP2 may also affect the BL transporters making this a futile exercise. Hence, quantitative transport kinetics and inhibition studies for AG would best be determined in single transporter transfectant models. Some of the transfectant models also have endogenous transporters that make kinetic and substrate specificity studies challenging. These studies use the nontransfectant mock cells as control cells to distinguish between endogenous vs. transfectant (transporter expressing) cells. There are no mock cells for the HK-2 cell model.

Overall transport of AG in the HK-2 model is consistent with the Duggin and Mudge (1975) finding that AG is secreted at low plasma concentrations and reabsorbed at higher concentrations in the dog. Consequently, the HK-2 model may be more useful for simulation of in vivo effects, or end-results, rather than kinetic analysis and substrate specificity studies.

The choice of AG as the model glucuronide-substrate for renal organic anion transporters was made due to the limited glucuronides available. Ideally, an acyl-

glucuronide associated with renal toxicity would have been studied. These compounds, however, are highly labile and are difficult to synthesize. Synthesis and concern of degradation would have severely limited the progress of the project. $E_2 17\beta G$, available radiolabeled, would have been the only feasible alternative. Since more information regarding transporter handling of $E_2 17\beta G$ is available, this would seem to have been a favorable choice over AG. However, many of the renal transporters are recognized for their ability to transport steroids or steroid conjugates, thus, transporter affinity for $E_2 17\beta G$ due to the steroid moiety is a possibility. Low solubility and high viscosity of $E_2 17\beta G$ also make it an unfavorable substrate. Another alternative to AG would have been MUG. However, little data exist concerning the transport of this compound.

Summary and Conclusion

HK-2 cells grown on Transwell-Clear inserts were studied to demonstrate both the presence and the function of transporters. OAT1 and OAT3, but not OAT2 were found to be present in the membrane fractions of HK-2 cells by Western blot analysis. Transport and self-inhibition of PAH and ES were demonstrated, indicating function of OAT1 and OAT3. Inhibition experiments with ouabain and probenecid confirmed OAT1 and/or OAT3 function. Transport of AG and FL demonstrated polarization of the monolayer on the insert membranes and a higher permeability of the BBM to both substrates.

Time-dependent studies with FL, as well as diffusion studies with FLD, indicate that HK-2 monolayers are leaky. Therefore, transport studies were designed to minimize the effects of diffusion by short incubation periods and uptake rather than or in addition to transepithelial studies. Short incubation periods were also favored to minimize upregulation of transporters.

Uptake experiments for AG indicated transporter-mediated uptake at the BLM as evidenced by time-, concentration- and temperature-dependent uptake. Kinetic analysis of the concentration-dependent uptake of AG yielded a K_m of 330 µM, suggesting low-affinity transport. Studies that demonstrated lack of inhibition of AG transport by coincubation with probenecid, ouabain, PAH and DHEAS suggest that uptake of AG is primarily mediated by a transporter other than OAT1 or OAT3. The OAT3 substrate $E_2 17\beta G$ demonstrated no significant inhibitory effect on AG transport. Decreased net accumulation of AG by ES was not high enough to indicate transport of AG primarily by OAT3. Together, these findings indicate the possibility of an unidentified transporter at the BLM responsible for uptake of AG or noncompetitive OAT3-mediated transport of AG

145

in that a purely competitive process would have yielded much greater inhibition of AG transport.

Upregulation or stimulation of BBM transporters, most likely MRP2, by ouabain, and probenecid offered the best explanation for the findings in this study. Increased clearance of AG was shown when AG was coincubated with ouabain and increased PSa (BBM permeability) was demonstrated for probenecid. Results also suggest possible downregulation of BBM transporters, such as MRP2, by AG. These findings are consistent with literature reports of MRP2 upregulation by ouabain, probenecid and ES and downregulation of MRP2 by $E_2 17\beta G$. Because upregulation of MRP2 can cause a decrease in net accumulation of substrate, it was determined that uptake experiments for AG are best interpreted along with parallel clearance studies.

The biphasic concentration-dependent uptake of AG with an increased rate of cellular accumulation at high concentrations of AG (> 1 mM) are consistent with in vivo studies that found reabsorption at high AG concentrations. Lack of inhibition of transport by probenecid also supports in vivo studies. Together with the difficulties attributed to upregulation, these findings indicate that the HK-2 model may be more appropriate for the study of net effects for glucuronides rather than kinetic analysis and transporter specificity.

Future Directions

The current study was limited to exploration of the BLM transporters responsible for the transport of the majority of organic anions. However, numerous findings were best explained by the presence of BBM transporters. Further characterization of the HK-2 model regarding the expression and function of the BBM transporters MPR2, MPR4, NPT1, and URAT1 and the BLM transporter SAT1 would be valuable. A literature search would be required to determine the expected MW, substrates and inhibitors of the transporters as well as availability of antibodies. Western blot analysis would determine expression of the transporters. Utilizing the HK-2 model developed in the current study, combined uptake and clearance studies of the prototypical substrates and inhibitors for each transporter would be performed.

Additionally, further characterization of transport of the prototypical OAT1 and OAT3 substrates PAH and ES would be performed to provide combined uptake and clearance data in time-dependent and concentration-dependent studies. To minimize modulatory effects as demonstrated in the current study, 2 min incubation periods with minimum tracer concentrations would be used for the concentration-dependent studies. The minimum concentration would be determined by pretesting in uptake experiments to achieve radioactivity levels well above background for a 2 min incubation. From these studies, kinetic analysis of the HK-2 transport system for PAH and ES could be determined.

Transduction of the HK-2 cell line with metallothionein isoform 3 by Kim et al. (2002) resulted in dome formation in the cell line and increased cell density. Domes are associated with tight junctions and vectorial transport function in renal cells. Use of these cells for the study of organic anion transport may yield improved confluence, increased cell density of the monolayer, decreased

diffusion and vectorial transport of organic anions. Initial studies would be side-by-side comparison of FLD diffusion and PAH uptake and clearance. In the event this cell line proves superior for transport studies, the proposed characterization studies described above should be performed in this cell line.

Further work with AG would best be performed in single and double transfectant systems. Use of oocytes or inside-out insect membrane vesicles are the most common models used for such systems. A feasibility study should be performed to determine if development of these models at the current facilities is practical. Development of this technology would open the door to a screening program for chemicals and toxins as substrates or inhibitors of the transduced transporters and provide a valuable complement to the transport and toxicity studies currently performed in the HK-2 cell model and renal tissue slices in the toxicology lab.

Bibliography

Aleo MD, Wyatt RD, Schnellmann RG. Mitochondrial dysfunction is an early event in ochratoxin A but not oosporein toxicity to rat renal proximal tubules. *Tox Appl Pharm* 107: 73-80, 1991.

Appiwattanakul N, Sekine T, Chairoungdua A, Kanai Y, Nakajima M, Sophasan S and Endou H. Transport Properties of Nonsteroidal Anti-inflammatory Drugs by Organic Anion Transporter 1 Expressed in Xenopus laevis Oocytes. *Mol Pharm,* 55: 847-54, 1999.

Audus KL, Bartel RL Hidalgo IJ, Borchardt RT. The Use of Cultured Epithelial and Endothelial Cells for Drug Transport and Metabolism Studies. *Pharm Res* 7(5):435-51, 1990.

Babu E, Takeda M, Narikawa S, Kobayashi Y, Enomoto A, Tojo A, Cha SH, Sekine T, Sakthisekaran D, Endou H. Role of human organic anion transporter 4 in the transport of ochratoxin A. *Biochim Biophys Acta* 1590(1-3):64-75, 2002.

Bahn A, Prawitt D, Buttler D, Reid G, Enklaar T, Wolff NA, Ebbinghaus C, Hillemann A, Schulten HJ, Gunawan B, Fuzesi L, Zabel B, Burckhardt G. Genomic structure and in vivo expression of the human organic anion transporter 1 (hOAT1) gene. *Biochem Biophys Res Commun* 275(2):623-30, 2000.

Bailey MJ, Dickinson RG. Acyl glucuronide reactivity in perspective: biological consequences. *Chem Biol Interact.* Review. 145(2):117-37, 2003.

Bergwerk AJ, Shi X, Ford AC, Kanai N, Jacquemin E, Burk RD, Bai S, Novikoff PM, Stieger B, Meier PJ, Schuster VL, Wolkoff AW. Immunologic distribution of an organic anion transport protein in rat liver and kidney. *Am J Physiol* 271(2 Pt 1): G231-8, 1996.

Berkhin EB and Humphreys MH. Regulation of renal tubular secretion or organic compounds. *Kidney Int* 59:17-30, 2001.

Bodo A, Bakos E, Szeri F, Varadi A, Sarkadi B. The role of multidrug transporters in drug availability, metabolism and toxicity. *Toxicol Lett* 140-141:133-43, 2003a.

Bodo A, Bakos E, Szeri F, Varadi A, Sarkadi B. Differential modulation of the human liver conjugate transporters MRP2 and MRP3 by bile acids and organic anions. J Biol Chem 278(26): 23529-37, 2003b.

Burckhardt BC, Brai S, Wallis S, Krick W, Wolff N, Burckhardt G. Transport of cimetidine by flounder and human renal organic anion transporter 1. *Am J Physiol Renal Physiol* 284: F503-9, 2003a.

Burckhardt BC and Burckhardt G. Transport of organic anions across the basolateral membrane of proximal tubule cells. *Rev Physiol Biochem Pharmacol* 146:95-158, 2003b.

Burckhardt G and Wolff NA. Structure of renal organic anion and cation transporters. *Am J Physiol Renal Physiol* 278:F853-F866, 2000.

Burckhardt G, Bahn A, Wolff N. Molecular physiology of renal p-aminohippurate secretion. *News Physiol Sci* 16:114-118, 2001.

Bradford MM. A rapid and sensitive method for the quantitation of microgram quantities of protein utilizing the principle of protein-dye binding. *Anal Biochem* 72:248-54, 1976.

Cappiello M, Giuliani L, Pacifici GM. Distribution of UDP-glucuronosyltransferase and its endogenous substrate uridine 5'-diphosphoglucuronic acid in human tissues. *Eur J Clin Pharmaco.* 41(4):345-50, 1991.

Cha SH, Sekine T, Kusuhara H, Yu E, Kim JY, Dim DK, Sugiyama Y, Danai Y and Endou H. Molecular cloning and characterization of multispecific organic anion transporter 4 expressed in the placenta. *J Biological Chemistry* 275:4507-4512, 2000.

Cha SH, Sekine T, Fukushima JI, Kanai Y, Kobayashi Y, Goya T and Endou H. Identification and characterization of human organic anion transporter 3 expressing predominantly in the kidney. *Mol Pharmacol* 59(5):1277-86, 2001.

Cihlar T, Lin DC, Pritchard JB, Fuller MD, Mendel DB, Sweet DH. The antiviral nucleotide analogs cidofovir and adefovir are novel substrates for human and rat renal organic anion transporter 1. *Mol Pharmacol* 56(3):570-80, 1999.

Cihlar T and Ho ES. Fluorescence-based assay for the interaction of small molecules with the human renal organic anion transporter 1. *Analy Biochem* 283: 49-55, 2000.

Dantzler, WH. Renal organic anion transport: a comparative and cellular perspective. *Biochim Biophys Acta* 1556: 169-181, 2002.

Deguchi T, Ohtsuki S, Otagiri M, Takanaga H, Asaba H, Mori S, Terasaki T. Major role of organic anion transporter 3 in the transport of indoxyl sulfate in the kidney. *Kidney Int* 61(5): 1760-8, 2002.

Dickinson RG, Harland RC, Ilias AM, Rodgers RM, Kaufman SN, Lynn RK, Gerber N. Disposition of valproic acid in the rat: Dose-dependent metabolism, distribution, enterohepatic recirculation and choleretic effect. *J Pharmacol Exp Ther* 211(3): 583-595, 1979.

Dickinson RG. Acyl glucuronide conjugates: Reactive metabolites of non-steroidal anti-inflammatory drugs. *Proc West Pharmacol Soc* 36: 157-162: 1993.

Duggin GG and Mudge GH. Renal tubular transport of paracetamol and its conjugates in the dog. *Br J Pharmac* 54:359-366, 1975.

Enomoto A, Takeda M, Shimoda M, Narikawa S, Kobayashi Y, Yamamoto T, Sekine T, Cha SH, Niwa T, Endou H. Interaction of human organic anion transporters 2 and 4 with organic anion transport inhibitors. *J Pharmacol Exp Ther* 301(3):797-802, 2002.

Enomoto A, Kimura H, Chairoungdua A, Shigeta Y, Jutabha P, Cha SH, Hosoyamada M, Takeda M, Sekine T, Igarashi T, Matsuo H, Kikuchi Y, Oda T, Ichida K, Hosoya T, Shimokata K, Niwa T, Kanai Y, Endou H. Molecular identification of a renal urate-anion exchanger that regulates blood urate levels. *Nature* 417:447-452, 2002.

Garcia-Ocana A, Galbraith SC, van Why SK, Yang K., Golovyan L, Dann P, Zager RA, Stewart AF, Siegel NJ and Orloff JJ. Expression and role of parathyroid hormone-related protein in human renal proximal tubule cells during recovery from ATP depletion. *J Am Soc Nephrol* 10:238-244, 1999.

Gao B, Hagenbuch B, Kullak-Ublick GA, Benke D, Aguzzi A, Meier PJ. Organic anion-transporting polypeptides mediate transport of opioid peptides across blood-brain barrier. *J Pharmacol Exp Ther* 294(1): 73-9, 2000.

Gerk P, Vore M. Regulation of expression of the multidrug resistance-associated protein 2 (MRP2) and its role in drug disposition. *J Pharmacol Exp Ther* 302(2):407-15, 2002.

Gesek FA, Wolff EW, Strandhoy JW. Improved separation method for rat proximal and distal renal tubules. *Am J Physiol* 253: F358-F365, 1987.

Goodman Gillman A, Rall TW, Nies AS, Taylor P. The Pharmacological Basis of Therapeutics, Eighth Edition, Chapter 30 Inhibitors of tubular transport of organic compounds. Irwin M Weiner. *Pergamon Press*, Elmsford, New York, pp. 745-746, 1990.

Groves CE, Evans KK, Dantzler WH, Wright SH. Peritubular organic cation transport in isolated rabbit proximal tubules. *Am J Physiol* 266: F450-8, 1994.

Groves CE, Morales M, Wright SH. Peritubular Transport of Ochratoxin A in Rabbit Renal Proximal Tubules. *JPET* 284:943-8, 1998.

Groves CE and Morales MN. Chlorotrifluoroethylcysteine interaction with rabbit proximal tubule cell basolateral membrane organic anion transport and apical membrane amino acid transport. *J Pharm Exp Ther* 291:555-561, 1999a.

Groves CE, Nowak G, Morales MN. Ochratoxin A Secretion in Primary Cultures of Rabbit Renal Proximal Tubule Cells. *J Am Soc Nephrol* 10:13-20, 1999b.

Hagenbuck B, Meier PJ. The superfamily of organic anion transporting polypeptides. *Biochim Biophys Acta* 1609(1):1-18, 2003.

Handler JS. Studies of kidney cells in culture. *Kidney Int* 30(2):208-15, 1986.

Hasegawa M, Kusuhara H, Sugiyama D, Ito K, Ueda S, Endou H, Sugiyama Y. Functional involvement of rat organic anion transporter 3 (rOat3; Slc22a8) in the renal uptake of organic anions. *J Pharmacol Exp Ther* 300(3):746-53, 2002.

Heckman P, Russel FG and vanGinneken CA. Renal transport of the glucuronides of paracetamol and p-nitrophenol in the dog. *Drug Met Dispo* 14(3): 370-371, 1986.

Hickey EJ, Raje RR, Reid VE, Gross SM and Ray SD. Diclofenac induced in vivo nephrotoxicity may involve oxidative stress-mediated massive genomic DNA fragmentation and apoptotic cell death. *Free Radical Biology & Medicine* 31(2): 139-152, 2001.

Hirohashi T, Suzuki H, Sugiyama Y. Characterization of the transport properties of cloned rat multidrug resistance-associated protein 3 (MRP3). *J Biol Chem* 274: 15181-5, 1999.

Hosoyamada M, Sekine T, Kanai Y, Endou H. Molecular cloning and functional expression of a multispecific organic anion transporter from human kidney. *Am J Physiol* 276: F122-F128, 1999.

Houser MT, Berndt WO. Unilateral nephrectomy in the rat: effects on mercury hamdling and renal coritcal subcellular distribution. *Toxicol Appl Pharmacol* 93: 187-194, 1988.

Ilias A, Urban Z, Seidl TL, Le Saux O, Sinko E, Boyd CD, Sarkadi B, Varadi A. Loss of ATP-dependent transport activity in pseudoxanthoma elasticum-mutants of human ABCC6 (MRP6). *J Biol Chem* 277(19): 16860-7, 2002.

Inui K, Masuda S, and Saito H. Cellular and molecular aspects of drug transport in the kidney. *Kidney Int* 58:944-958, 2000.

Ji L, Masuda S, Saito H, Inui K. Down-regulation of rat organic cation transporter rOCT2 by 5/6 nephrectomy. *Kidney Int* 62(2):514-24, 2002.

Jones SG, Morrisey K, Williams JD and Phillips AO. TGF-β1 stimulates the release of pre-formed bFGF from renal proximal tubular cells. *Kidney Int* 56:83-91, 1999.

Jones DP, Sundby GB, Ormstad Kand Orrenius S. Use of isolated kidney cells for study of drug metabolism. *Biochem Pharmacol* 28: 929-935, 1979.

Joshi MD and Jagannathan V. Hexokinase*. Methods Enzymol* 9:371-375, 1966.

Jung KY, Takeda M, Kim DK, Tojo A, Narikawa S, Yoo BS, Hosoyamada M, Cha SH, Sekine T. Characterization of ochratoxin A transport by human organic anion transporters. *Life Sci* 69: 2123-35, 2001.

Juteau H, Gareau Y and Labelle M. A convenient synthesis of β-acyl glucuronides. *Tetrahedron Lett* 38(9): 1481-1484, 1997.

Kanai N, Lu R, Boa Y, Wolkoff AW, Vore M, Schuster VL. Estradiol 17 beta-glucuronide is a high-affinity substrate for oatp organic anion transporter. *Am J Physiol* 270(2 Pt 2):F326-31, 1996.

Keppler D, Kamisako T, Leier I, Cui Y, Nies AT, Tsujii H, Konig J. Localization, substrate specificity, and drug resistance conferred by conjugate export pumps of the MRP family. *Adv Enzyme Regul* 40:339-49, 2000.

Kikuchi R, Kusuhara H, Sugiyama D, Sugiyama Y. Contribution of organic anion transporter 3 (Slc22a8) to the elimination of p-aminohippuric acid and benzylpenicillin across the blood-brain barrier. *Pharmacol Exp Ther* 306(1):51-8, 2003.

Kim D, Garrett SH, Sens MA, Somji S, Sens DA. Metallothionein isoform 3 and proximal tubule vectorial active transport. *Kidney Int* 61(2): 464-72, 2002.

King AR and Dickinson RG. Studies on the reactivity of acyl glucuronides-IV, Covalent binding of diflunisal to tissues of the rat. *Biochem Pharmacol* 45:1043-7, 1993.

Kipp H, Pichetshote N, Arias IM. Transporters on demand: Intrahepatic pools of canalicular ATP binding cassette transporters in rat liver. *J Biol Chem* 276(10): 7218-24, 2001.

Klaassen, CD. Casarett & Doull's Toxicology, 6th Edition. Absorption, Distribution, and Excretion of Toxicants, *McGraw-Hill,* New York, 2001.

Koepsell H, Endou H. The SLC22 drug transporter family. *Pflugers Arch* 447(5):666-76, 2004. Epub Jul 19, 2003.

Kojima R, Sekine T, Kawachi M, Cha SH, Suzuki Y, Endou H. Immunolocalization of multispecific organic anion transporters, OAT1, OAT2, and OAT3, in rat kidney. J *Am Soc Nephrol* 13(4):848-57, 2002.

Konig J, Nies A, Cui Y, Leier I, Keppler D. Conjugate export pumps of the multidrug resistance protein (MRP) family: localization, substrate specificity, and MRP2-mediated drug resistance. *Biochim Biophys Acta* 1461(2): 377-94 Review, 1999.

Kretz-Rommel A.and Boelsterli UA. Diclofenac covalent protein binding is dependent on acyl glucuronide formation and is inversely related to P450-mediated acute cell injury in cultured rat hepatocytes. *Toxicol Appl Pharmicol* 120: 155-161, 1993.

Kretz-Rommel A and Boelsterli UA. Selective protein adducts to membrane proteins in cultured rat hepatocytes exposed to dicolfenac: radiochemical and immunochemical analysis. *Mol Pharm* 45: 237-244, 1993.

Kubitz R, D'urso D, Keppler D, Haussinger D. Osmodependent dynamic localization of the multidrug resistance protein 2 in the rat hepatocyte canalicular membrane. *Gastroenterology* 113(5):1438-42. 1997.

Kubitz R, Huth C, Schmitt M, Horbach A, Kullak-Ublick G, Haussinger D. Protein kinase C-dependent distribution of the multidrug resistance protein 2 from the canalicular to the basolateral membrane in human HepG2 cells. *Hepatology* 34(2): 340-50, 2001.

Kumar CK, Yanagawa N, Ortiz A and Said HM. Mechanisms and regulation of riboflavin uptake by human renal proximal tubule epithelial cell line HK-2. *Am J Physiol* 274 (43):F104-F110, 1998.

Kusuhara H, Sekine T, Utsunomiya-Tate N, Tsuda M, Kojima R, Cha SH, Sugiyama Y, Kanai Y, Endou H. Molecular cloning and characterization of a new multispecific organic anion transporter from rat brain. *Biol Chem* 274(19):13675-80, 1999.

Lash LH and Tokarz JJ. Isolation of two distinct populations of cells from rat kidney cortex and their use in the study of chemical-induced toxicity. *Analytical Biochem* 182: 271-279, 1989.

Lash LH, Tokarz JJ, Pegouske DM. Susceptibility of primary cultures of proximal tubular and distal tubular cells from rat kidney to chemically induced toxicity. *Toxicology* 103: 85-103, 1995.

Lash LH. Use of freshly isolated and primary cultures of proximal tubular and distal tubular cells from rat kidney. *Methods in Renal Toxicology*, Eds. Zalups R.K., Lash L.H., CRC Press, New York: 189-215, 1996.

Lash LH. In Vitro Methods of Assessing Renal Damage. *Toxicologic Pathology* 26(1):32-42, 1998.

Leach MW, Frank DW, Berardi MR, Evans EW, Johnson RC, Schuessler DG, Radwanski E and Cartwright ME. Renal changes associated with naproxen sodium adminisration in cynomolgus monkeys. *Toxicol Pathol* 27(3): 295-306, 1999.

Leier I, Hummel-Eisenbeiss J, Cui Y, Keppler D. ATP-dependent para-aminohippurate transport by apical multidrug resistance protein MRP2. *Kidney Int.* 57(4): 1636-42, 2000.

Lever JE. Expression of Differentiated Functions in Kidney Epithelial Cell Lines. *Mineral Electrolyte Metab* 12:14-19, 1986.

Lock EA, Reed CJ. Xenobiotic metabolizing enzymes of the kidney. *Toxicol Pathol.* Review. 26(1):18-25, 1998.

Lohr JW, Willsky GR, Acara MA. Renal drug metabolism. *Pharmacol Rev* 50(1):107-41, 1998.

Lopez-Nieto CE, You G, Bush KT, Barros EJ, Beier DR, Nigam SK., Molecular cloning and characterization of NKT, a gene product related to the organic cation transporter family that is almost exclusively expressed in the kidney. *J Biol Chem* 272(10):6471-8, 1997.

Lu R, Chan BS, Schuster VL., Cloning of the human kidney PAH transporter: narrow substrate specificity and regulation by protein kinase C. *Am J Physiol* 276(2 Pt 2): F295-303, 1999.

Malo C, Berteloot A. Analysis of kinetic data in transport studies: new insights from kinetic studies of Na(+)-D-glucose cotransport in human intestinal brush-border membrane vesicles using a fast sampling, rapid filtration apparatus. J Membr Biol. 122(2):127-41, 1991.

Masereeuw R, Moons MM, Toomey BH, Russel FG and Miller DS. Active Lucifer Yellow secretion in renal proximal tubule: Evidence for organic anion transport system crossover. *J Pharmacol Exp Ther* 289:1104-1111, 1999.

Masuda S, Ibaramoto K, Takeuchi A, Saito H, Hashimoto Y, Inui K. Cloning and functional characterization of a new multispecific organic anion transporter, OAT-K2, in rat kidney*. Molec Pharm* 55:743-752, 1999.

Masuda S, Saito H, Nonoguchi H, Tomita K, Inui K. mRNA distribution and membrane localization of the OAT-K1 organic anion transporter in rat renal tubules. *FEBS Lett* 407: 127-131, 1997.

McGurk KA, Remmel RP, Hosagrahara V, Tosh D and Burchell B. Reactivity of mefenamic acid 1-o-acyl glucuronide with proteins *in vivo* and *ex vivo*. *Drug Met Dispo* 24(8): 842-849, 1996.

Miller DS, Prichard JB. Dual Pathways for Organic Anion Secretion in Renal Proximal Tubule. *J Exp Zool* 279(5):462-70, Dec 1, 1997.

Miners JO, MacKenzie PI. Drug glucuronidation in humans. *Pharmac Ther* 51:347-369, 1991.

Moolenaar F, Crancrinus S, Visser J, de Zeeuw D, Meijer DKF. Clearance of indomethacin occurs predominantly by renal glucuronidation. *Pharm Weekbl Sci.* 14(4):191-5, 1992.

Morris ME, Levy G, Renal Clearance and Serum Protein Bidking of Acetaminophen and Its Major Conjugates in Humans. *J Pharm Sci* 73(8):1038-41, Aug 1984.

Motohashi H, Sakurai Y, Saito H, Masuda S, Urakami Y, Goto M, Fukatsu A, Ogawa O, Inui K. Gene Expression Levels and Immunolocalization of Organic Ion Transporters in the Human Kidney. *J Am Soc Nephrol* 13(4):866-74, 2002.

Mottino AD, Cao J, Veggi LM, Crocenzi F, Roma MG, Vore M. Altered localization and activity of canalicular Mrp2 in estradiol-17beta-D-glucuronide-induced cholestasis *Hepatology* 35(6):1409-19, 2002.

Mottino AD, Veggi LM, Wood M, Velez Roman JM, Vore M. Biliary secretion of glutathione in estradiol 17{beta}-d- glucuronide-induced cholestasis. *J Pharmacol Exp Ther* [Epub ahead of print]. Jul 31, 2003.

Mulder GJ, Coughtrie MWH and Burchell B. *Conjugation reactions in drug metabolism*, Chapter 4. Taylor & Francis Ltd, 1990.

Mulder GJ. Glucuronidation and its role in regulation of biological activity of drugs. *Annu Rev Pharmacol Toxicol* 32:25-49, 1992.

Nagata Y, Kusuhara H, Endou H, Sugiyama Y. Expression and functional characterization of rat organic anion transporter 3 (rOat3) in the choroid plexus. *Mol Pharmacol* 61(5):982-8, 2002.

Newton JF, Braselton JR, Kuo CH, Kluwe WM, Gemborys MW, Mudge GH, Hook JB. Metabolism of acetaminophen in the isolated perfused kidney. *J Pharmacol Exp Ther* 221(1): 76-79, 1982.

Nowak G.and Schnellmann RG. L-Ascorbic acid regulates growth and metabolism of renal cells: improvement in cell culture. *Am J Physiol* 271:C2072-C2080, 1996.

Nowak G and Schnellmann R. Improved culture conditions stimulate gluconeogenesis in primary cultures of renal proximal tubule cells. *Am J Physiol* 268 (*Cell Physiol* 37)): C1053-C1061, 1995.

O'Neill PJ, Yorgey KA, McKown LA. Dose-dependent pharmacokinetics and renal handling of zomepirac in rhesus monkeys. *J Pharmacol Exp Ther* 219(3): 665-8, 1981.

Pantuck EJ, Pantuck CB, Kappas A, Conney AH, Anderson KE. Effects of protein and carbohydrate content of diet on drug conjugation. *Clin Pharmacol Ther* 254-8, September, 1991.

Podelski V, Johnson A, Wright S, Dela Rosa V and Zager RA. Ethylene glycol mediated tubular injury: identification of critical metabolites and injury pathways. *Amer J Kidney Dis* 38(2):339-348, 2001.

Prescott LF. Kinetics and metabolism of paracetamol and phenacetin. *Br J Clin Pharmacol* Suppl 2:291S-298S, 1980.

Pritchard JB. Coupled transport of p-aminohippurate by rat kidney basolateral membrane vesicles. *Am J Physiol* 255(4 Pt 2): F597-604, 1988.

Pritchard JB and Miller DS. Renal secretion of organic anions and cations. *Kidney Int* 49: 1649-54, 1996.

Raucusen LC, Monteil C, Sgrignoli A, Lucskay M, Marouillat S, Rhim JGS and Morin J. Cell lines with extended in vitro growth potential from human renal proximal tubule: Characterization, response to inducers, and comparison with established cell lines. *J Lab Clin Med* 129(3):318-329, 1997.

Race JE, Grassl SM, Williams WJ, Holzman EJ, Molecular Cloning and Characterization of Two Novel Human Renal Organic Anion Transporters (hOAT1 and hOAT3), *Biochem Biophys Res Commun*, 225, 508-514, 1999.

Reid G, Wolff NA, Dautzenberg FM, Burckhardt G. Cloning of a human renal p-aminohippurate transporter, hROAT1. *Kidney Blood Press Res.* 21(2-4):233-7, 1998.

Reid G, Wielinga P, Zelcer N, van der Heijden I, Kuil A, de Haas M, Wijnholds J, Borst P. The human multidrug resistance protein MRP4 functions as a prostaglandin efflux transporter and is inhibited by nonsteroidal antiinflammatory drugs. *Proc Natl Aca Sci USA*, 100(16):9244-9, 2003.

Romiti N, Tramonti G, Chieli E, Influence of different chemicals on MDR-1 P-glycoprotein expression and activity in the HK-2 proximal tubular cell line. *Toxicol Appl Pharmacol.*, 3(2):83-91, Sep 1, 2002.

Russel FG, Massereeuw R, van Aubel RA, Molecular Aspects of Renal Anionic Drug Transport *Annu Rev Physiol.*, 64:563-94, 2002.

Ryan MJ, Johnson G, Kirk J, Fuerstenberg SM, Zager RA and Torok-Storab B, HK-2: An immortalized proximal tubule epithelial cell line from normal adult human kidney. *Kidney Int*, 45:48-57, 1994.

Saito H, Masuda S, Inui K, Cloning and functional characterization of a novel rat organic anion transporter mediated basolateral uptake of methotrexate in the kidney. *J Biol. Chem.* 271(34): 20719-20725, 1996.

Sakhrani LM, Fine, LG, Renal Tubular Cells in Culture. *Mineral Electrolyte Metab.* 9:276-81, 1983.

Sallustio BC, Sabordo L, Evans AM, Nation RL. Hepatic disposition of electrophilic acyl glucuronide conjugates . *Curr Drug Metab* 1(2): 163-80, 2000.

Sasaki M, Suzuki H, Ito K, Abe T, Sugiyama Y., Transcellular transport of organic anions across a double-transfected Madin-Darby canine kidney II cell monolayer expressing both human organic anion-transporting polypeptide (OATP2/SLC21A6) and Multidrug resistance-associated protein 2 (MRP2/ABCC2). *J Biol Chem* 277(8):6497-503, 2002.

Sauvant C, Holzinger H, Gekle M, Modulation of the Basolateral and Apical Step of Transepithelial Organic Anion Secretion in Proximal Tubular Opossum Kidney Cells, *J. Biol. Chem.* 276(18); 14695-14703, 2001.

Savina PM, Brouwer KL. Probenecid-impaired biliary excretion of acetaminophen glucuronide and sulfate in the rat. *Drug Metab Dispos.* 20(4): 496-501, 1992.

Schmitt M, Kubitz R, Lizun S, Wettstein M, Haussinger D. Regulation of the dynamic localization of the rat Bsep gene-encoded bile salt export pump by anisoosmolarity. *Hepatology.* 33(3):509-18, 2001.

Seitz S and Boelsterli UA. Diclofenac acyl glucuronide, a major biliary metabolite, is directly involved in small intestinal injury in rats. *Gastroenterology* 115: 1476-1482, 1998.

Sekine T, Watanabe N, Hosoyamada M, Kanai Y, Endou H. Expression cloning and characterization of a novel multispecific organic anion transporter. *J Biol Chem* 272: 18526-18529, 1997.

Sekine T, Cha SH, Tsuda M, Apiwattanakul N, Nakajima N, Kanai Y, Endou H. Identification of multispecific organic anion transporter 2 expressed predominantly in the liver. *FEBS Lett* 429:179-82, 1998.

Sekine T, Cha SH and Endou H. The multispecific organic anion transporter (OAT) family. *Pflugers Arch - Eur J Physiol* 440:337-350, 2000.

Shimada H, Moewes B, Burckhardt G. Indirect coupling to Na$^+$ of p-aminohippuric acid uptake into rat renal basolateral membrane vesicles. *Am J Physiol.* 253(5 Pt 2): F795-801, 1987.

Simonson GD, Vincent AC, Roberg KJ, Huang Y, Iwanij, V. Molecular cloning and characterization of a novel liver-specific transport protein. *J Cell Sci* 107:1065-1072, 1994.

Spahn-Langguth H and Benet LZ. Acyl glucuronides revisited: is the glucuronidation process a toxification as well as a detoxification mechanism? *Drug Metab Rev* 24:5-48, 1992.

Spahn-Langguth H, Dahms M, Hermening A. Acyl glucuronides: covalent binding and its potential relevance. *Adv Exp Med Biol* 387:313-28, 1996.

Smith PC and Liu JH, Covalent binding of suprofen to renal tissue of rat correlates with excretion of its acyl glucuronide. *Xenobiotica* 25(5):531-540, 1995.

Sugiyama D, Kusuhara H, Shitara Y, Abe T, Meier PJ, Sekine T, Endou H, Suzuki H, Sugiyama Y. Characterization of the efflux transport of 17beta-estradiol-D-17beta-glucuronide from the brain across the blood-brain barrier. *J Pharmacol Exp Ther* 298(1):316-22, 2001.

Sugiyama D, Kusuhara H, Shitara Y, Abe T, Sugiyama Y. Effect of 17beta-estradiol-D-17beta-glucuronide on the rat organic anion transporting polypeptide 2-mediated transport differs depending on substrates. *Drug Metab Dispos* 30(2):220-3, 2002.

Sun W, Wu RR, Van Poelje PD and Enrion MD. Isolation of a family of organic anion transporters from human liver and kidney. *Biochem Biophys Res Commun* 283(2):417-22, 2001.

Sweet DH, Wolff NA and Pritchard JB. Expression cloning and characterization of ROAT1. *J Biol Chem* 272:30088-30095, 1997.

Sweet DH, Bush KT and Nigam SK. The organic anion transporter family: from physiology to ontogeny and the clinic. *Am J Physiol Renal Physiol* 281:F197-F205, 2001.

Sweet DH, Miller DS, Pritchard JB, Fujiwara Y, Beier DR, Nigam SK. Impaired Organic Anion Transport in Kidney and Choroid Plexus of Organic Anion Transporter 3 (O*at3 (Slc22a8))* Knockout Mice. *J Biol Chem* 277(30): 26934-26943, 2002.

Sweet DH, Chan LM, Walden R, Yang XP, Miller DS, Pritchard JB. Organic anion transporter 3 (Slc22a8) is a dicarboxylate exchanger indirectly coupled to the Na+ gradient. *Am J Physiol Renal Physiol.* 284(4): F763-9, 2003.

Takeda M, Sekine T, Endou H. Regulation by protein kinase C of organic anion transport driven by rat organic anion transporter 3 (rOAT3). *Life Sciences* 67:1087-93, 2000.

Takeda M, Narikawa S, Hosoyamada M., Cha SH, Sekine T, Endou H. Characterization of organic anion transport inhibitors using cells stably expressing human organic anion transporters. *Eur J Physiol* 419:113-20, 2001.

Takeda M, Khamdang S, Narikawa S, Kimura H, Kobayashi Y, Yamamoto T, Cha SH, Sekine T, Endou H. Human organic anion transporters and human organic cation transporters mediate renal antiviral transport. *J Pharm Exp Ther* 300: 918-924, 2002.

Takano M, Hirozane K, Okamura M, Takayama A, Nagai J and Hori R. ρ-Aminohippurate transport in apical and basolateral membranes of the OK kidney epithelial cells. *J Pharm Exp Ther* 269(3): 970-975, 1994.

Tamai I, Nozawa T, Koshida M, Nezu J, Sai Y and Tsuji A. Functional Characterization of Human Organic Anion Transporting Polyeptide B (OATP-B) in Comparison with Liver-Specific OATP-C. *Pharmaceutical Research* 18(9): 1262-9, 2001.

Terlouw SA, Masereeuw R, Russel FG. Modulatory effects of hormones, drugs, and toxic events on renal organic anion transport. *Biochem Pharmacol.* 65(9): 1393-405, 2003.

Tirona RG, Kim RB. Pharmacogenomics of organic anion-transporting polypeptides (OATP). *Advanced Drug Delivery Reviews* 54: 1343-52, 2002.

Tojo A, Sekine T, Nakajima N, Hosoyamada M, Kanai Y, Kimura K, Endou H. Immunohistochemical localization of multispecific renal organic anion transporter 1 in rat kidney. *Am Soc Nephrol.* 10(3):464-71, 1999.

Tramonti G, Romiti N, Norpoth M and Chieli E. P-glycoprotein in HK-2 proximal tubule cell line. *Renal Failure* 23(3&4):331-337, 2001.

Tukey RH, Strassburg CP.   Human UDP-glucuronosyltransferases: metabolism, expression, and disease. *Annu Rev Pharmacol Toxicol.* Review. 40:581-616, 2000.

Uchino H, Tamai I, Yamashita K, Minemoto Y., SAai Y, Yabauuchi H, Miyamoto K, Takesa E, Tsuji A. p-Aminohippuric acid transport at renal apical membrane mediated by human inorganic phosphate transporter NPT1. *Biochem Biophys Res Commun* 2;270(1):254-9, 2000.

Ullrich KJ, Rumrich G, Gemborys M, Dekant W. Transformation and transport: How does metabolic transformation change the affinity of substrates for the renal contraluminal anion and cation transporters? *Toxicol Lett* 53: 19-27, 1990.

Ullrich KJ. Renal transporters for organic anions and organic cations. Structural requirements for substrates. *J Membrane Biol* 158: 95-107, 1997.

Van Aubel RA, Masereeuw R, Russel FG. Molecular pharmacology of renal organic anion transporters. *Am J Physiol Renal Physiol* 279:F216-F232, 2000.

Van Aubel RA, Peters JG, Masereeuw R, Van Os CH, Russel FG. Multidrug resistant protein Mrp2 mediates ATP-dependent transport of the classic renal organic anion *p*-aminohippurate. *Am J Physiol Renal Physiol* 279:F713-F717, 2000.

Van Aubel RA, Smeets PH, Peters JG, Bindels RJ, Russel FG. The MRP4/ABCC4 gene encodes a novel apical organic anion transporter in human kidney proximal tubules: putative efflux pump for urinary cAMP and cGMP. *J Am Soc Nephrol*. 13: 595-603, 2002.

Van Crugten JT, Sallustio BC, Nation RL and Somogyi AA. Renal tubular transport of morphine, morphine-6-glucuronide, and morphine-3-glucuronide in the isolated perfused rat kidney. *Drug Met Dispo* 19(6): 1087-1092, 1991.

Van Montfoort JE, Hagenbuch B, Groothuis GM, Koepsell H, Meier PJ, Meijer DK. Drug uptake systems in liver and kidney. *Curr Drug Metab*. 4(3): 185-211, 2003.

Visarius TM, Putt DA, Schare JM, Pegouske DM, Lash LH. Pathways of glutathione metabolism and transport in isolated proximal tubular cells from rat kidney. Biochem Pharmacol. 52(2):259-72, 1996.

Whelton A. Nephrotoxicity of nonsteroidal anti-inflammatory drugs: Physiologic foundations and clinical implications. *Am J Med* 106(5B):13S-24S, 1999.

Whitin JC, Bhamre S, Tham DM, Cohen HJ. Extracellular glutathione peroxidase is secreted basolaterally by human renal proximal tubule cells. *Am J Physiol Renal Physiol* 283(1):F20-8, 2002.

Xiong H, Turner K, Ward E, Jansen P, Brouwer K. Altered hepatobiliary disposition of acetaminophen glucuronide in isolated perfused livers from multidrug resistance-associated protein 2-deficient TR(-) Rats. *J Pharmacol Exp Ther*. 295(2): 512-8, 2000.

Zager RA and Burkhart K. Differential effects of glutathione and cysteine on Fe^{2+}, Fe^{3+}, H_2O_2 and myoglobin-induced proximal tubular cell attack. *Kidney Int* 53(6):1661-1672, 1998.

Zager RA and Burkhart K. Myoglobin toxicity in proximal human kidney cells: Roles of Fe, Ca^{2+}, H$_2$O$_2$, and terminal mitochondrial electron transport. *Kidney Int* 51:738-738, 1997.

Zelcer N, Reid G, Wielinga P, Kuil A, van der Heijden I, Schuetz JD, Borst P. Steroid and bile acid conjugates are substrates of human multidrug-resistance protein (MRP) 4 (ATP-binding cassette C4). *Biochem J* 371(Pt 2): 361-7, 2003.

Appendix

Buffer Preparation

<u>10 X Phosphate Buffered Saline (PBS) with 5 mM glucose, 500 ml</u>

1.38 M sodium chloride	40.32 g
26.82 mM potassium chloride	1.00 g
23.25 mM sodium phosphate, dibasic/anhydrous	1.65 g
14.70 mM potassium phosphate, monobasic/anhydrous	1.00 g
5.00 mM magnesium chloride	1.02 g
50 mM glucose	4.50 g

In approximately 460 ml of deionized distilled water, the ingredients were added while stirring. The pH was adjusted to 7.4 with HCl and NaOH. The buffer was brought to volume (500 ml) with deionized distilled water, sterile filtered and refrigerated. Dilute 1:10 with deionized distilled H_2O and adjust pH to 7.4.

<u>Waymouth's Buffered Transport Media (WBTM), 1 liter</u>

135 mM sodium chloride	7.889 g
13 mM HEPES	3.384 g
2.5 mM calcium chloride dehydrate	0.368 g
1.2 mM magnesium chloride hexahydrate	0.244 g
0.8 mM magnesium sulfate	0.194 g
5 mM potassium chloride	0.373 g
5.78 mM glucose	1.042 g

In approximately 950 ml of deionized distilled water, the ingredients were added while stirring. The pH was adjusted to 7.4 with HCl and NaOH. The buffer was brought to volume (1000 ml) with deionized distilled water, sterile filtered and refrigerated.

Compounds for Toxicity Studies

AG (200 μM and 500 μM)

A 50 mM stock of AG was prepared by adding 0.5 ml deionized water to 8.732 mg AG. A 20 mM stock was prepared from the 50 mM stock by adding 80 ml x 50 mM AG to 120 ml deionized water. Final concentration incubation buffers were prepared by adding 20 μl x 20 mM stock to 2 ml transport media (PBS, 5 mM glucose) for 200 μM AG and 20 μl x 50 mM stock to 2 ml transport media for 500 μM AG. Control transport media was prepared with 20 ml x deionized water to 2 ml transport media.

APAP (200 μM and 500 μM)

A 50 mM stock of APAP was prepared by adding 1.0 ml deionized water to 7.56 mg APAP. A 20 mM stock was prepared from the 50 mM stock by adding 80 ml x 50 mM APAP to 120 ml deionized water. Final concentration incubation buffers were prepared by adding 20 μl x 20 mM stock to 2 ml transport media (PBS, 5 mM glucose) for 200 μM APAP and 20 μl x 50 mM stock to 2 ml transport media for 500 μM APAP. Control transport media was prepared with 20 ml x deionized water to 2 ml transport media.

Diclofenac (200 μM and 500 μM)

A 50 mM stock of diclofenac was prepared by adding 0.5 ml deionized water to 7.952 mg diclofenac. A 20 mM stock was prepared from the 50 mM stock by adding 80 ml x 50 mM diclofenac to 120 ml deionized water. Final concentration incubation buffers were prepared by adding 20 μl x 20 mM stock to 2 ml transport media (PBS, 5 mM glucose) for 200 μM diclofenac and 20 μl x 50 mM stock to 2 ml transport media for 500 μM diclofenac. Control transport media was prepared with 20 ml x deionized water to 2 ml transport media.

<u>Solutions for Gel Preparation and Western Blot</u>

[†] Solutions were prepared by Dr. Kelley Kiningham

<u>Cell Fractionization</u>

<u>Homogenization Buffer (25 ml)</u>

20 mM HEPES ....5 ml x 100 mM

5 mM EGTA...1.25 ml x 0.1M

10 mM 2-mercaptoethanol (2ME)*...20 ul

1 ug/1 ml pepstatin .... 25 ul of (1 mg/1 ml)

1 ug/1 ml leupeptin .... 20 ul of (1 mg/1 ml)

1 ug/1 ml aprotinin... 20 ul of (1 mg/1 ml)

1 mM phenylmethylsufonyl fluoride (PMSF) ....500 ul x10mM

Diluted to 25 ml with deionized water

* 2ME was not included for nonreduced protein samples.

<u>Gel Preparation</u>

<u>30% Acrylamide, 0.8% Bisacrylamide</u>[†] (neurotoxic)

60 g acrylamide

1.6 g bisacrylamide

dilute to 200 ml with water

Use 37°C water bath to dissolve solids if necessary; sterile filter into foil

wrapped or brown bottle and store at 4°C.

<u>5X Separation Buffer</u>[†]

56.76 g TRIS

1.25 g sodium dodecyl sulfate (SDS)

pH to 8.8

Diluted to 250 ml with DI water

<u>5X Stacking Buffer</u>[†]

37.85 g TRIS

2.5 g SDS

pH to 6.8

Diluted to 500 ml with DI water

<u>10% Ammonium Persulfate (APS)</u>   (prepared fresh daily)

0.1 g APS in 1 ml deionized water

<u>2X Sample Buffer</u>[†]

0.76 g TRIS (125 mM)

2 g SDS (13.9 mM or 4%)

10 ml Glycerol (20%)

5 ml 2-mercaptoethanol (2ME)* (10%)

pH to 6.8

Diluted to 50 ml with DI water

Bromophenol blue (1-2 mg) added until deep blue color obtained

Sample Buffer was prepared without 2-ME which was added just before use (1:10). Note: If 2X sample buffer is prepared without 2ME, it can remain at room temperature.

* 2ME was not included for nonreduced protein samples. DI water was substituted for 2ME.

Separation Gel	8 % Gel (ml)	12.5% Gel (ml)
5X Separation Buffer	7.0	7.0
30% Acrylamine, 0.8% Bis	9.3	14.6
H_2O	18.5	13.2
10% Ammonium Persulfate*	0.15	0.15
TEMED	0.025	0.025
Total	35.0 ml	35.0 ml

N-butanol (~2 ml)

Stacking Gel	ml
5X Separation Buffer	3.0
30% Acrylamine, 0.8% Bis	1.5
H_2O	10.5
10% Ammonium Persulfate*	0.075
TEMED	0.015

After rinsing n-butanol from the set separation gel with a large volume of water then carefully drying the mold, Stacking Gel was prepared and poured over the separation gel then left at room temperature for one hour to set.

10X Electrode Buffer[†] (Dilute 1:10 prior to use)

30.3 g TRIS (250 mM)

144 g Glycine (1.92 M)

10 g SDS (34.68 mM)

pH to 8.3

Diluted to 1 L with deionized water

Solutions Needed for Western Analysis

Transfer Buffer[†]

12.12 g TRIS

57.6 g glycine

800 ml methanol

3.2 L distilled water

Solution should be precooled for high voltage transfers.

Ponceau S[†]

g Ponceau S

5 ml acetic acid

diute to 100 ml with deionized water

Solution is stored in a brown bottle and may be reused.

10X TBS[†] (Dilute 1:10 prior to use)

12.12 g TRIS

87.66 g NaCl

pH to 8.0

Dilute to 1 L with deionized water

1X TBST

Add 500 μl Tween-20 to 1 L 1X TBS

Blocking solution (Blotto A)

5% non-fat dry milk in TBST (2.5 mg to 50 ml)

Prepared fresh daily and refrigerated.

Stock Solutions for Transport Substrates/Inhibitors

Stock solutions were prepared according to the following formula:

Mass (g) = MW (g/mol) x desired molarity (mol/L) x 1L/1000 ml

Diluted to 1 ml with appropriate solution.

Transport media was prepared at 1:100 (26 μl stock to 2.6 ml WBTM). An equal volume (26 μl) of WBTM was added to the control treatment.

AG (MW 349.3)

A 5mM stock was prepared from 1.746 mg AG solubilized in 1 ml deionized distilled water. Dilutions were prepared from this stock. Typically a 1:100 dilution (30 μl in 3 ml transport media) was prepared.

DHEAS (100 mM) MW 390.5

3.905 mg DHEAS was dissolved in 0.1 ml 100% methanol (solubility, 50 mg/ml methanol) and vortexed for 1 min. This 100 mM stock was used at 1:100 for final concentration of 1 mM or diluted 1:10 (100 μl to 1 ml) with WBTM and used 1:100 for 100 μM final concentration. Final concentration of methanol was 1% for 1 mM DHEAS or 0.1% for 10 μM DHEAS. An equal amount of methanol was added to control and all other treatments run simultaneously.

$E_2 17\beta G$ (21.254 mM) MW 470.5

25 mg $E_2 17\beta G$ was dissolved in 2.5 ml 0.1 M NaOH yielding a 21.254 mM solution; 37.6 μl x 21.254 mM $E_2 17\beta G$ was added to a volume of 8 ml WBTM for a final concentration of 0.1 mM.

<u>ES</u> (10 mM) MW 372.4

3.729 mg ES was dissolved in 200 μl ethanol and brought to 1 ml with distilled water. This 10 mM stock was used 1:100 for a final concentration of 100 μM ES/ 0.2% ethanol. An equal amount of ethanol was added to control and all other treatments run simultaneously. Due to light sensitivity, containers were wrapped in foil and experiments were conducted in a dark environment.

<u>FL</u> (400 μM) MW 376.3

Stock FL (400 μM) was prepared by bringing 1.51 mg of FL to a volume of 10 ml with distilled water. The stock was prepared in a dark environment and stored in a foil wrapped microcentrifuge tube.   This stock was used at 1:100 in transport medium for a final concentration of 4 μM FL.

<u>FLD</u> (10 mM) MW 4300

Stock FLD (10 mM) was prepared by the addition of 2.32 ml of distilled water to a bottle of 100 mg FLD. The stock was prepared in a dark environment and stored in a foil wrapped microcentrifuge tube.   This stock was used at 1:100 in transport medium for a final concentration of 100 μM FLD.

<u>MUG</u> (MW 352.3)

A 5mM stock was prepared from 1.76 mg MUG solubilized in 1 ml deionized distilled water. Dilutions were prepared from this stock. Typically a 1:100 dilution (30 μl in 3 ml transport media) was prepared.

<u>Ouabain</u> (100 mM) MW 728.8

Ouabain (72.8 mg) was dissolved in 1 ml of water and heated at 95°C for 15 min. The stock was prepared in a dark environment and stored in a foil wrapped microcentrifuge tube.   The stock was used at 1:100 or 1:1000.

<u>PAH</u> (100 mM) MW 194.2 g/mol

19.42 mg PAH was dissolved in 1 ml WBTM (solubility, 50 mg/ml water), heated at 95°C x 5 min and vortexed (according to Sigma technical services, PAH is reported to decompose if dissolved in HCl or NaOH). The 100 mM PAH stock was used 1:100 for 1 mM PAH or diluted 1:10 to make a 10 mM PAH stock and used 1:100 for 100 µM PAH final concentration.

<u>Probenecid</u> (100 mM) 285.4

290 µl x 1.0 M NaOH was added to 28.54 mg probenecid (solubility, 100 mg/ ml 1 M NaOH, Sigma Technical) and brought to 1 ml with distilled water or WBTM. This 100 mM stock was used 1:100 or 1:1000 for a final concentration of 1 mM or 100 µM.

<u>Radiolabeled Working Solutions (WS) for Transport Studies</u>

[^{14}C]AG Working Solution (40 µCi/ml, 820 µM)

Activity: 48.8 µCi/µmol

Prepared from 1 uCi/ml Stock

1. Transfer 0.5 ml Stock to [^{14}C]AG WS vial.
2. Rinse stock bottle x 3 with 0.25 ml distilled H$_2$O.
3. Using hot pipette tip, transfer each rinse to AG WS vial.
4. Use 1:100 (26 µl per 2.6 ml media) → 0.4 µCi/ml, 8.2 µM
5. Or use 1:200 (13 µl per 2.6 ml media) → 0.2 µCi/ml, 4.1 µM

[^{3}H]DHEAS Working Solution (20 µCi/ml, 253 nM)

Activity: 79.1 Ci/mmol

Prepared from 1.0 mCi/ml Stock (250 µCi [^{3}H]DHEAS in 0.25 ml)

1. Add 2.45 ml distilled H$_2$O to [^{3}H]DHEA WS vial.
2. Add 0.05 ml STOCK solution to WS vial.
3. Pipette WS in and out to ensure all STOCK is rinsed into WS.
4. Use 1:100 (26 µl per 2.6 ml media) → 0.2 µCi/ml, 2.53 nM

[^{3}H]ES Working Solution (20 µCi/ml, 435 nM)

Activity: 46.0 µCi/nmol

Prepared from 1 mCi/ml Stock in a dimly lit room due to light sensitivity

1. Add 2.45 ml distilled H_2O to [^{3}H]ES WS foil wrapped vial.

2. Add 0.05 ml STOCK solution to WS vial.

3. Pipette WS in and out to ensure all STOCK is rinsed into WS.

4. Use 1:100 (26 µl per 2.6 ml media) → 0.2 µCi/ml, 4.35 nM

5. Or use 1:200 (13 µl per 2.6 ml media) → 0.1 µCi/ml, 2.17 nM

[^{14}C]PAH Working Solution (40 µCi/ml, 760 µM)

Activity: 52.7 µCi/µmol

Prepared from 100 µCi/ml Stock (50 µCi [^{14}C]PAH in 0.5 ml)

1. Transfer 0.5 ml Stock to [^{14}C]PAH WS vial.

2. Rinse stock bottle x 3 with 0.25 ml distilled H_2O.

3. Using hot pipette tip, transfer each rinse to PAH WS vial.

4. Use 1:100 (26 µl per 2.6 ml media) → 0.4 µCi/ml, 7.6 µM

5. Or use 1:200 (13 µl per 2.6 ml media) → 0.2 µCi/ml, 3.80 µM

Solutions for Isolation of F344 renal proximal tubules

Perfusion Buffer A

	pH 7.36
Chemical	Concentration
NaCl	115.0 mM
KCl	5.0 mM
$NaHCO_3$	25.0 mM
NaH_2PO_4	2.0 mM
$MgSO_4 \cdot 7H2O$	1.0 mM
Alanine	1.0 mM
Glucose	5.0 mM
Deferoxamine	0.1 mM
Mannatol	25.0 mM
Lactate	4.0 mM
Dextran	0.6 % (w/v)
Penicillin G	100 units/ml
$CaCl_2$	1.0 mM

bubble with 95% O_2/ 5% CO_2 for 30 min

Perfusion Buffer B

Chemical	Concentration
Collagenase	130 units/ml
SBTI	0.01 % (w/v)

diluted in 25 ml Perfusion buffer A

Incubation Buffer A

	pH 7.36
Chemical	Concentration
NaCl	115.0 mM
KCl	5.0 mM
$NaHCO_3$	25.0 mM
NaH_2PO_4	2.0 mM
$MgSO_4 \cdot 7H2O$	1.0 mM
Alanine	1.0 mM
Glucose	5.0 mM
Deferoxamine	0.1 mM
Malic acid	5.0 mM
Butyric acid	2.0 mM
Lactate	5.0 mM
$CaCl_2$	1.0 mM
Penicillin G	100 units/ml

bubble with 95% O_2/ 5% CO_2 for 30 min

Incubation Buffer B

Chemical	Concentration
Collagenase	150 units/ml
SBTI	0.02% (w/v)
BSA	0.2% (w/v)
Dnase	70 units/ml

diluted in 50 ml Incubation buffer A

Krebs-Henseleit Buffer Concentrate (KHB 10x)

	Concentration
NaCl	118.0 mM
KCl	4.8 mM
$NaHCO_3$	0.12 mM
$MgSO_4 \cdot 7H2O$	25.0 mM
Hepes	25.0 mM

bubble with 95% O_2/ 5% CO_2 for 30 min

Krebs-Henseleit Buffer (1x)

Chemical	Amount
	pH 7.36
KHB 10x	20.0 ml
$_dH_2O$	180.0 ml

bubble with 95% O_2/ 5% CO_2 for 30 min

45% Percoll Density Gradient

Chemical	Amount
	pH 7.36
KHB 10x	6.0 ml
$_dH_2O$	27.0 ml
Percoll	27.0 ml

bubble with 95% O_2/ 5% CO_2 for 30 min

mixed in exact order